UNDERSTANDING THE EFFECTS OF SPATIAL AND TEMPORAL VARIABILITY OF MAIZE (*Zea Mays* L.) EMERGENCE ON CROP GROWTH, YIELD, AND NITROGEN UPTAKE

By

Susana Maria Albarenque

A DISSERTATION

Submitted to
Michigan State University
in partial fulfillment of the requirements
for the degree of

Crop and Soil Sciences – Doctor of Philosophy

2023

ABSTRACT

Spatial and temporal variability in maize emergence causes a decrease in crop yield and resource use efficiency, impacting the environment and producers' profit. The overarching goal of this dissertation was to evaluate the effect of the spatial and temporal variability of maize emergence on the crop growth, yield, nitrogen (N) uptake, and N use efficiency (Chapter 1).

Chapter 2 aims to compare the timing of maize plant emergence across and within sub-field yield stability zones, evaluate the impact of delayed emergence on crop yield and yield components by yield stability zone, and compare the effect of spatial and temporal variation of plant emergence on crop yield and yield components. Temporal variability has a higher impact than within-row plant spatial variability on crop yield and its components. The decrease in maize yield caused by the delay in emergence was not statistically related to yield stability zones but had a more negative impact in the low yield stability zones.

Chapter 3 investigates maize biomass accumulation and variation in plants with temporal variability in the emergence by yield stability zones and evaluates the plant nitrogen concentration, uptake and use efficiency in plants with temporal variability in emergence. Emergence delay caused a reduction in grain per plant through a reduction in plant growth rate (PGR) around silking. Although the delay in emergence did not affect nitrogen concentration in the grain, it caused a decrease in plant biomass and consequently an increase in biomass nitrogen concentration, resulting in less nitrogen accumulated in late emerged plants compared with early emerged plants. late emerged plants set fewer grains than early emerged plants and this lack of sink caused a change in plant N partitioning.

Chapter 4 presents an approach to determine maize plant emergence time by using plant height obtained from LIDAR images and Machine Learning (ML) techniques and uses the estimated emergence as an input in SALUS model to estimate yield accounting for spatial and

temporal variation. LiDAR images provided an accurate plant height in the three evaluated plant growth stages (V6, V14, and R1). Emergence was adequately estimated with the ML model and an “accurate” yield map was obtained using SALUS model. The integration of several digital tools allowed us to adequately simulate the spatial and temporal effect of emergence on crop yield.

Conclusions from the research projects and recommendations on managing fields with spatial and temporal variation in maize emergence are outlined in Chapter 5.

To Emilio and Miguel

AKNOWLEDGEMENTS

First and foremost, I would like to express my heartfelt gratitude to my family. Their encouragement and support lead me to successfully complete my degree. Further, thanks are owed to my son, who has always supported me at every stage of my career path. I am also grateful to Miguel, my loved one, for his support, encouragement, and company.

I am deeply grateful to my advisor, Dr. Bruno Basso, for placing his trust in my abilities, which has allowed me to grow both professionally and personally. My gratitude goes to my other four committee members, Dr. Jeff Andresen, Dr. Karen Renner, Dr. Kurt Thelen, and Dr. Maninderpal Singh for supporting my research goals.

I would like to extend my heartfelt thanks to Ricardo Melchiori for his continuous encouragement and belief in my potential, starting from my undergraduate years and guiding me throughout my academic journey. Additionally, I am grateful to all my friends and colleagues at INTA for their unwavering support and camaraderie.

Throughout every stage of my life, I have been exceptionally fortunate to be surrounded by friends who have consistently stood by me with their support. I extend my most sincere gratitude to them for sharing in my moments of joy and success, as well as providing comfort during challenging times. I am profoundly grateful to my lab mates, whose daily presence has illuminated my journey with joy and laughter. Their unwavering support for both me and my son during times of need has been truly heartwarming and made us feel in “home”.

TABLE OF CONTENTS

LIST OF TABLES

LIST OF FIGURES

LIST OF ABBREVIATIONS

CV	Coefficient of Variation
DAP	Emergence in days after planting (day)
DEM	Digital elevation model
FAO	United Nations Food and Agriculture Organization
GDD_E	Emergence in thermal time (°C day^{-1})
GN	Grain number
HS	High stable
LS	Low stable
MAE	Mean Absolute Error
ML	Machine learning
MS	Medium stable
N	Nitrogen
N_fUEb	Nitrogen fertilizer use efficiency in the biomass
N_fUEg	Nitrogen fertilizer use efficiency in the grains
NHI	Nitrogen harvest index
NUEb	Nitrogen use efficiency in the biomass
NUEg	Nitrogen use efficiency in the grains
$N_{up}b$	Biomass Nitrogen uptake (g N $plant^{-1}$)
$N_{up}g$	Grain Nitrogen uptake (g N $plant^{-1}$)
$N_{up}t$	Total Nitrogen uptake (g N $plant^{-1}$)
PA	Precision Agriculture
PGR	Plant growth rate

PGS	Plant growing space
PSV	Plant spatial variability
RMSE	Root Mean Square Error
RRMSE	Relative Root Mean Square Error
SALUS	System Approach to Land Use Sustainability
UAV	Unmanned aerial vehicle
UN	Unstable
VRS	Variable rate seeding
YSZ	Yield stability zone

CHAPTER 1: INTRODUCTION TO THE DISSERTATION

1.1. Rationale and Background

Over the last two centuries, the global population has significantly increased and is projected to reach 9.7 billion by 2050 (Waqas et al., 2023). To meet the needs of this growing population, food production must increase by 60-110% before 2050 (Pradhan et al., 2015) without further incorporation of land. However, this increase must also consider consumption patterns and the impacts of climate change. Unfortunately, agricultural land is being converted into urban areas at an alarming rate, especially in lower-middle-income countries, which are projected to experience the fastest rates of urbanization (United Nations, 2018). This trend has resulted in the loss of critical ecosystems, such as rainforests, wetlands, and grasslands, which causes a significant reduction in biodiversity and depletion of water resources (Lark et al., 2020). Therefore, it is critical to adopt sustainable land-use practices that balance the demands of urbanization and food production while preserving natural resources. Maize has the highest global production rate, has a considerable potential yield (Tollenaar & Lee, 2002), is highly sensitive to the availability of resources and inputs (Mueller et al., 2019), improves resources and inputs use efficiency (Caviglia et al., 2013) increasing the sustainability of productive systems, and adds carbon inputs and residues to the soil, among other benefits. Consequently, maize plays a crucial role in enhancing both the amount and quality of food production while also reducing the environmental impact associated with agriculture (Andrade et al., 2023).

Originally from southern Mexico, maize was introduced in the United States thousands of years ago, and native communities embraced it as a staple crop. Maize is produced in 141 countries worldwide, totaling 1147 Mt in 2022 (Table 1). On a yearly basis, the US is the top global producer (392 Mt y^{-1}), followed by China (257 Mt y^{-1}), Brazil (88 Mt y^{-1}), the European

Union (69 Mt y^{-1}), and Argentina (51 Mt y^{-1}). The continuous increase in US maize production during the last 60 years (Fig. 1a) is linked to the production area growth (Fig. 1b) and the steady increase in crop yield (Fig. 1c), which went from 3.9 Mg ha^{-1} to 11 Mg ha^{-1} in the 1961-2021 period (UN FAO, 2023). Maize, along with wheat (*Triticum aestivum* L.) and rice (*Oryza sativa* L.*)*, fulfills 30% of the total intake of food calories for over 4.5 billion individuals, playing a crucial role in current and future global food security (Shiferaw et al., 2011) and production system sustainability (Andrade et al., 2022; Otegui et al., 2020). In addition to being a source of nutrition for both humans and animals, maize serves as a fundamental component for producing various products such as starch, oil, protein, alcoholic beverages, food sweeteners, fuel, and is a highly traded agricultural commodity across nations (Wu & Guclu, 2013).

Table 1. Maize main production areas production and cultivated land (FAO, 2023).

Country	Production (Mt y^{-1})	Cultivated land (M ha)	Average yield (Mg ha^{-1})
USA	384	34.6	11.1
China	273	43.4	6.3
Brazil	88	19	4.6
EU	69	9.2	7.5
Argentina	61	8.1	7.4
Ukraine	42	5.5	7.7
India	32	9.9	3.2
Mexico	28	7.1	3.9
Indonesia	20	3.5	5.7
South Africa	17	3.1	5.4
Russia	15	2.9	5.3
Rest of the world	454	103	5.0
Total	1483	249	6.1

EU: Austria, Belgium, Bulgaria, Croatia, Republic of Cyprus, Czech Republic, Denmark, Estonia, Finland, France, Germany, Greece, Hungary, Ireland, Italy, Latvia, Lithuania, Luxembourg, Malta, Netherlands, Poland, Portugal, Romania, Slovakia, Slovenia, Spain, and Sweden.

The importance of maize in crop sequences is related to the large biomass productivity and high water and radiation use efficiencies of the crop system (Caviglia et al., 2013). Maize improves carbon balance and physical properties of the soil (i.e., infiltration and stability of aggregates) as its residues have a high C:N ratio (C:N~60) (Janssen, 1996). However, it can reduce N in the soil (high C:N residues), penalizing the following crop if non-fertilized and can

result in the following crop having a higher yield response to N fertilization (Semmartin et al., 2023).

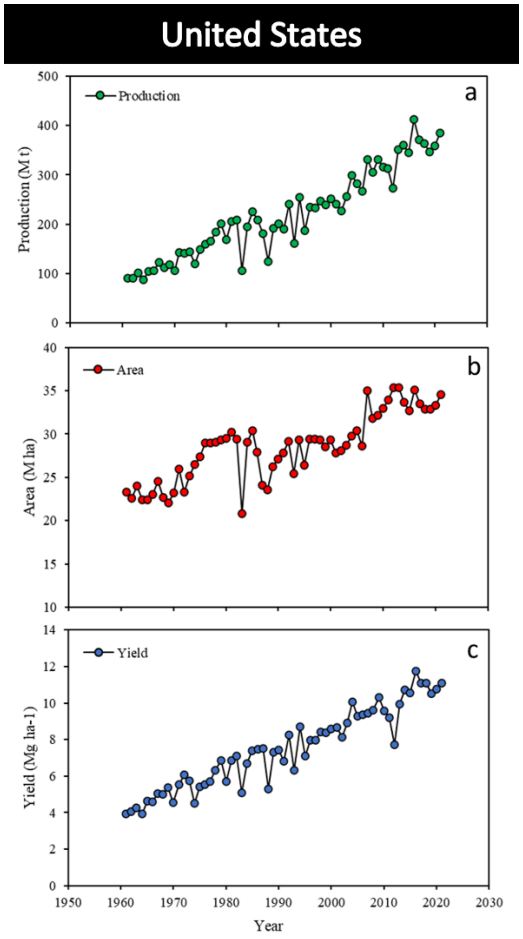

Figure 1. Annual maize production statistics for USA, 1960-2021 for a) production, b) area cropped, and c) yield. Based on UN FAO (2023).

The success in providing food security in the face of increasing global food demand is tightly related to narrowing the gap between actual farmer's yield and maximum attainable yield (yield gap). This yield gap is highly associated with the level of available labor, fertilizer, and plant protection inputs (Hoffmann et al., 2018). In recent decades, genetic improvements and newly developed technologies for better field management have contributed to reducing this gap and increasing potential yield limits (Cammarano et al., 2023). Increases in crop production have been related to the introduction of new cultivars with increased harvest index, greater use of

inputs (water, nutrients, and agrochemicals), and significant investment in irrigation areas. However, the current scenario differs in several critical aspects from that of 50 years ago and there are regions where yields have reached a plateau (Van Ittersum & Cassman, 2013). Additional improvements in genetic yield potential or water-limited yield are challenging, as the likelihood of significant advancements in genetic enhancement of photosynthesis or drought tolerance remains low (Hall & Richards, 2013) and the limited possibility to increase the harvest index (Alexandratos & Bruinsma, 2012). The improvement has also been related to social factors like governments supporting research, education, improvement in knowledge transference, subsidies to fertilizers, cooperative banks, and road network development, among others (Aggarwal et al., 2019).

Nitrogen supply through synthetic fertilizers has been highly adopted and related to the steady increase in yield since 1970 (Robertson & Vitousek, 2009). The discovery of the direct synthesizing of ammonia from hydrogen and nitrogen (Haber-Bosch process) and its increased use after World War II offered an important N source for the world's agriculture-increasing needs (Smil, 2004). By 1960 artificial fertilizer usage in the US was close to 7500 tons -nitrogen, phosphate, and potash- scaling up to 22,000 in 2015, being 10,400 tons used in maize fertilization (USDA, 2023). The inadequate management of nitrogen (N) in agriculture can have negative consequences on the environment and economy, which makes it increasingly important to improve the use of N fertilizer for sustainable agroecosystems (Smil, 1999). Generally, developed countries use N fertilizer rates that exceed crop demand, while developing countries, have a negative soil N balance, i.e., higher export of N from grain crops than N supplied by fertilizers (Liu et al., 2010). The excessive use of fertilizers has resulted in various environmental issues such as nitrate leaching to groundwater, phosphates causing eutrophication in surface

water, and an increase in greenhouse gas emissions from both fertilizer production and crop production (Novelli et al., 2023). To minimize the adverse impacts of fertilization on the environment, some countries (e.g., the European Union) have regulated the amount of organic and inorganic nitrogen that farmers can apply in certain areas (Cammarano et al., 2023; Moll et al., 1982). On the other hand, in the regions of the world where N application is below crops needs and the N balance in the soils is usually negative, there is a depletion of fertility with the consequent soil degradation associated with the decrease in organic matter, water retention, nutrients, and increased erosion risk (Vitousek et al., 2009). Therefore, the development of tools to evaluate crop N status is crucial for improving N fertilizer prescriptions and achieving higher crop yields with minimal environmental impact.

Precision agriculture involves the application of both technologies and principles to effectively manage the spatial and temporal variability that exists in agricultural fields to improve productivity while maintaining environmental quality (Pierce & Nowak, 1999). Common N fertilizer management uses uniform rates at a field-level, where soil N and crop requirements are spatially and temporally variable, causing mismatches between N supply and crop demand (Huggins & Pan, 1993), reducing the N use efficiency (NUE) and increasing the negative impacts on the environment and farmers profit (Lemaire & Gastal, 2019). Among the practices listed towards a more intensified and sustainable agriculture, the adoption of variable N rates is one of the most important to reduce the N emissions to the atmosphere in places where rates are higher than crop demand, and to increase soil N balances in places where rates are bellow crop requirements (Martinez-Feria et al., 2018). The use of N variable rates has been proven to increase NUE and reduce the environmental impacts, while improving farmer's profit (Basso et al., 2011).

Spatial and temporal variability in both crop yield and N fertilizer requirements is related to natural variation in soil properties, climate, and different management practices, and the interactions between them (Wang, 2021). Moreover, this variation is responsible for the uneven emergence of maize crops, which leads to increased interplant competition and yield reduction (Andrade & Abbate, 2005). Early emerged plants become taller and develop a root system earlier in the growing season (Liu et al., 2004a), having an advantage in resource uptake when compared with late-emerged plants, which remain shaded and smaller and have lower yields (Fig. 2, Fig. 3a). In addition, the variable distance between emergent and growing plants is mainly caused during planting operations (Liu et al., 2004c) and can contribute to plant stand variability (plant m^{-2}) (Fig. 2, Fig. 3b). Heterogeneity in the distance between plants may cause variable yield loss associated with very closely placed plants that is not compensated for by the additional yield of plants located in gaps, thereby decreasing overall yield (Novak & Ransom, 2018). Even crops (Fig. 2, low spatial and temporal variability) can outyield uneven stands when growing conditions and management are favorable (Lawles et al., 2012).

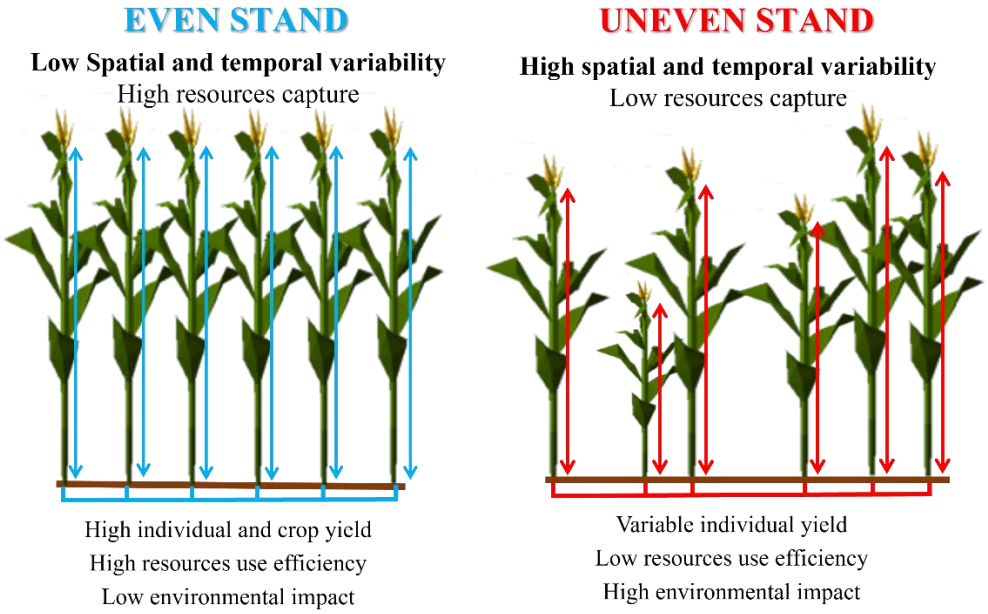

Figure 2. Even and Uneven crop stand schematic representation.

The literature is consistent in reporting the negative effect of delayed emergence on crop yield (Andrade & Abbate, 2005; Liu et al., 2004a, 2004b; Nafziger et al., 1991; Tollenaar & Wu, 1999) with reported reductions ranging from 5 to 22% (Carter & Nafziger, 1991; Ford & Hicks, 1992; Nemergut et al., 2021), highlighting that late-emerged plants could not compete with early emerged plants for resources. In contrast, the impact of within-row plant spatial variability has shown less consistent results, resulting in lower yield in some cases (Kolling et al., 2019; Sangoi et al., 2012) but not causing an effect in others (Liu et al., 2004d).

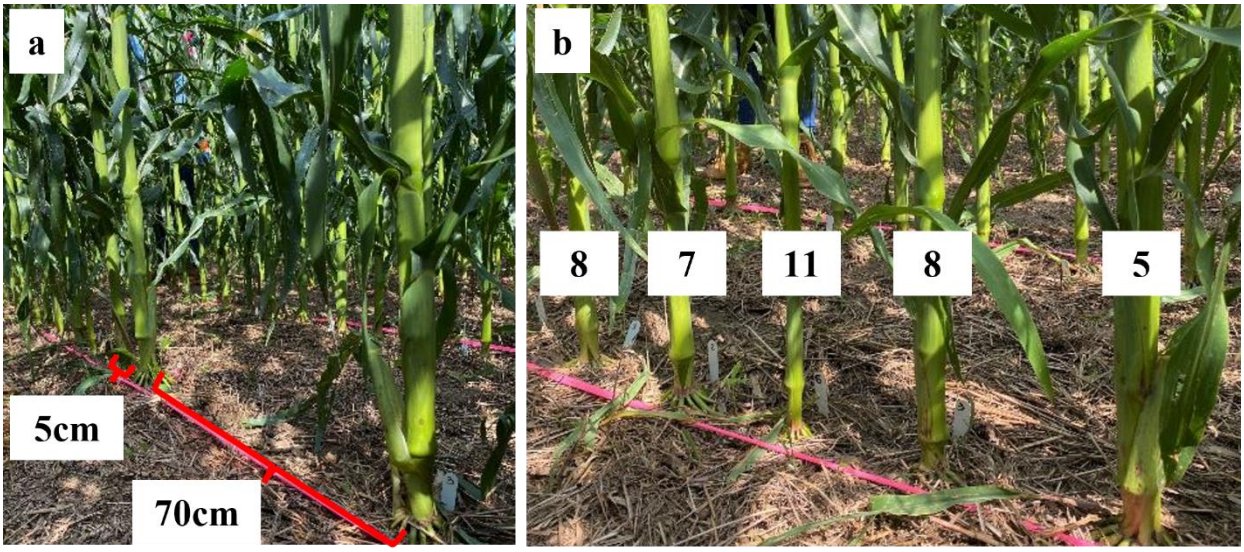

Figure 3. Spatial and temporal variation in a maize field. a) plant spatial variability and b) emergence variability. The numbers in the figures represent the number of days from planting to emergence.

These contrasting results and the influence of complex temporal interactions throughout the growing season make crop yield evaluation a challenging task. Additionally, assessing soil, weather, and management aspects demands considerable time and resources. To address the temporal variation effects of management practices on crop yield, crop models offer a valuable solution. These models consider the intricate temporal interactions occurring during the growing season and provide insights into the impact of different management approaches (Albarenque et

al., 2016; Basso et al., 2007; Batchelor et al., 2002). Unfortunately, crop models do not account for the spatial and temporal variations that exist in the field related to unevenness in emergence, thus missing a yield-reduction effect. The mechanisms that explain the effects of spatial and temporal variation in delayed emergence on crop yield should be incorporated into simulation models to improve their accuracy in crop yield forecasting at small and large scales. Additionally, assessment of plant temporal variation associated with the emergence time is not possible to do at field scale. Currently, farmers can easily access remote sensing technologies , such as Unmanned Aerial Vehicles (UAV) images, which have been shown to be useful in determining plant density in maize and wheat (Gnädinger & Schmidhalter, 2017; Velumani et al., 2021), plant spacing (Shuai et al., 2019), and recently (Vong et al., 2022) used them in combination with Machine Learning (ML) techniques to detect corn emergence at early stages (V2). Guo et al. (2022) used plant height obtained using UAV to identify maize phenology. However, no studies have integrated the use of crop models, UAV images, and ML to accurately estimate crop yield while accounting for the simulation of the effect of the spatial and temporal variation of emergence.

1.2. Objectives and Structure of the Dissertation

The overarching goal of this dissertation is to understand the effect of spatial and temporal variability of maize emergence on crop growth, yield, and nitrogen uptake and to incorporate this variation into crop models to improve their accuracy in crop yield forecasting at small and large scales. This dissertation consists of an introductory chapter, four research chapters, and a concluding chapter with summaries and recommendations. Chapter 2 presents the first study where maize emergence was studied across ten farmers' fields to evaluate its effect on crop yield and yield components by yield stability zones. This chapter has been submitted to

Field Crops Research. Chapter 3 portrays the effect of the spatial and temporal variability that exists in maize crop stands caused by uneven plant emergence on plant biomass accumulation, N uptake and N use efficiency. Chapter 4 integrates the use of UAV, Machine Learning techniques and crop growth models to improve crop yield estimation in fields with spatial and temporal variation in the emergence.

CHAPTER 2: YIELD STABILITY ZONE AND PLANT EMERGENCE EFFECTS ON MAIZE (*Zea mays* L.) YIELD

A version of this chapter has been submitted to a peer-review journal (*Field Crops Research)*

2.1. Abstract

Uneven crop stands result from natural variation in emergence time that is related to soil moisture and temperature, and variation of within-row plant-to-plant distance caused during planting operations. Understanding the effect of the spatial and temporal variation of plant emergence on crop yield can help farmers make more informed decisions about planting. The objectives of this work were to i) compare the timing of maize plant emergence across and within sub-field yield stability zones, ii) evaluate the impact of delayed emergence on crop yield and yield components by yield stability zone, and iii) compare the effect of spatial and temporal variation of plant emergence on crop yield and yield components. Ten experiments were conducted in farmers' maize fields in Springport (Michigan, US) Portland (Michigan, US), and Parana (Entre Rios, Argentina). Several years of yield monitored data for each field were used to develop yield stability zones (YSZ). Individual plant emergence was recorded daily, across yield stability zones. Emerged plants were tagged and the distance between plants within the row was recorded and used to calculate plant growing space (cm^2), and to classify them as uniform, double or skips. Marked plants were hand harvested to analyze the individual plant yield and number, weight of grains, and total crop yield. Individual plant emergence time ranged from 3 to 31 days after planting (DAP). The variation in timing of plant emergence had a greater impact than the variation of within-row plant spacing on crop yield and yield components. In general, the impact was larger in low yield areas. On average, plant yield was reduced by 7%, grain number by 6%, and final crop yield by 8.5% per day of emergence delay after planting. The

greater variation in the days of emergence delay when compared to within-row plant spacing variation can be related to the small overall spatial variability within the rows. Temporal variability had a higher impact than within-row plant spatial variability on crop yield and its components. The decrease in maize yield caused by the delay in emergence was not statistically related to yield stability zones. However, a trend of a more negative impact in the low yield stability zones was evident. Understanding factors affecting the spatial and temporal emergence patterns of crops can help farmers manage their planting operation and may help them with decisions on using more precise and tailored inputs (such as nitrogen fertilizer) on different sub-field yield stability zones. Incorporating emergence data and information into crop models will also help improve yield simulation results.

2.2. Introduction

Uniform crop stands can outyield non-uniform stands when the growing conditions and management are favorable (Andrade & Abbate, 2005; Lawles et al., 2012). Unevenness might result from natural variation in emergence that is mainly related to soil moisture and soil temperature variability (Andrade & Abbate, 2005). Early emerging plants have an advantage in obtaining resources when compared to those emerging later. They become taller have a better-developed root system earlier in the growing season (Liu et al., 2004a), which can lead to higher yields. There is evidence of an asymmetric competition for light, as the initially suppressed plants (dominated) exhibited the highest level of responsiveness to thinning (Pagano & Maddonni, 2007). The variable distance between emergent and growing plants is mainly caused during planting operations (Liu et al., 2004b) and can contribute to plant stand variability (emerged plants m^{-2}) (Daynard & Muldoon, 1983). Heterogeneity in the distance between plants may cause variable yield loss associated with very closely placed plants that is not compensated

for by the additional yield of plants located in gaps, thereby decreasing overall yield (Novak & Ransom, 2018).

The literature is consistent in reporting the negative effect of delayed emergence on crop yield (Andrade & Abbate, 2005; Liu et al., 2004a, 2004b; Nafziger et al., 1991; Tollenaar & Wu, 1999). Carter et al. (1990) planted maize at several dates to simulate delayed emergence and reported between 10 and 22% yield reduction in plants with a 21-day delay in the emergence, noting that late emerged plants could not compete with early emerged plants for resources. Nafziger et al. (1991), studied several hybrids in different environments in Illinois and Wisconsin, and reported a 0.69 Mg ha^{-1} yield loss when emergence was delayed between 10 and 12 days, and up to 1.44 Mg ha^{-1} with 22-day delays. Moreover, grain yield has been shown to be lower in uneven emerged stands with increased density, where early emerging plants produced more grain per plant than late emerging plants (Ford & Hicks, 1992). Recently, Nemergut et al. (2021) reported per-plant yield reductions of 5.25% per day of delay in emergence when the plants emerged nearly 7 days after planting.

Unlike emergence delay, the impact of within-row plant spatial variability has shown contrasting results. Liu et al. (2004c), evaluated different standard deviations of within-row plant spacing and reported no significant effect on yield, leaf number, plant height, leaf area index, and harvest index. Similarly, Lauer & Rankin (2004) reported that grain yield was rarely affected by plant spacing variability and that maize plants can compensate for plant spacing variability when plant density is adequate. In contrast, other authors observed significant yield decreases ranging from 83 to 128 kg ha^{-1} for every 10% increase in the plant spacing variation coefficient, mainly related to grain number decreases (Sangoi et al., 2012; Kolling et al. 2019). Contrasting results in within-row spatial variability might be related to variations in the procedures used to simulate

plant spacing variability, which range from the more basic hand planting and plant thinning once the plants emerged, to the more complex, including herbicide use in Roundup-ready and traditional seed mixtures (Kolling et al., 2019; Liu et al., 2004c; Pommel et al., 2002).

While these and other studies have added to our knowledge of emergence delay and spatial variability of planting, the conditions under which they were performed, the methods used to generate spatial and temporal variability, and the objectives of the studies still leave a number of further questions to be investigated. We are not aware of any studies that have been performed under commercial production conditions; a more complex scenario where many additional factors and interactions can affect yield. Similarly, while prior studies have analyzed emergence variation and within-row spatial variation, separately or together, the majority have been manipulative, i.e., the variation in emergence was obtained with different specified planting dates and the variation of within-row planting spacing through post emergence thinning. Likewise, while studies have explored the relationships between delayed emergence and individual plant yield, height, and growth rate, they have not explored the effect on yield components. Therefore, questions that remain unanswered include: Is emergence delay related to the spatial variability of the soil and prior yields? Which yield component is more affected by emergence delay? Our study aims to answer these questions. Thus, in this study, we i) compared the delay in plant emergence across sub-field yield stability zones under varying commercial operating conditions; ii) evaluate the impact of emergence delay on crop yield and yield components by yield stability zones, and iii) compare the effect of spatial and temporal variation of emergence on maize crop yield and yield components.

2.3. Methods

2.3.1. Site description and general characteristics

Field experiments were conducted in nine commercial maize producers' fields located in Portland (MI) (42.8971°N, 84.9776°W) and Springport (MI) (42.3471°N, 84.7097°W), and in one commercial field located at the National Institute of Agricultural Technology Research Station in Parana (INTA EEA Parana, Argentina) (32.2336°S, 60.5338°W) (Table 2). According to the Köppen climate classification the Michigan study areas are characterized as cold, without dry season, hot summer (Dfb) with a mean average daily temperature of 7.9°C and precipitation averaging 895 mm annually in the, whereas the Parana study area is characterized as temperate, without dry season, hot summer (Cfa) with an average daily temperature of 18.9°C and precipitation averaging 1101 mm annually. Fields varied in soil properties and management practices, such as tillage system, plant density, row spacing, hybrid relative maturity, and planting date (Table 2). The Springport fields were planted with a White planter 9924VE, Portland fields with a John Deere 1770 NT and a pneumatic Giorgi Precisa 8000 was used in Parana field.

2.3.2. Yield stability zones

Yield stability zones (YSZ) in the Michigan fields were delineated from several years of yield monitor data collected from farmers in each studied field following (Basso et al., 2007; Maestrini & Basso, 2018). Briefly, standardized yield maps were used to calculate the mean (μ) and standard deviation (σ) of the yield for every pixel of the field, considering a pixel as stable when $\sigma < 0.75$ and as unstable when $\sigma \geq 0.75$. Similarly, pixels with $\mu < 0$ were classified as low-yielding and high-yielding when $\mu > 0$. This methodology classifies field pixels as High Stable (HS), Low Stable (LS), Medium Stable (MS) and Unstable (UN). As Parana fields lacked

yield maps data, zones were determined based on detailed soil maps, soil productivity index maps, and using farmer experience (Hornung et al., 2006). It was therefore not possible to estimate the temporal variation in the productivity and the unstable zones in this field.

2.3.3. Experimental design

Three replicate plots were established in each field and in each identified yield stability zone shortly after corn planting (0-2 days after planting, DAP), covering an area of two meters by four-rows in 2016 (Field 222), 2017 (Field 222 and Field JS1), and 2018 (Field 105 and Field NC12) and five meters by two-rows in 2019 (Field 304 and Field MG1), 2020 (Field 308 and Field 11), and 2021 (Field 210). In each case plot size allowed for up to 60 plants per plot (Fig. 1). Fields in Springport, except for 2019-F304, had cover crop coverage at planting, which were terminated one week after planting.

2.3.4. Plant emergence measurements

In 2016 and 2017, emergence dates were estimated from time-lapse images (one per hour) taken between dawn and dusk by 'Stealth Cam' cameras (16-22 MP resolution) that were attached to a post five rows in front of each replicate plot. The emergence dates were determined by analyzing the imagery using the ESRI ArcGIS Image Analysis toolbox, and the distance between the plants within each row was measured in the field.

From 2018 to 2021, emergence was recorded by visiting each plot in each field once per day during the period of emergence. Each emerged plant was individually identified using white stakes labeled with permanent ink that indicated the number of days after planting to emerge (Fig.4), and the distance between the plants within the row was measured and recorded (Fig.4). In order to evaluate plant spatial variation (PSV), plant growing space (GS, cm^2) was calculated

as the sum of the half distances between a plant and its two neighbors multiplied by the row spacing (Eq. 1; (Martin et al., 2005)):

$$GS_i=[(d_i-d_{i-1})/2+(d_{i+1}-d_i)/2)xR] \quad \text{Equation 1}$$

where GS_i is the *i*th plant space available to grow, d_i, d_{i-1}, and d_{i+1}, are the distances to the *I*, *i*-1, and *i*+1 plant, and R is the row spacing. Additionally, each plant or space between plants was classified according to the distance within the row as a double, skip or uniform (Novak & Ransom, 2018). The classification was made based on the standard deviation of the distance between plants within the row and the theoretical distance between the plants i.e., expected distance between plants based on plant density and row spacing. According to plant density and row spacing in Table 1, the calculated theoretical distance was 18, 20 and 27 cm, for Springport, Portland, and Parana, respectively. Thus, doubles were identified as consecutive plants less than 5cm from each other. Skips were gaps greater than the theoretical distance between plants plus one standard deviation, and uniform were plants with distances between 5 and the theoretical distance plus one standard deviation. At the end of the growing season, each labeled plant was individually harvested (n=4186 plants) to analyze the individual plant yield, grain number, grain weight, and cob weight. Additionally, the cob weight to grain weight ratio was calculated.

Figure 4. Representative plot photos at Springport, MI in 2019 and 2021 (42.3471°N, 84.7097°W): a) field 2019-304 no-till before emergence, b) field 2019-304 after emergence, and c) field 2021-210, no-till and cover crop, after emergence. The numbers in the white stakes indicate emergence in days after planting, from left to right: 23, 4, 11, and 6.

Table 2. Experimental sites and locations with soil and management data.

Site	Year-Field	Predominant Soil Taxonomic class	Tillage System†	Plant density (plants ha^{-1})	Row spacing (cm)	Field Size (ha)	Relative maturity	Planting date	Silking date
Springport	**2016-222**	Fine-loamy, mixed, active, mesic Typic Hapludalfs	NT	74131	76.2	35	96	21-May	26-Jul
	2017-222	Fine-loamy, mixed, active, mesic Typic Hapludalfs	NT	74131	76.2	35	96	25-May	30-Jul
	2018-105	Fine-loamy, mixed, active, mesic Typic Hapludalfs	NT	74131	76.2	106	96	4-Jun	5-Aug
	2019-304	Very-fine, mixed, active, frigid Aquic Glossudalfs	NT	74131	76.2	32	95	8-Jun	8-Aug
	2020-308	Very-fine, mixed, active, frigid Aquic Glossudalfs	NT	74131	76.2	29	102	11-May	23-Jul
	2021-210	Very-fine, mixed, active, frigid Aquic Glossudalfs	NT	74131	76.2	150	95	15-May	27-Jul
Portland	**2017-JS1**	Coarse-loamy, mixed, semiactive, nonacid, frigid Mollic Endoaquepts	C	93899	50.8	34	95	18-May	24-Jul
	2018-NC12	Coarse-loamy, mixed, semiactive, nonacid, frigid Mollic Endoaquepts	C	93899	50.8	28	95	1-May	17-Jul
	2019-MG1	Fine, mixed, active, mesic Haplic Glossudalfs	C	93899	50.8	25	104	8-Jun	12-Aug
Parana	**2020-11**	Fine, montmorillonitic, thermic Vertic Argiudolls	NT	70000	52	17	122	29-Dec	5-Mar

†NT*:* no-till, *C:* conventional

Table 3. Observed precipitation and temperatures at each experiment site and season for periods near emergence (May-June at Springport and Portland, December-January at Parana) and growing season (May-October at Springport and Portland, December-April at Parana) versus historical normal (1991-2020).

Site	Year-Field	Cumulative precipitation (mm)							Temperature (°C)			
		-2wk[†]	-1wk[§]	+1wk[ǂ]	+2wk[‡]	R1±2wk[⁋]	Total in-season	Total historical	Em period	Em Historical	Average in-season	Historical Average
Springport	2016-222	25	0	2	12	58	414	447	18	15.5	20	17.7
	2017-222	63	55	6	6	32	238	447	17	15.5	19	17.7
	2018-105	34	26	16	16	84	407	447	19.5	15.5	20.5	17.7
	2019-304	49	20	88	47	19	420	446	16.5	15.5	19.3	17.7
	2020-308	32	10	63	103	84	418	446	17.5	15.5	19.3	17.7
	2021-210	10	1	3	43	154	607	446	18	15.5	19.9	17.7
Portland	2017-JS1	0	0	0	0	82	294	454	16.6	16.7	18.4	18.5
	2018-NC12	6	2	19	64	44	425	454	18.8	16.7	19.9	18.5
	2019-MG1	52	23	40	89	44	576	454	15.8	16.7	18.6	18.5
Parana	2020-11	24	1	2	28	91	680	541	23.5	23.9	23	22.9

[†]-2wk: two weeks before planting, [§]-1wk: one week before planting, [ǂ]+1wk: one week after planting, [‡]+2wk: two weeks after planting, [⁋]R1±2wk: 30-d period around flowering.

Total in-season: cumulative precipitation during the growing season

Total historical: cumulative precipitation during the growing season for 30-Year average (1991–2020).

Em period: average temperature during the emergence period (May-June for Springport and Portland, and December-January for Parana)

Em historical: average temperature during the emergence period for 30-Year average (1991–2020).

Average in-season: average temperature during the growing season (May-October and December-April, for Michigan and Parana sites, respectively).

Historical average: average temperature during the growing season period for the 30-Year average (1991–2020).

2.3.5. Weather conditions

A summary of long-term patterns of precipitation and temperature around planting and for the growing season are presented in Table 3. Rainfall during the growing season was closer (90 to 110%) to the average (1991-2020) for the same period in most evaluated fields, whereas, in 2017 (Field 222 and JS1) in-season precipitation was between 28 and 46% lower than the average. Temperatures were slightly higher than historical averages in Springport fields, while they were within the range of historical values for the other four fields. The average temperature during the emergence period (May-June) ranged from 14 to 22°C in Springport, around 14% higher than the 30 yr average for the same period. In contrast, temperatures in Portland were 16% higher than average in May but 7% lower in June. In Parana, temperatures during the emergence period (Dec-Jan) were slightly lower (2%) than the 30-yr average. The average precipitation during the evaluated crop emergence period was slightly below the 30-yr average in May (4%) and above it in June (12%) in Springport, and in Portland, it was slightly below the 30-yr average in May (6%) and June (3%). Parana showed below-average precipitation in December (21%) and above average in January (56%) (Table 3).

2.3.6. Data analysis

Data was analyzed using the GLIMMIX procedure in SAS version 9.4 (SAS Inst., Inc.), to test the effects of Year-Field and YSZ and their interaction (Year-Field x YSZ) on plant emergence and growing space, YSZ and Year-Field x YSZ were considered fixed effects and Year-Field random. Individual plants were nested within each plot and included as a random factor to identify them as subsamples. Additionally, emergence was described using the 10, 50, and 90 percentiles of the emergence distribution, emergence uniformity was calculated as the time between the 10% and 90% of emergence (Egli & Rucker, 2012). Plant yield, grain number,

grain weight, and crop yield were analyzed by field to test the effect of yield stability zone, considering DAP and GS as covariates. Mean separation between groups was analyzed using Tukey's method, performing pairwise comparisons to identify differences greater than the expected standard error. In addition, to make results comparable among Year-Fields the relative to the maximum per Year-Field plant yield (RPY), grain number (RGN), and crop yield (RY) were calculated and a regression analysis was performed using the JMP® Pro Version 15.2.0 (SAS Institute Inc., Cary, NC, 1989–2021) to determine relationships with DAP using the mean RPY, RGN, and RY per day of emergence per plot. Slopes and intercepts were compared by yield stability zones, when no differences among slopes were detected, multiple regressions were performed using YSZ as a dummy variable to select a model that best describes the relationship. Three models were compared: i) Full model, describe the relationship using four or three functions one per YSZ (8 or 6 parameters), ii) Simple model with YSZ, describes the relationship using a unique function (5 or 4 parameters) using dummy variables, and iii) Simple model that describes the relationships with a unique function (2 parameters) (Supplemental Table S3). Models were compared with a F test (Mead et al., 2003) selecting the simplest model (less parameters) that better described the relationships.

2.4. Results

2.4.1. Emergence by year-field and yield stability zones

Across all fields, emergence ranged from 3 to 31 days after planting (DAP). The emergence range was highest in Springport (3 to 31 DAP), and narrower in Portland (5 to 25 DAP) and Parana (6 to 25 DAP). All yield stability zones (YSZ) showed variability in emergence and emergence was significantly affected by YSZ in 7 out of 10 field site years ($p<0.05$) (Table 4). In Springport, the average DAP to emergence ranged from 5.5 to 14.4, 6.4 to

14.6, 5.2 to 14.7, and from 4.9 to 14.7 days, in the HS, LS, MS, and UN zones, respectively. In Portland, emergence ranged from 6.8 to 11.6, 6.8 to 10.5, 6.5 to 11.4, and from 6.9 to 10.7 days in the HS, LS, MS, and UN stability zones, respectively. The average time to emergence in Parana was 7.5, 6.9, and 7.1 days in the HS, LS, and MS stability zone, respectively.

Table 4. Emergence statistics and emergence uniformity (T10-90) from ten year-fields by yield stability zone (YSZ). Variation coefficient in brackets.

Site	Year-Field	Emergence- days after planting†				Emergence uniformity (T_{10-90})†			
		HS	MS	LS	UN	HS	MS	LS	UN
Springport	**2016-222**	10.9b(11)§	11.5a(13)	11.4a(12)	10.7b(6)	1.6	2.3	2.4	1.0
	2017-222	5.5b(32)	5.2b(41)	6.4a(47)	4.9b(26)	2.7bc	3.5ab	5.4a	1.0c
	2018-105	7.0(10)	7.2(13)	---	7.1(19)	3.0	3.0	---	3.0
	2019-304	8.1(8)	8.0(8)	---	8.2(12)	1.4	1.5	---	1.3
	2020-308	14.4(10)	14.7(9)	14.7(9)	14.7(15)	4.0a	1.6b	2.1b	1.5b
	2021-210	10.8c(17)	11.2cb(22)	13.2a(26)	11.8b(9)	2.6b	4.2ab	6.8a	4.3ab
Portland	**2017-JS1**	10.3a(11)	10.4a(15)	10.5a(8)	9.8b(11)	2.0	1.3	1.4	2.0
	2018-NC12	11.6a(14)	10.1b(12)	---	10.7b(13)	3.0	3.0	---	4.0
	2019-MG1	8.9c(10)	11.4a(16)	9.8b(6)	9.4bc(6)	1.4b	3.4a	1.0b	1.0b
Parana	**2020-11**	7.5ab(31)	7.1ab(12)	6.9b(27)	---	3.0	2.0	2.0	---
		ANOVA							
Year-Field		ns				ns			
YSZ		ns				ns			
Year-Field x YSZ		***				*			

†Means not sharing the same letter within the same row are different ($p<.05$) from each other. HS: High and stable, LS: Low and stable, MS: Medium and stable, and UN: Unstable.

No difference was detected between Year-Field, YSZ, and no interaction (Year-Field x YSZ) was detected (APPENDIX A Table 20). In Springport the time taken for 10% of the plants to emerge (10% emergence) (Fig.5a-f) was 8.5 DAP for all YSZs, similarly in Parana it was 6.1 DAP (Fig.5j), whereas in Portland it was 9.5 DAP (Fig.5g-i). The time to 50% emergence in Springport was 9.4 DAP for all the YSZs. Similarly, Portland time to 50% emergence was 10.2 days. In Parana, the time to 50% emergence was 6.7 DAP. The time to 90% emergence in

Springport was 11 DAP. In Portland, the time to reach 90% emergence was 11.6, and in Parana was 8.8 DAP.

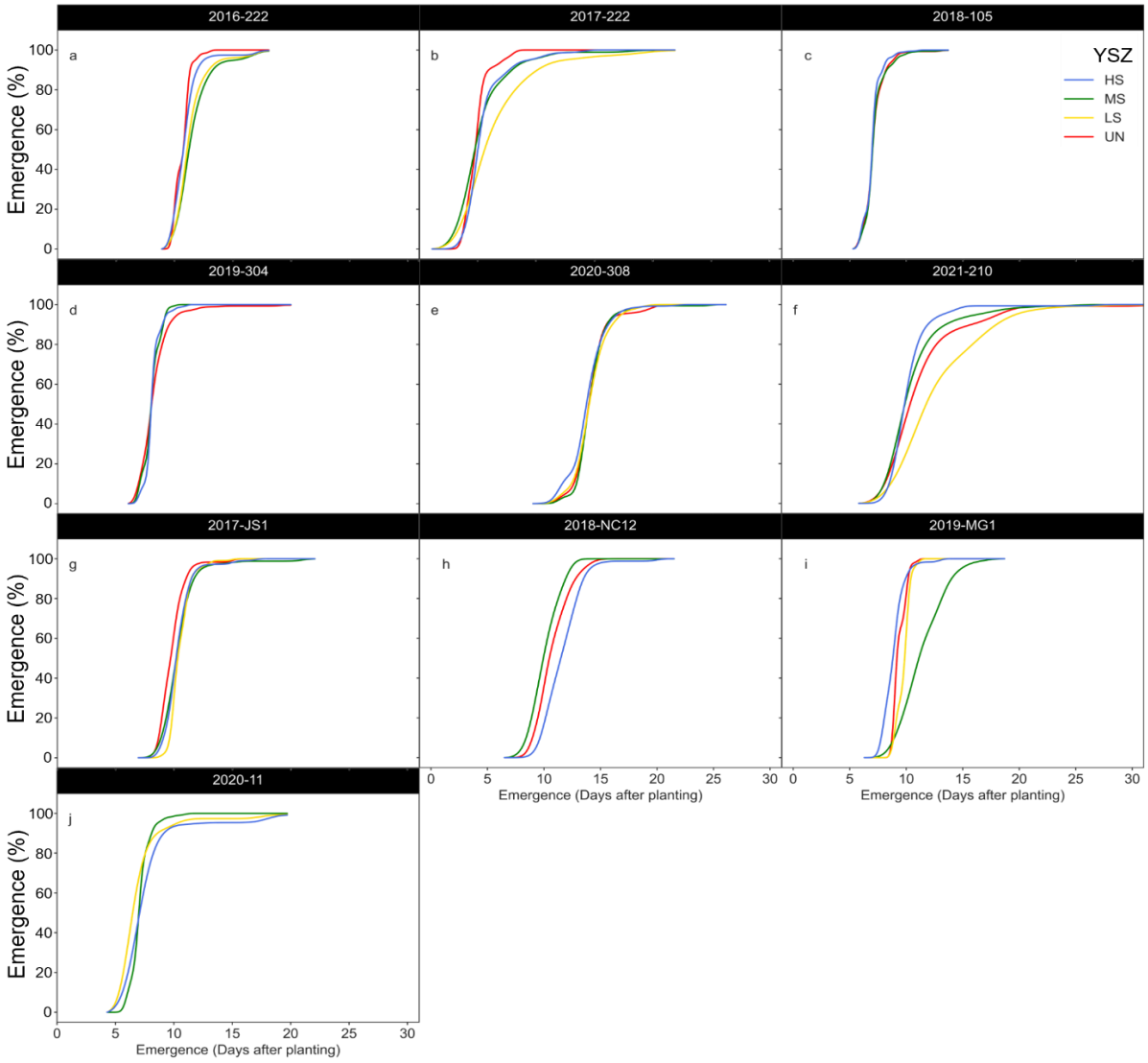

Figure 5. Cumulative probability distributions of maize emergence by Year-Field and Yield Stability Zone at Springport (a, b, c, d, e, and f), Portland (g, h, and i), and Parana (j). For field a) 2016-222, b) 2017-222, c) 2018-105, d) 2019-304, e) 2020-308, f) 2021-210, g) 2017-JS1, h) 2018-NC12, i) 2019-MG1, and j) 2020-11 and for High and stable (HS), Low and stable (LS), Medium and Stable (MS), and Unstable (UN).

2.4.2. Plant spatial variability by yield stability zones

The available space that plants had for growth (GS) calculated to evaluate the plant spatial variability, ranged from 998 to 1632 cm^2 per plant. In Springport, three fields showed significant differences in GS ($p<0.05$) between YSZ (Table 5), ranging from 1217 to 1524, 1423 to 1697, 1220 to 1570, and 1205 to 1923 cm^2, in the HS, LS, MS, and UN YSZs, respectively. The GS in Portland fields ranged from 1042 to 1632, 998 to 1564, 1001 to 1622, and 1008 to 1488 cm^2, in the HS, LS, MS, and UN YSZs, respectively. In Parana, GS was 1578, 1617, and 1601 cm^2, in the HS, LS and MS YSZs, respectively.

Table 5. Mean growing space (cm^2 $plant^{-1}$) by yield stability zone (YSZ) at three locations (Springport, Portland, and Parana) across fields and years (2016-2021).

Location	Year-Field	YSZ *P*-value	Growing space (cm^2) †			
			HS	MS	LS	UN
Springport	2016-222	ns	---	---	1568	1528
	2017-222	<0.0001	1395b	1244b	1697a	1205b
	2018-105	ns	1313	1349	---	1368
	2019-304	ns	1217	1220	---	1269
	2020-308	0.0021	1524b	1570b	1649ab	1923a
	2021-210	<0.0001	1313b	1302b	1423a	1259b
Portland	2017-JS1	ns	1042	1001	998	1008
	2018-NC12	ns	1067	1068	---	---
	2019-MG1	ns	1632	1622	1564	1488
Parana	2020-11	ns	1578	1601	1617	---
ANOVA						
Year-Field				ns		
YSZ				ns		
Year-Field x YSZ				*		

---: Not measured. † Means not sharing the same letter within the same row and Year-Field are different ($p<0.05$) from each other.

Based on within row plant spacing, plant spatial variability was also evaluated by classifying individual plants as uniform, skip or double. In Springport, plots contained between 76 and 96% uniform plants, between 4 and 23% skips, and between 0 and 3% doubles. In Portland uniform plants were between 81 and 91%, skips represented 4 to 17%, while doubles

were between 1 to 4%. Similarly, the Parana field had 87% uniform plants, 12% skips, and 1% doubles (Fig. 6).

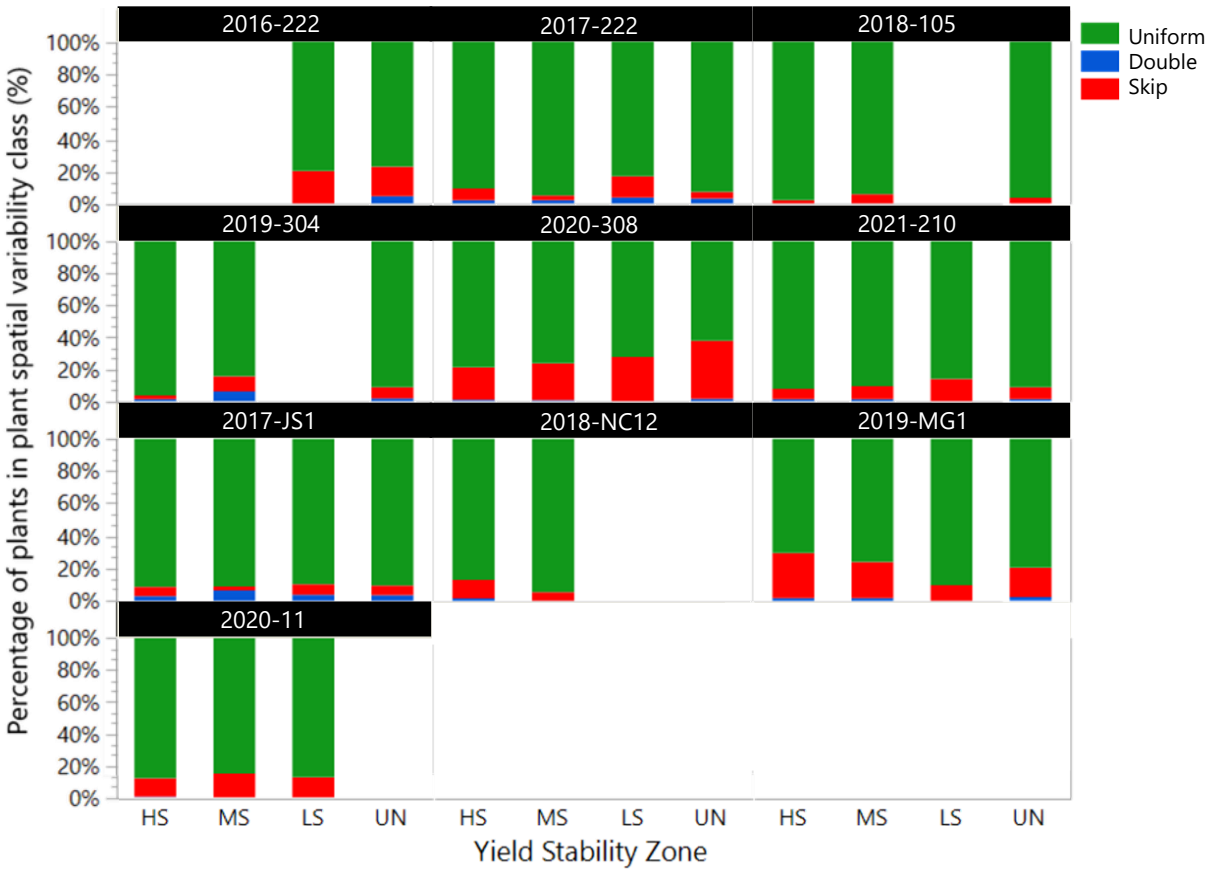

Figure 6. Plant spatial variability within the maize's row as percentage of uniform, skip, and double plants by yield stability zones across fields and years. Uniform plants are defined as plants with distances between 5 cm and the theoretical distance plus one standard deviation; plants next to gaps greater than the theoretical distance between plants plus one standard deviation, and Doubles were consecutive plants with less than 5 cm from each other. Yield stability zones are HS: High stable, MS: Medium stable, LS: Low stable, and UN: Unstable.

2.4.3. Plant yield, crop yield and yield components

Mean individual plant yield at Springport ranged from 130 to 308, 109 to 150, 131 to 202, and 108 to 308 g plant^{-1} in the HS, LS, MS, and UN YSZs, respectively. In Portland, the range was between 98 to 137 g plant^{-1} in the HS zone, 86 and 99 g plant^{-1} in the LS zone, 113 and 167 g plant^{-1} in the MS zone, and between 117 and 120 g plant^{-1} in the UN zone. At Parana

there were lower individual plant yields, with 101, 71, and 113 g plant^{-1} averages for HS, LS, and MS, respectively (Table 4). The mean grain number per plant in Springport was 638 grain plant^{-1} (465-638), 515 (403-657), 545 (470-644), 513 (415-713) grain plant^{-1}, for HS, LS, MS, and UN YSZ. Portland had the lowest grain number, with 436 (414-462), 304 (278-329), 432 (377-525), and 406 (370-475) in the HS, LS, MS, and UN YSZs, respectively. Similarly, grain number in Parana were 447, 309 and 442, for the HS, LS, and MS YSZs, respectively. The crop yield ranged between 7.51 and 13.33 Mg ha^{-1} in Springport, 6.40 and 15.40 Mg ha^{-1} in Portland, and 4.50 and 7.27 Mg ha^{-1} in Parana (Table 6).

Table 6. Average plant yield (g plant^{-1}), grain number (grains plant^{-1}), grain weight (g grain^{-1}), and crop yield (Mg ha^{-1}) by yield stability zone (YSZ) at three locations (Springport, Portland, and Parana) across fields and years (2016-2021).

Site	Year-Field	YSZ	Plant yield† g plant^{-1}	Grain number† grains plant^{-1}	Grain weight† g grain^{-1}	Yield† Mg ha^{-1}
Springport	2016-222	HS§	163	553	0.294	11.83a
		MS‡	162	536	0.304	10.50b
		LS¶	150	496	0.306	10.70b
		UN‡	160	506	0.318	11.60a
	2017-222	HS	130a	465	0.280b	12.37b
		MS	150a	499	0.300a	13.33a
		LS	109b	403	0.271c	7.70d
		UN	116a	415	0.278bc	10.60c
	2018-105	HS	141	480	0.293	10.83
		MS	133	470	0.285	10.1
		UN	146	496	0.296	10.8
	2019-304	HS	173	572	0.302	12.95
		MS	142	511	0.275	10.62
		UN	150	510	0.291	10.81
	2020-308	HS	208b	638b	0.328a	12.67
		MS	202b	644b	0.313b	11.85
		LS	143c	657ab	0.215c	7.51
		UN	238a	713a	0.336a	11.66
	2021-210	HS	145a	557a	0.262	10.20a
		MS	131b	533ab	0.249	9.40b
		LS	126b	503b	0.251	8.44c
		UN	108c	437c	0.265	8.00c
Portland	2017-FJS1	HS	131	414	0.315	9.31
		MS	118	393	0.301	8.91
		LS	86	278	0.312	6.39
		UN	117	370	0.318	8.64
	2018-FNC12	HS	98	432	0.233	9.32
		MS	167	525	0.319	15.39
		UN	120	475	0.25	11.12
		HS	137	462	0.293	11.39
	2019-MG1	MS	113	377	0.304	9.5
		LS	99	329	0.309	8.48
		UN	119	375	0.324	10.93
Parana	2020-11	HS	101a	447a	0.23	6.64a
		MS	113a	442a	0.253	7.30a
		LS	71b	309b	0.236	4.50b

†Means not sharing the same letter within the same column and field-year are different ($p<0.05$) from each other. HS: High and stable, LS: Low and stable, MS: Medium and Stable, and UN: Unstable.

2.4.4. Impact of emergence delay on plant yield, crop yield and yield components

The relative individual plant yield across year-fields was negatively affected by emergence delay (Fig. 5 a, b, c). The average relative plant yield decrease per day of emergence

delay was 2 % in Springport and it did not show differences among YSZ (Table 7 and APPENDIX A Table 19). Although, there were no significant differences between YSZs (i.e., no significant difference in slopes, $p>0.05$) in the emergence effect, Portland and Parana relative plant yield was best explained with a model that included the zones as dummy variables (Table 7 and APPENDIX A Table 19). Similarly, relative grain number was significantly reduced by the delay in emergence (Fig. 5 d, e, and f). In Springport the relationship was best explained with a simple model and the reduction in RGN was 2% per day of delay in emergence. In Portland and Parana, the model that included YSZs as dummy variables explained the best the reduction in RGN (Table 7 and APPENDIX A Table 19). In Springport, the relative crop yield relationship with emergence was best explained by a simple model, and the reduction was 3% per day of delay. In Portland and Parana, a model including YZS as dummy variables best explained the relationship with emergence, the reduction in RY were 7 and 5% per day of delay in the emergence in Portland, and Parana, respectively (Table 7 and APPENDIX Table 19). The effect of emergence delay on individual grain weight (APPENDIX A Table 19) was not significant ($P>0.05$).

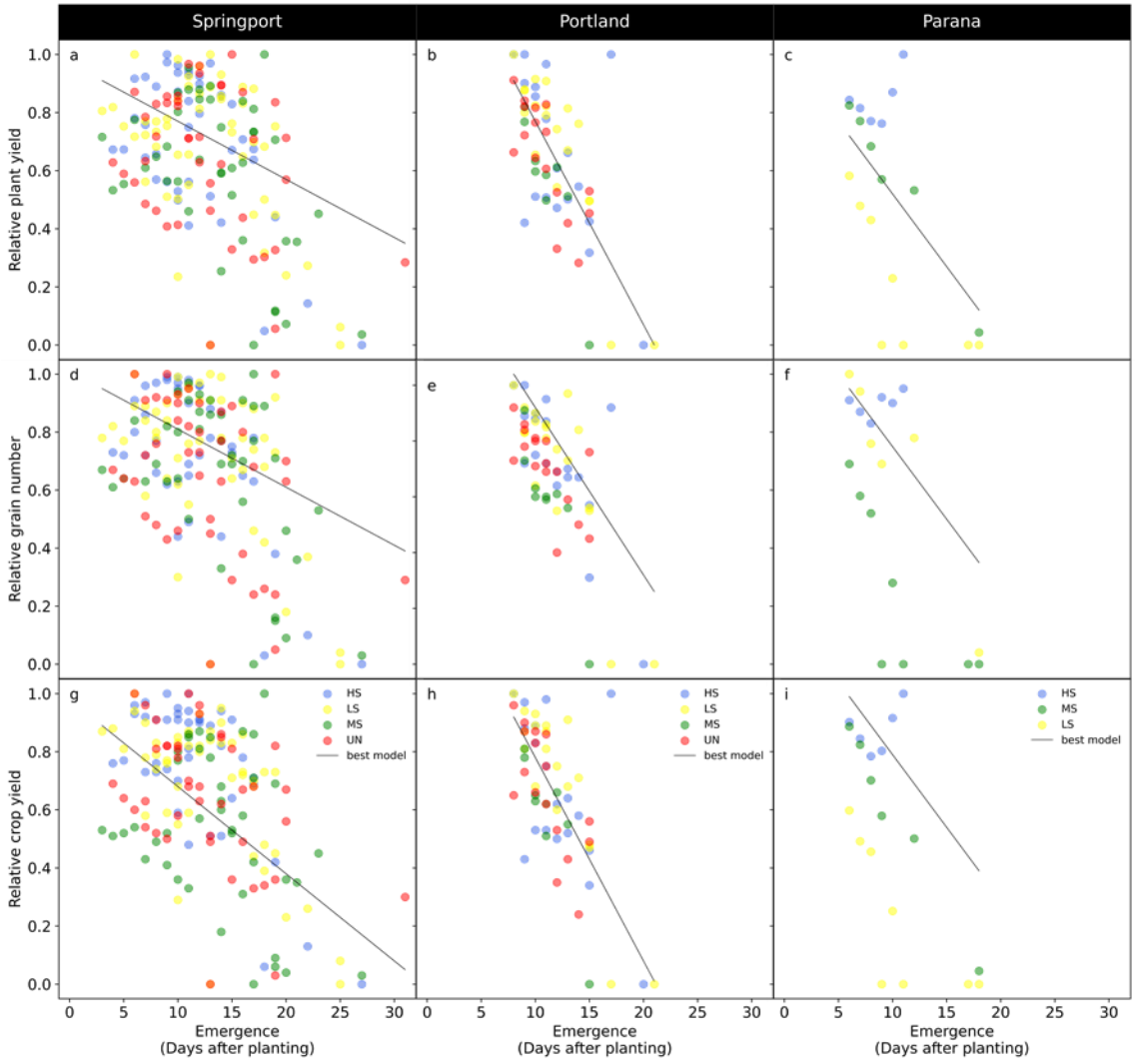

Figure 7. Relative plant individual yield (a, b, c), relative grain number (d, e, f) and relative crop yield (g, h, i) versus time to emergence (days after planting) by yield stability zone for Springport, Portland, and Parana across all seasons. Each point represents the mean value per emergence day in each plot. HS: High and stable, LS: Low and stable, MS: Medium and Stable, and UN: Unstable.

Table 7. Statistical correlation between emergence (days after planting) with relative plant individual yield (RPY), relative grain number (RGN), and relative yield (RY), for Springport, Portland, and Parana site locations across fields and seasons.

Site	Variable	Model	R^2	p
Springport	**Relative Plant yield**	RPY = 0.97 -0.02DAP	0.24	<0.0001
	Relative grain number	RGN = 1.01 -0.02DAP	0.25	<0.0001
	Relative crop yield	RY = 0.98 -0.03DAP	0.27	<0.0001
Portland	**Relative Plant yield**	RPY = 1.47 +0.04MS -0.15LS -0.08UN -0.07DAP	0.58	<0.0001
	Relative grain number	RGN = 1.52 -0.02MS -0.21LS -0.09UN -0.06DAP	0.63	<0.0001
	Relative crop yield	RY = 1.48 +0.05MS -0.14LS -0.06UN -0.07DAP	0.57	<0.0001
Parana	**Relative Plant yield**	RPY = 1.02 -0.32MS -0.20LS -0.04DAP	0.84	<0.0001
	Relative grain number	RGN = 1.25 -0.40MS -0.11LS -0.05DAP	0.83	<0.0001
	Relative crop yield	RY = 1.29 -0.21MS -0.54LS -0.05DAP	0.85	<0.0001

2.4.5. Impact of plant available growing space variation on plant yield, crop yield and yield components

Although some fields showed a significant effect of growing space on individual plant yield, grain number, grain weight, and crop yield (APPENDIX A Table 18), none of the regressions were significant (APPENDIX A Fig.24). Plant yield was significantly ($p<0.05$) affected by within row plant separation (uniform, skip or double) in field 2017- FJS1 in favor of plants classified as skips (Table 7), and in 2018-FNC12 in favor of plants classified as uniform. The grain number was significantly affected by the within row plant separation in two fields (2017-FJS1 and 2020-F308) where the plants located in skips produced more grains. The individual grain weight was affected by the distance between plants in field 2017-F222, where plants located in skips reached higher individual grain weight. Similarly, crop yield showed a significant variation with the variation in the distance between plants in the three fields (2016-F222, 2017- FJS1, and 2018-FNC12), and yield was higher in the uniform plants except in 2017-FJS1 where yield was higher in the skips (Table 7).

Table 8. Average plant yield (g plant^{-1}), grain number (grains plant^{-1}), grain weight (g grain^{-1}), crop yield (kg ha^{-1}), by plant spatial variability class (Uniform, Skip, and Double) at three locations (Springport, Portland, and Parana) across fields.

Location	Year-field	Plant yield† (g plant^{-1})			Grain number† (grain plant^{-1})			Grain weight† (g grain^{-1})			Yield† (kg ha^{-1})		
		Uniform	**Skip**	**Double**	**Uniform**	**Skip**	**Double**	**Uniform**	**Skip**	**Double**	**Uniform**	**Skip**	**Double**
Springport	**2016-F222**	155	148	156	501	484	507	0.313	0.307	0.312	11334a	9747b	11289ab
	2017-F222	127	131	109	447	441	405	0.282ab	0.292a	0.265b	11085	9894	9697
	2018-F105	141b	181a	---	494	552	----	0.290	0.328	-----	11614	13155	-----
	2019-F304	154	182	146	529	602	522	0.289	0.301	0.277	11408	13328	10896
	2020-F308	189	230	158	643b	734a	593b	0.294	0.314	0.265	10924	11915	9374
	2021-F210	126	142	145	503	546	546	0.256	0.266	0.264	8888	9831	10134
Portland	**2017-FJS1**	112b	137a	121ab	361b	430a	376ab	0.311	0.320	0.327	8230b	9737a	8949ab
	2018-FNC12	134a	103b	104ab	483	383	350	0.277	0.252	0.277	12491a	9307b	9837ab
	2019-FMG1	117	134	94	385	418	327	0.307	0.320	0.290	10004	11424	8230
Parana	**2020-F11**	96	93	73	403	391	320	0.240	0.239	0.225	6224	5942	4848

†Means not sharing the same letter within the same row are different ($p<0.05$) from each other. Uniform: plants with distances between 5cm and theoretical distance plus one standard deviation; Skip: plants located in gaps greater than theoretical distance plus one standard deviation, and Double: consecutive plants less than 5 cm from each other.

2.5. Discussion

The impacts of emergence time and spatial variability of within row planting are rarely studied outside the confines of small experimental research plots. In this study we worked almost exclusively on active, commercial farmer fields that experienced a range of management practices (e.g., seeding rate, soil type and conditions, cover crop, tillage, and crop hybrid) with single planting dates at each site to evaluate the spatial and temporal variation of corn emergence in the various sub-field yield stability zones. Our results showed that emergence delay has a greater impact than plant spatial variation on crop yield and its components, and in general the impact is larger in low yield stability zones. The greater impact in the low yield stability zones might be related to spatial variation in the conditions that promote emergence (Knappenberger & Köller, 2012) i.e., less plant available water and reduced soil fertility in the low yielding areas. It is noteworthy that the LS zones in Michigan sites were typically located in the header of the fields, where field operation transit is higher, likely leading to compaction and decreasing soil water retention. In Parana, the LS zone was in a severely eroded area that retains less water and has lower fertility.

In our study, emergence across years and fields varied between 3 and 31 DAP, a broader range than reported by Nemergut et al. (2021), who evaluated in-field corn emergence in different soils and at different planting depths and reported emergence between 4 and 13 DAP. This narrower emergence range may be related to their observation period – results were reported over 14 consecutive DAP, so later emerging plants were not included in the analysis. Overall, emergence time variation was higher in Springport than in Portland and Parana (Fig.5a-f). The difference in emergence between the Michigan sites might be explained by different tillage practices adopted; Springport fields were under no-till with cover crops in some years,

which may have resulted in colder and wetter soils than in Portland where conventional tillage was used. Differences in surface residue cover related to tillage systems have been shown to affect soil temperature and consequently corn emergence (Gupta, 1985). Even though the Parana field was under no-till, there was a higher uniformity in emergence time when compared with Springport and Portland. This could be related to the higher mean temperature at the Parana site along with the later planting date that can lead to higher soil and near soil surface air temperatures, major factors known to affect emergence (Knappenberger & Köller, 2012). Planting speed is an important contributing factor to plant emergence time and one that farmers can directly control. Planting speed is related to the depth that the seed is placed; greater speeds increase the variability in the seed depth placement, which in turn increases the variation in timing of plant emergence (Nielsen, 1993). Seeds planted in a shallower position with enough water and appropriate temperature for emergence will do so faster than seeds planted deeper. However, seeds that are planted at shallower depths and that do not have good soil-seed contact, or where the soil is dry (Cox & Cherney, 2015), will not emerge, leading to a greater stand variability with more exposure to bird and other animal predation.

Our results showed a significant negative effect of the increasing delay of emergence on relative individual plant yield, relative grain number and relative crop yield ($p<0.05$, Fig.5). Although the degree of decrease per day of delay in the emergence (slopes) of the relationships for the variables (relative plant yield, relative grain number, and relative yield) and emergence did not significantly differ among YSZ, in Portland and Parana the models that best explained the relationship between the variables and emergence, included the YSZ as dummy variables (Table 7) generally penalizing LS zones. This penalization in relative yield and yield components of emergence delay likely caused a higher impact in the LS zone than in the other yield zones.

Consequently, by considering variable rate seeding based on YSZs, farmers have the opportunity to reduce their seeding rate in the LS zones, thereby reducing seed cost, a major portion of total planting costs. For each day of delay in emergence, individual plant yield was reduced on average by 7%, a similar magnitude to those found by Andrade & Abbate (2005), (Liu et al., 2004b), and (Nafziger et al., 1991). Emergence delay appears to promote the formation of plant 'health' hierarchies, where plants that emerge earlier have an advantage in that they have access to more readily available resources and can uptake their requirement, when compared to plants that emerge later that may not (Carter et al., 1990).

A significant reduction was found in the number of grains per plant (Fig. 5d, e, and f, Table 6), whereas the effect on grain weight per plant was less consistent (APPENDIX A Table 18). This result is similar to Pommel et al. (2002), who evaluated heterogeneity in three emergence treatments (normal, late, and delayed) and found a more frequent negative effect of treatment on grain number than on individual grain weight as emergence time increased. When corn planting date is delayed, grain number is reduced due to a limitation in the availability of assimilates during grain filling (Bonelli et al., 2016); corn plants that emerge late experience this source limitation and a higher resource competition from the early emerged plants. Additionally, as the late emerged plants will have a phenological delay, postharvest damage and costs might increase due to grains from late emerging plants that will have higher grain moisture content at harvest.

Although the individual grain weight was generally not significantly affected by the emergence delay (APPENDIX A Table 18), the reduction in the grain number was sufficient alone to significantly reduce the final crop yield, with reductions ranging from 416 to 903 kg ha^{-1} per day of delay (3-14% decrease), higher than the 293 kg ha^{-1} reduction in yield per day of

delay reported by Liu et al. (2004a) and the 122 kg ha^{-1} per day found by Rutto et al. (2014). Differences probably related to the methodology; these authors used manipulative treatments to achieve the delayed emergence (i.e., planting at different dates) in contrast with our experiments where the natural variation of emergence was captured. The temporal variability in emergence affects resource capture and utilization by the plants, causing a decrease in grain yield through a reduction in harvest index (Tollenaar et al., 2006).

The plant available growing space varied between site location (Table 4), an expected outcome due to the differences in plant density and row spacing between the fields (Table 1). We found that the plant spatial variability differs with YSZ in three of the ten fields, and in general plants in the low stable YSZ had a larger available space than in the other YSZs. This can be related to a higher percentage of skips in the low stable yielding zones. Although the GS had a significant effect in some fields, there was no significant relationship between growing space and yield and yield components (APPENDIX A Table 18). Tollenaar et al. (2006) demonstrated that plants located next to a gap (i.e., a 'missing' plant) increased their yield, but that this is insufficient to compensate for the gap. However, Liu et al. (2004b) does not cause plant competition, a range that includes the standard deviation in our experiments (6 to 10 cm).

The availability of precision planting equipment has allowed producers to reduce the variability within the row and obtain a more consistent distance between the plants, as demonstrated by the small percentage of skips and doubles found in our fields (Fig 3), where for example, the pneumatic planter used in Parana – specially developed for the no-tillage system – will likely have contributed to a more uniform stand. Shuai et al. (2019) analyzed corn stand heterogeneity using unmanned aerial vehicles (UAVs) across YSZs and concluded that variability in plant spacing across YSZs was not a major cause of yield variability. This result

agrees with other studies that found that plants can partially compensate for grain yield penalties due to greater plant spatial variability if the plant density is adequate (Lauer & Rankin, 2004), which is likely the case in our experiments where fields are managed by their owners who have optimized the inputs.

Variation in plant emergence time has a stronger effect than variation of within-row plant spacing (APPENDIX A Table 18), agreeing with previous studies (Lauer & Rankin, 2004; Liu et al., 2004a; Pommel et al., 2002a), and likely related to lower overall spatial variability when compared to temporal variability. In addition, the plants may have compensated for within row variations (i.e., missing plants or doubles), but were unable to do so for temporal variations where plant hierarchies developed due to resource availability and capture.

2.6. Conclusions

Temporal variability of crop emergence has a larger impact than within-row plant spatial variability on final crop yield and its components. The delay in emergence causes a decrease in maize total yield and yield components that was not statistically related to yield stability zone type but was more prevalent in low yield stability zones. The reduction in total crop yield could be explained by the reduction in the grain number per plant.

Our findings can be incorporated into crop models that currently do not consider naturally occurring emergence variation, but rather assume uniform emergence that might lead to yield overestimation. Future work is needed to incorporate the relationship of emergence delay with plant individual yield, grain number and grain yield into crop models to improve model accuracy.

2.7. Acknowledgements

The authors wish to thank Rich Price, Ruben Ulbrich, Lydia Price, and Neville Millar for their valuable support in field activities, data processing and comments on the manuscript. The authors are grateful to the funding provided by the US Department of Agriculture National Institute of Food and Agriculture: 2020-67021-32799, 2015-68007-23133, and Natural Resource Conservation Service award numbers NR213A750013G001 and MSU AgBioResearch.

CHAPTER 3: EMERGENCE DELAY REDUCES MAIZE (*Zea mays* L.) NITROGEN UPTAKE AND USE EFFICIENCY

3.1. Abstract

Spatial and temporal variability in plant emergence may cause differences in N uptake by crops at field scale leading to a mismatch between plants requirements and nitrogen supply with negative environmental and economic impacts. We aimed to understand nitrogen uptake and concentration in unevenly emerged plants. We conducted four experiments in farmers' fields with available data to determine yield stability zones (YSZ) and found that emergence ranged from 64 and 124.1 °C day^{-1}, with significant variability between zones in three out of four fields. Plant biomass at R6 ranged from 54 to 736 g $plant^{-1}$ and was significantly affected by YSZ ($p<0.05$), with a decrease in biomass variation from V6 to R1. We observed a curvilinear relationship between plant growth rate around R1 and grain number per plant, and a threshold in emergence (76°C day^{-1}) beyond which plant growth rate was negatively impacted, resulting in lower yield. Late-emerging plants accumulated less nitrogen than early emerged plants and the plant nitrogen partition changed with the delay. Nitrogen concentration in the grains was not affected by the delay, whereas the concentration of nitrogen in biomass increased, related to a lower total biomass and a lack of sink (i.e. less grains per plant). The number of grains set by the plants was reduced due to a decreased plant growth rate during the period around R1. Understanding the impact of spatial and temporal variability in plants N uptake is important to improve nitrogen prescriptions, nitrogen use efficiency and reduce environmental losses.

3.2. Introduction

Nitrogen (N) is one of the most worldwide limiting factors in crop production (Andrade et al., 1996;Cassman & Dobermann, 2022). Over the past decades, the continuous increase in

maize yield has been mainly linked to an increase of mineral fertilizers utilization (Lemaire & Gastal, 2019) leading to serious environmental impacts (Vitousek et al., 2009). The application of uniform N rates, where requirements and nutrient availability varies spatially, generates mismatches between the supply and demand (Huggins & Pan, 1993). Nitrogen variable rates have been developed to match crop needs with fertilizer supply and prevent these consequences (Cassman & Dobermann, 2022). Although variable N rate considers spatial variability in crop demand and soil availability, it does not consider the temporal variability that exists in maize crop stands caused by uneven plant emergence. Uneven emergence can generate a variability in crop N demand and increase the disparity between plant requirements and nitrogen supply with the known negative impact for the environment and farmers' profit.

Soil N availability during the maize growing season varies according to the initial content of N in the soil, fertilization supply, and mineralization during the growing season. It has been reported that over 60% of soil-applied fertilizer-N can be lost (Kant et al., 2011; Raun & Johnson, 1999), and these losses are due to a combination of volatilization, denitrification, runoff, leaching, and consumption by microorganisms (i.e. immobilization). Crop yield is highly related with the N status at silking (R1), since close to 60% of the nitrogen that a maize crop needs is taken up during the pre-flowering period (Ciampitti & Vyn, 2013; Lemaire & Gastal, 2019). Past studies evaluating N uptake in uneven plant stands reported differences in nitrogen uptake and use efficiency in plants that develop size hierarchies and compete differently for the use of resources (Caviglia & Melchiori, 2011; Mayer et al., 2012; Rossini et al., 2012, 2018). Under uneven crop stands, nitrogen is allocated preferentially to dominant plants and the lack of light interferes in the response of N supply of dominated plants (Lemaire and Gastal, 2019). A reported response of maize to the presence of neighbors is a change in the biomass partitioning

(Kasperbauer & Karlen, 1994) and shoot elongation (Maddonni et al., 2002). This reduction in assimilate allocation to roots might impact the dominated plants' competitive capabilities of resources capture from the soil. However, in areas of low resources availability dominant plants might develop larger root systems that allows them to reach more resources compared with dominated plants (Boomsma et al., 2009). Indeed, plants that compete for light also compete for nutrients (specifically nitrogen uptake). Moreover, the competition has been suggested as symmetric (Maltese et al., 2023), i.e. larger plants tend to capture more light and nutrients than smaller ones (Casper & Jackson, 1997).

Studies evaluating plant-to-plant variability have shown that dominant plants outyield dominated plants, but the higher yield of the dominant plants does not compensate for the lower yield of dominated plants and the overall yield in a heterogeneous crop stand is reduced (Novak & Ransom, 2018; Parra et al., 2022). One of the causes of heterogeneous crop stand is the variability in crop emergence usually associated with soil moisture and temperature spatial variability. Effects of temporal variability (uneven emergence) have been widely studied (Andrade & Abbate, 2005; Carter et al., 1990; Carter et al., 2019; Liu et al., 2004; Tollenaar & Wu, 1999) but there is still a gap in knowledge of the impact of emergence delay on N uptake and use efficiency. Between 10 and 22% of yield reduction when emergence is delayed 21 days (Carter et al., 1990), and 5.25% reduction in per-plant yield per day of delay (Nemergut et al., 2021) were reported impacts of emergence delays. Unlike the impact of emergence on yield, the impact of uneven emergence on N uptake has been less explored. The heterogeneity in N capture and use efficiency may contribute to a mismatch between N supply and N consumption, contributing to increased environmental risk, reduced N use efficiency, and decreased farmer’s profit. It is important to understand if plant N uptake is affected by the delay in emergence and if

the effect of the delay is related to the spatial variability in the fields, as well as to learn if plant hierarchies (dominant and dominated) are related to emergence delay. Our hypothesis is that plants that emerge late accumulate less nitrogen than early emerged plants and the nitrogen partitioning in the plant changes with the delay. Thus, the objectives of this research were to i) evaluate the biomass accumulation and variation in maize plants with temporal variability in emergence within yield stability zones, and ii) evaluate the nitrogen concentration, N uptake and N use efficiency in plant hierarchies with temporal emergence variability in four commercial fields.

3.3. Methods

3.3.1. Field experiments and Yield stability zones

Field experiments were conducted in four corn commercial fields, located in Springport (MI) (42.3471°N, 84.7097°W), and in Portland (MI) (42.8971°N, 84.9776°W). Fields varied in soils and management practices, such as tillage system, row spacing, hybrid relative maturity, and planting date. Fields in Springport were planted with a White planter 9924VE, and a John Deere 1770 NT was used in Portland field. N fertilizer (46− 0− 0) was applied at planting and side dressed around V6 (V6 stage; Ritchie et al., 1997) (Table 1).

Yield stability zones (YSZ) were delineated from several years of yield monitor data collected from farmers in each studied field (Basso et al., 2007; Maestrini & Basso, 2018; Maestrini & Basso, 2021). Briefly, standardized yield maps were used to calculate the mean (μ) and standard deviation (σ) of the yield for every pixel of the field, considering a pixel as stable when $\sigma < 0.75$ and as unstable when $\sigma \geq 0.75$. Similarly, pixels with $\mu < 0$ were classified as low-yielding and high-yielding when $\mu \geq 0$. This methodology classifies field pixels as High Stable (HS, consistently higher than the average), Low Stable (LS, consistently lower than the

average), Medium Stable (MS, consistently average) and Unstable (UN, yields fluctuate, high some years and low in others).

The experiments consisted of five meters by two-row plots with three replicates in each yield stability zone (YSZ) established shortly after corn planting (one to two days after planting). Plots from all the experiments were outlined by orange marking stakes, and the plot size allowed for a maximum of up to 60 plants per plot (1648 total for the four fields). Emergence (DAP, days after planting) was recorded by visiting each plot from each field once a day during the period of emergence. Each emerged plant was individually labeled using white stakes marked with the day of emergence, and phenology was recorded bi-weekly on each tagged plant using the (Ritchie et al., 1986) scale. At the end of the growing season tagged plants were individually harvested to determine the individual plant yield and grain number. Individual plant biomass at R6 was weighed wet and ground using a woodchipper, and a subsample was weighed before and after forced air oven drying (60°C) to get whole plant dry weight.

For each Year-field, plants were classified as Early, when the emergence was ranked in the lowermost 33% of the data, Medium when they were within 34 and 66%, and Late, when they were within the uppermost 33% of the data set.

3.3.2. In season plant biomass

Plant biomass was estimated in three maize growing stages, V6, V14, and R1 (Ritchie et al., 1986) using allometric models such as in Maddonni & Otegui (2004). For this intent, plant height (H) from the ground to the ligule of the last fully expanded leaf, and stem diameter (D) at the base of the stalk from every tagged plant in every plot from every experiment (total of 1648 plants) were measured. Between twenty and thirty plants per field (total of 360 plants) were harvested at every sampling stage (V6, V14, R1) and used to calibrate (280 plants) and validate

(82 plants) the allometric models. Harvested plants were also measured and oven dried at 70°C until constant weight to determine observed total plant biomass. The relationship between morphometric variables (H and D) and plant biomass was evaluated through regression models. Although, there were not significant differences in slopes and intercepts among models per stage, a single model per stage was used to describe biomass in all the evaluated fields (Table 2) since the lower RMSE (Equation 2) and RRMSE (Equation 3) compared with a general model to estimate biomass at all the stages.

$$RMSE = \sqrt{\frac{\sum_{i=1}^{n}(E_i - O_i)^2}{n}} \quad \text{Equation 2}$$

$$RRMSE = \frac{RMSE}{\frac{1}{n}\sum_{i=1}^{n} O_i} \quad \text{Equation 3}$$

where E_i is the estimated plant emergence (°C day^{-1}), O_i is the observed emergence, n is the total number of observations, and i is the ith observation.

For each Year-field and YSZ, plants were classified in hierarchies according to its estimated plant biomass at V6 (Pagano & Maddonni, 2007). Plants were considered dominated when they were ranked in the lowermost 33%, dominant when they were in the uppermost 33%, and Uniform when their biomass was within the lowermost and uppermost 33%.

.

Table 9. Soil classification and management practices at Springport, MI and Portland, MI experimental sites, 2019-2021.

Site	Year-Field	Predominant Soil Taxonomic class	Tillage System*	Row spacing (cm)	Relative Maturity	Planting Date	Seeding rate (seeds ha^{-1})	N fertilizer (kg ha^{-1})	Side-dress date
Springport	2019-304	Very-fine, mixed, active, frigid Aquic Glossudalfs	NT	76.2	95	8-Jun	74132	184	30-Jul
	2020-308	Very-fine, mixed, active, frigid Aquic Glossudalfs	NT	76.2	102	11-May	74132	192	21-Jul
	2021-210	Very-fine, mixed, active, frigid Aquic Glossudalfs	NT	76.2	95	15-May	74132	192	28-Jul
Portland	2019-MG1	Fine, mixed, active, mesic Haplic Glossudalfs	Conv	50.8	104	8-Jun	93900	186	11-Jul

*NT: No-till, Conv: conventional

Table 10. Allometric model parameters and model validation statistics for the estimation of plant biomass (g plant^{-1}) at V6, V14, and R1 crop growth stages at Springport, MI and Portland, MI experimental sites, 2019-2021.

Model	Stage	Model parameters		n	adj R^2	RMSE (g plant^{-1})	RRMSE (%)
		a	b				
By stage	V6	0.172	0.09	90	0.88	1.2	24
	V14	0.261	0.28	90	0.85	11.5	18
	R1	0.272	4.03	100	0.88	24.0	24
General	Overall	0.272	-1.20	280	0.93	14.1	30

3.3.3. Plant Nitrogen uptake

At harvest, ten (2019) or six (2020 and 2021) consecutive plants per plot (345 plants total) were selected from every plot trying to represent each emergence variability class, the grain and biomass were ground individually to analyze the nitrogen content per plant (%Ng and %Nb, nitrogen concentration in the grains and in the biomass, respectively) via dry combustion on a Perkin Elmer TN 2410. Total N uptake by the plants ($N_{up}t$) at maturity (R6) was calculated as the sum of the N uptake in the grain ($N_{up}g$) and the N uptake in the biomass ($N_{up}b$). The N uptake in the biomass and the grain was obtained by the product of the biomass (or grain) and its %N. Biomass, grain yield and N uptake were expressed in grams per plant.

3.3.4. Calculations

Thermal time was computed for emergence (GDD_E, °C day^{-1}) as:

$$GDD_E\ (°C\ day^{-1}) = \sum_{planting}^{emergence} (Tm - Tb)$$

where Tm is the daily mean temperature and Tb is maize base temperature (Tb 10°C).

Plant growth rate (PGR) was estimated as the weight difference between consecutive samplings expressed as a function of chronological days (g $plant^{-1}$ day^{-1}).

Nitrogen use efficiency was calculated as the ratio between N uptake in the grain and the biomass (NUEg and NUEb) and N applied, and N fertilizer efficiency as the ratio between yield (grain and biomass) (N_fUEg and N_fUEb) and N applied. Nitrogen harvest index (NHI) was computed as the ratio between N uptake in the grains and total N uptake (Rossini et al., 2018). All the variables were calculated at the plant level.

3.3.5. Weather conditions

The study areas are characterized as Cold, without dry season, hot summer (Dfb) with an average daily temperature of 7.9°C and rain totals averaging 880-910 mm annually. Rainfall during the growing season was closer (90 to 110%) to the average (1991-2020) for the same period in the evaluated fields. Temperatures were slightly higher than historical averages in Springport fields, while they were within the range of historical values for Portland. The average temperature during the emergence period (May-June) ranged from 14 to 22°C in Springport (Fig.8a, c, and d), around 14% higher than the 30 yr average for the same period. In contrast, temperatures in Portland (Fig.8b) were 16% higher than average in May but 7% lower in June.

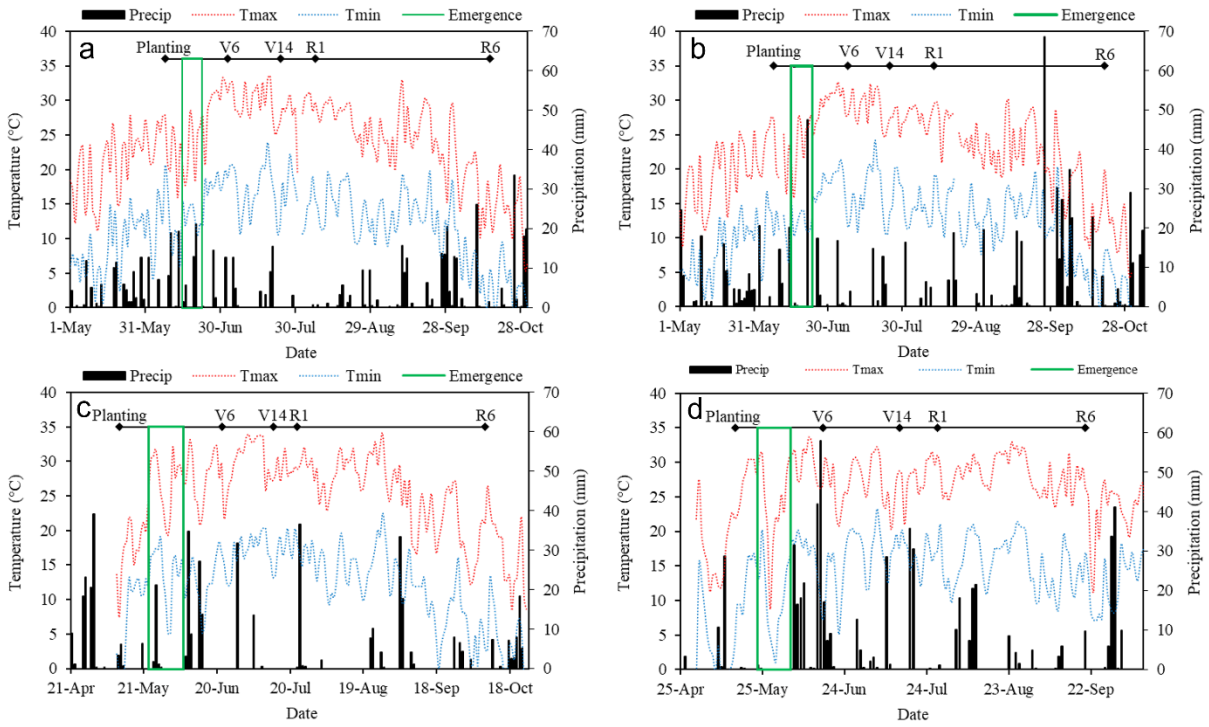

Figure 8. Daily precipitation (mm), and maximum, mean, and minimum temperatures (°C) at Springport, MI (42.3471°N, 84.7097°W) and Portland, MI sites (42.8971°N, 84.9776°W) for a) 2019-F304, b) 2019-FMG1, c) 2020-F308, and d) 2021-210.

3.3.6. Data analysis

Data was analyzed using the GLIMMIX procedure in SAS version 9.4 (SAS Inst., Inc.) to determine the yield stability zone effect, considering emergence (DAP) days after planting as a covariate. Individual plants variables were nested within each plot and included as a random factor to identify them as subsamples. Mean separation between groups was analyzed using Tukey's method, performing pairwise comparisons to identify differences greater than the expected standard error. Plant biomass was analyzed considering crop growth stage as a repeated measure.

Regression analysis was performed using the JMP® Pro Version 15.2.0 (SAS Institute Inc., Cary, NC, 1989–2021) to determine relationships between plant yield, grain number, plant biomass, $N_{up}t$, $N_{up}g$, $N_{up}b$, and crop yield with emergence (GDD_E, °C day^{-1}). Sigmoid functions (Gompertz equation, best fit) were fitted between plant biomass and thermal time. A non-linear model was fitted to plant grain number vs PGR. Models were fitted by Year-Field and yield stability zone, when models did not differ ($p>0.05$) among Year-Field, a single model was fitted to the whole dataset. Bi-linear models were fitted to evaluate the relationship of PGR, GN and NHI with emergence in thermal time (GDD_E, °C day^{-1}), using piecewise-regression in Python (Pilgrim, 2021).

3.4. Results

3.4.1. Emergence, plant biomass, and plant yield

Emergence ranged from 8 to 14.7 days after planting (64 and 124.1 °C day^{-1}). The emergence range was highest in field 2021-210 (9 to 27 DAP, and 87.8 to 259.8 °C day^{-1}), and narrower in 2019-MG1 (8 to 17 DAP, and 61 to 135.8 °C day^{-1}). All yield stability zones (YSZ)

showed variability in emergence (Table 11, variation coefficient in brackets) and emergence was significantly affected by YSZ in 3 out of 4 field site years ($p<0.05$) (Table 11).

Table 11. Maize average emergence in days after planting and thermal time (°C day^{-1}), from four year-fields by yield stability zone (YSZ). Variation coefficient in brackets.

Year-Field	YSZ	Emergence- in days after planting (DAP)†			
	P-value	HS	LS	MS	UN
2019-F304	0.3244	8.1 (8)	----	8.2 (8)	8.2 (12)
2020-F308	<.0001	14.4b (10)	14.7a (9)	14.7a (9)	14.7ab (15)
2021-F210	<.0001	10.8b (17)	13.2a (26)	11.2b (22)	10.5b (9)
2019-FMG1	<.0001	8.9c (10)	9.8b (6)	11.4a (16)	9.4b (6)
Year-Field	**YSZ *P*-value**	**Emergence- in thermal time (GDD_E, °C day^{-1})†**			
2019-F304	0.8607	73.2 (7)	----	73.5 (7)	73.4 (11)
2020-F308	<.0001	84.3b (23)	93.7a (17)	92.4a (21)	89.1ab (20)
2021-F210	<.0001	109.4b (16)	124.1a (18)	110.3b (17)	105.1b (13)
2019-FMG1	<.0001	64.0b (7)	67.3b (6)	87.0a (21)	66.1b (11)

†Means not sharing the same letter within the same row are different ($p<.05$) from each other. HS: High and stable, LS: Low and stable, MS: Medium and stable, and UN: Unstable.

Plant biomass ranged from 54 to 736 g plant^{-1} at R6 and was significantly affected by YSZ ($p<0.05$) (Fig.9). In general, higher biomass was accumulated in the HS YSZ, except in 2021-F210 where final biomass did not differ among YSZs (Fig.9d). There were no differences among YSZs in early stages and R1, except in 2019-FMG1, where accumulated biomass at R1 significantly differed among YSZ (Fig.9b).

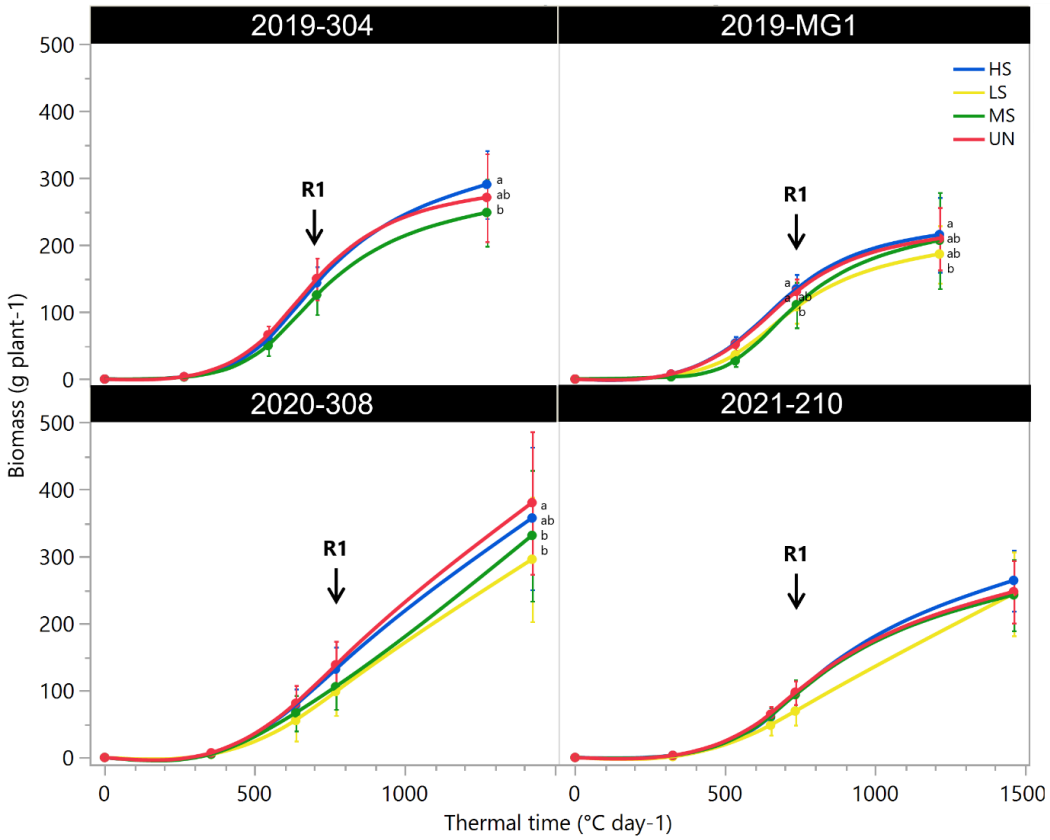

Figure 9. Maize plant biomass accumulation at Springport, MI (42.3471°N, 84.7097°W) and Portland, MI sites (42.8971°N, 84.9776°W) for a) 2019-F304, b) 2019-FMG1, c) 2020-F308, and d) 2021-FF10 seasons and fields for High stable (HS), Low stable (LS), Medium stable (MS), and Unstable (UN) yield stability zones. Bars represent one standard deviation.

A decrease in the plant-to-plant variability in the biomass was associated with the progression in the growing season (i.e. higher CV in early stages). For all fields, plant biomass CV decreased from V6 (20-60%) to R1 (14-34%) (Fig.10) and remained similar until R6. In general, high yielding zones (HS) had consistently lower CVs compared to low, medium, and unstable yielding zones (LS, MS, UN, respectively). Even though no significant differences ($p>0.05$) among YSZ were found in Field 2019-F304, HS zone had a lower CV during all the evaluated stages (V6, V14, R1, and R6). Field 2019-MG1 showed significant differences ($p<0.05$) among YSZ in plant-to-plant variability at V6, as the HS zone had a CV of 18% and the other zones had 37% variation. The variation decreased as the season progressed, and by R6 there were no significant differences among YSZ. Field 2020-F308 (Fig.10), had the highest variability in plant biomass, with non-significant ($p>0.05$) YSZ differences. However, the plant biomass CV in the HS zone was always lower compared to the others YSZs. In 2021 (Fig.10), plant biomass variability was significantly affected by the YSZ at V6 and R6, and the LS zone had a consistently higher CV (58%) compared with the other zones.

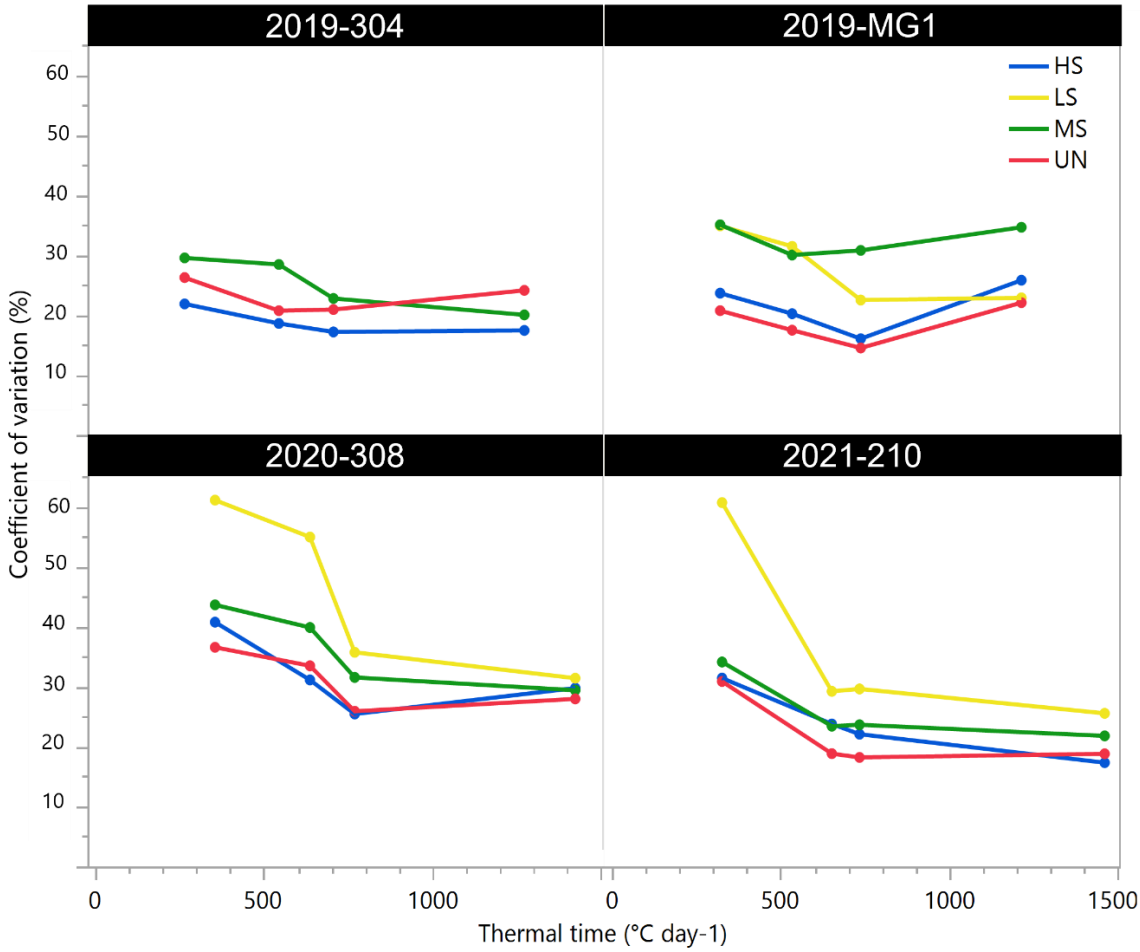

Figure 10. Coefficient of variation of maize plant biomass (CV) as function of thermal time at Springport, MI (42.3471°N, 84.7097°W) and Portland, MI sites (42.8971°N, 84.9776°W) for a) 2019-F304, b) 2019-FMG1, c) 2020-F308, and d) 2021-FF10 seasons and fields for High stable (HS), Low stable (LS), Medium stable (MS), and Unstable (UN) yield stability zones.

Plants in each hierarchy segregated into the emergence classes (early, medium, late) in different proportions in every Year-Field (Fig.11). Dominant plants in 2019-304 and 2019-MG1 were mainly late (42-45%) and medium plants (33-42%), whereas early emerged plants represented a smaller proportion (13-25). In contrast, in 2020-F308 and 2021-F210, dominant plants were mainly early plants (60-64%), followed by medium (28-35%) and a small percentage of late (5-8%) emerged plants. The proportion of emergence classes in the dominated plants was similar in 2019-F304 and 2020-F308, where 21% of the dominated plants emerged Early, between 31 and 43% late, and between 36 and 49% medium. In 2019-FMG1 and 2021-F210,

dominated plants were in majority (90-97%) late and medium emerged plants, with a small proportion of early plants (3-10%).

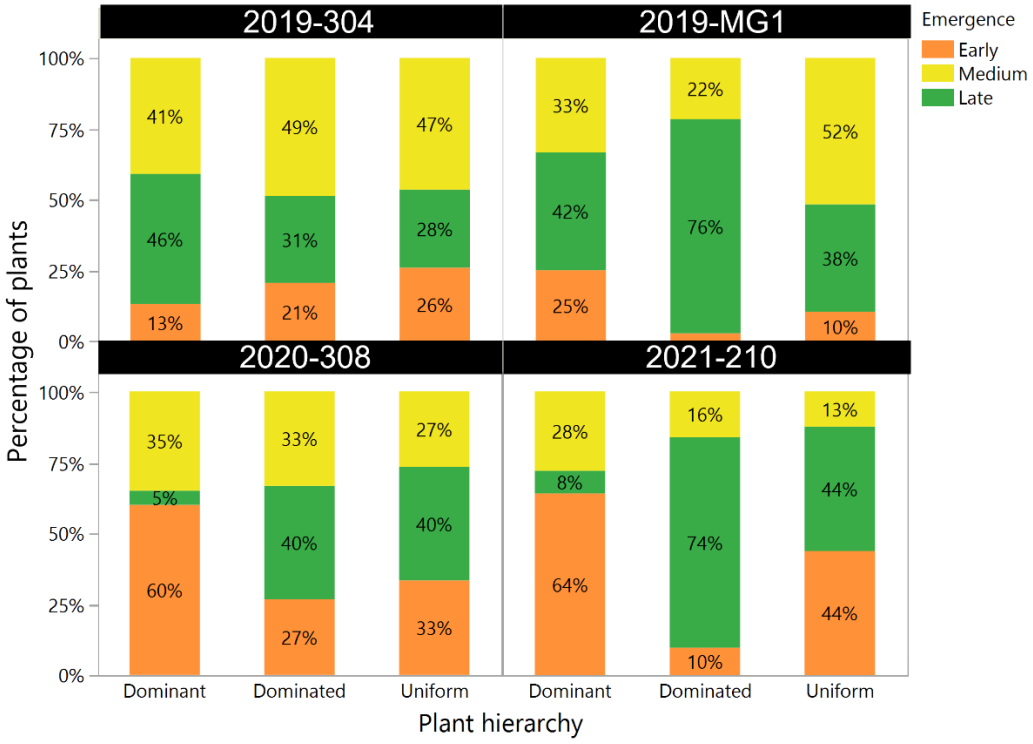

Figure 11. Percentage (%) of plants in each emergence class (Early, Late, and Medium) and plant hierarchy (Dominant, Dominated, and Uniform) at Springport, MI (42.3471°N, 84.7097°W) and Portland, MI sites (42.8971°N, 84.9776°W) for 2019-F304, 2019-FMG1, 2020-F308, and 2021-F210 season field combinations.

Average individual plant yield (Table 12) ranged from 82 to 217 g plant^{-1}. Fields in 2019 showed significant differences between YSZ, with the highest plant yield in the HS zone. In 2020 and 2021plant yield did not significantly differ among YSZ. Field 2019-F304 and 2020-F308 showed a small variation in emergence, compared with Field 2019-FMG1 and 2021-F210 where emergence had a higher variation (Fig.12). In general, plant yield decreased with the delay in the emergence. In Fig.12a, plants that were in gaps (i.a. 2020-F308) reached higher individual yields compared with those that were evenly distributed within the row; also, plants that emerged late next to plants emerged earlier, had lower yields.

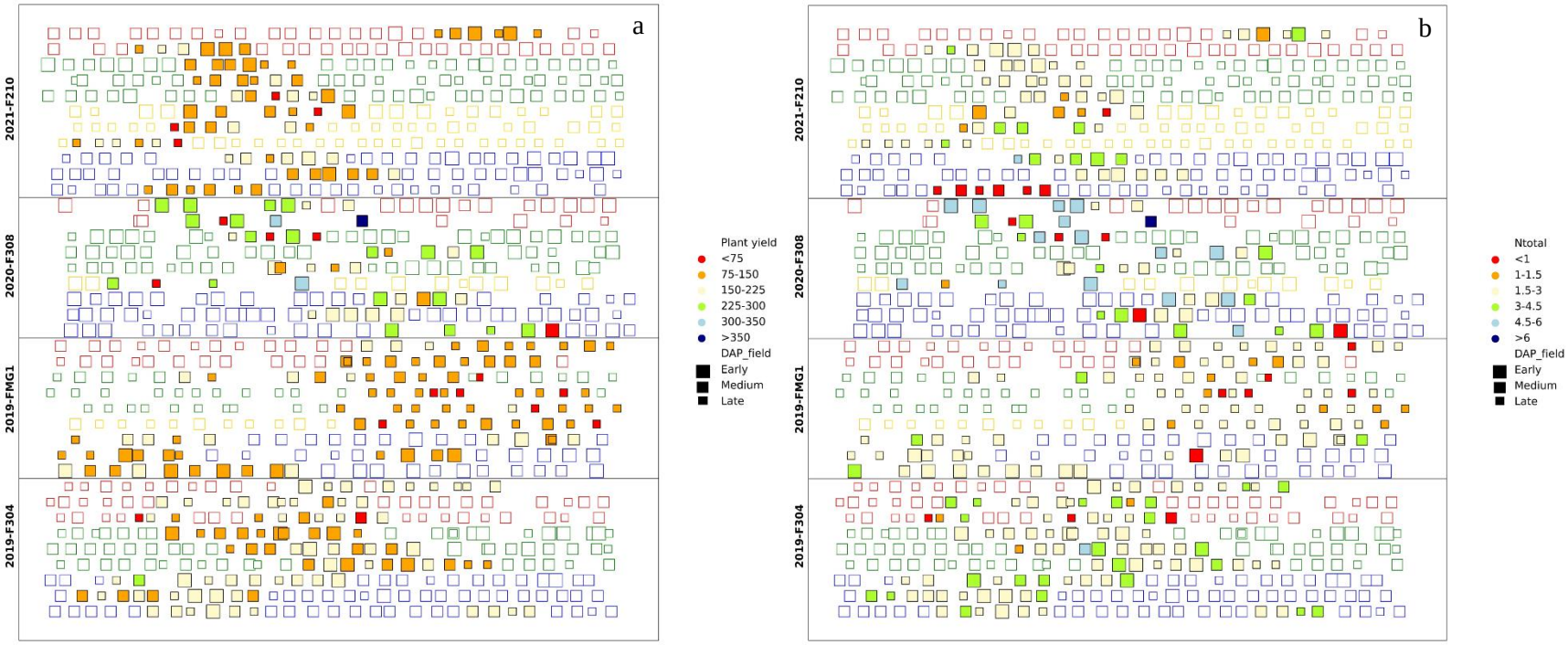

Figure 12. Yield plant-to-plant variability (g plant^{-1}) (a) and total N uptake plant-to-plant variability (g N plant^{-1}) (b) for sampled plants. The scheme denotes the distribution of the plants within the 5 m row (distance between the squares represent the distance between plants within the row in the field) for the 4 evaluated fields, 2019-F304, 2019-FMG1, 2020-F308, and 2021-F210. Filled squares represent each sampled plant, the size of the square refers to the emergence category (early, medium, late). Empty squares denote plants that were not selected for nitrogen analysis but were monitored during the growing season to estimate biomass. Edge color denotes High stable (blue), Low stable (yellow), Medium stable (green), and Unstable (red) yield stability zones.

3.4.2. Nitrogen concentration, Nitrogen uptake, and Nitrogen use efficiency

Nitrogen concentration in the grain (%Ng) was significantly affected by YSZ in 2021-F210, while nitrogen concentration in the biomass (%Nb) showed a significant effect of YSZ in 2020-F308 and 2021-F210 (Table 12). Overall, %Ng ranged from 1.0 to 1.33%, and when affected by YSZ it was higher in the HS and lower in the LS zone. The %Nb had a wider range (0.53- 1.2%) than %Ng, showing higher values in HS and UN zone compared with MS and LS zones, when significantly affected by YSZ.

Plant nitrogen uptake in the grains ($N_{up}g$) was significantly affected by YSZ in 2019-304, 2021-F210 and 2019-FMG1 fields. Plants took up less nitrogen in YSZ with less yield potential (LS<MS<UN <HS). Field 2020-308 showed higher nitrogen uptake in the grains compared with the other fields (Table 12). Plant nitrogen uptake in the biomass ($N_{up}b$) was significantly affected by the YSZ in 2019-F304. There was greater uptake in the HS and UN zones, higher N uptake than the LS zone. The total plant nitrogen uptake ($N_{up}t$) was affected by YSZ in 2019-F304, as $N_{up}t$ was higher in the HS zone (Table 12). In general, plants located in gaps took up more nitrogen than those placed in evenly distributed rows (Fig.12b).

NUEg ranged from 0.41 to 0.81, showing significant differences among YSZ in 2019-F304 and 2021-F210, and HS showed higher efficiency compared to the other zones. The NUEb did not show a YSZ significant effect and ranged from 0.14 to 0.44. The fertilizer efficiency ranged between 26 and 69 g grain g N^{-1}, showing a significant effect of YSZ in three fields (Table 12). In 2019-F304 the plants in the HS reached higher NUEfg, in 2019-MG1, the LS NUEfg was 30% lower than the other zones fertilizer efficiency, and in field 2021-210 the LS and UN reached similar efficiency. The NUEfb ranged between 20 and 51 g biomass g N^{-1}, and it was significantly affected by the YSZ in 2019-F304, 2019-FMG1, and 2021-F210, being in

general less efficient in the use of the fertilizer in the MS, UN and LS, in 2019-F304, 2019-FMG1, and 2021-F210, respectively (Table 12).

Table 12. Average plant yield, nitrogen concentration in the grains (Ng), nitrogen concentration in the biomass (Nb), N uptake in the grains (Nupg), N uptake in the biomass (Nupb), total nitrogen uptake (Nupt), nitrogen use efficiency in the grains (NUEg), nitrogen use efficiency in the biomass (NUEb), nitrogen fertilizer efficiency in the grains (NfUEg), nitrogen fertilizer efficiency in the biomass (NfUEb) at R6 growth stage at Springport, MI (42.3471°N, 84.7097°W) and Portland, MI sites (42.8971°N, 84.9776°W) for 2019-F304, 2019-FMG1, 2020-F308, and 2021-F210 season field combinations.

Year-Field	YSZ	Plant yield	N concentration		Plant N uptake (g N plant^{-1})			NUEg	NUEb	NUEfg (g grain g N^{-1})	NUEfb (g biomass g N^{-1})
		(g plant^{-1})	Grain (%)	Biomass (%)	$N_{up}g$	$N_{up}b$	$N_{up}t$				
2019-F304	**HS**	169	1.15	0.64	2.04a	0.84a	2.88a	0.81a	0.32	69a	51a
	MS	144	1.14	0.62	1.62b	0.63b	2.26b	0.65b	0.25	56b	40b
	UN	151	1.14	0.60	1.81b	0.74ab	2.55b	0.67b	0.28	60b	47a
	p-value		ns	ns	**	**	**	**	*	**	**
2020-F308	**HS**	216	1.13	0.74a	2.53	1.17	3.70	0.73	0.37	69	50
	LS	160	1.32	0.69ab	3.22	1.33	4.55	0.71	0.29	53	43
	MS	186	1.21	0.61b	2.52	0.92	3.44	0.77	0.28	63	45
	UN	217	1.26	0.62b	2.91	1.26	4.17	0.63	0.25	53	42
	p-value		ns	**	ns	*	ns	ns	ns	ns	ns
2021-F210	**HS**	139	1.13a	1.10ab	1.64a	1.25	2.89	0.58a	0.44a	49a	38a
	LS	120	0.99b	0.92c	1.28b	1.06	2.34	0.43b	0.35b	42ab	37a
	MS	134	1.12a	1.03bc	1.49ab	1.15	2.64	0.56a	0.43ab	50a	42a
	UN	126	1.14a	1.20a	1.27b	1.03	2.30	0.43b	0.36b	42b	29b
	p-value		***	****	**	ns	ns	**	*	***	***
2019-FMG1	**HS**	137	1.26	0.60	1.59a	0.56	2.15	0.44	0.16	36a	27a
	LS	82	1.32	0.68	1.13b	0.47	1.60	0.34	0.14	26b	20b
	MS	114	1.22	0.60	1.55a	0.64	2.19	0.46	0.19	38a	31a
	UN	122	1.21	0.54	1.45ab	0.57	2.02	0.41	0.18	38a	32a
	p-value		ns	ns	**	ns	ns	ns	ns	***	<.0001

Differences significant at * p<0.10; **p<0.05; *** p<0.01; **** P<0.001

Table 13. ANOVA of nitrogen concentrations in the grains (Ng) and biomass (Nb), plant and crop N uptake in the grain ($N_{up}g$), biomass ($N_{up}b$) and total ($N_{up}t$), nitrogen use efficiency for grain (NUEg) and biomass (NUEb), and nitrogen fertilizer use efficiency for grain (NUEfg) and biomass (NUEfb) at R6 growth stage at Springport, MI (42.3471°N, 84.7097°W) and Portland, MI sites (42.8971°N, 84.9776°W) for 2019-F304, 2019-FMG1, 2020-F308, and 2021-F210 season field combinations.

Site	Year-Field	Effect	Plant yield	%Ng	%Nb	Plant N uptake (g N plant^{-1})			Crop N uptake (kg N ha^{-1})		
			g plant^{-1}			Npg	Npb	Nptotal	Ncg	Ncb	Nctotal
Springport	2019-F304	YSZ	***	ns	ns	**	ns	***	***	ns	ns
		DAP	ns	ns	ns	ns	ns	ns	ns	ns	ns
		YSZxDAP	ns	ns	ns	ns	ns	ns	ns	ns	ns
	2020-F308	YSZ	ns	ns	**	ns	ns	ns	ns	ns	ns
		DAP	***	ns	ns	***	ns	***	***	ns	**
		YSZxDAP	**	ns	ns	**	ns	ns	**	ns	ns
	2021-F210	YSZ	ns	****	***	ns	ns	ns	**	ns	ns
		DAP	****	ns	ns	***	***	***	**	***	***
		YSZxDAP	ns	ns	ns	ns	ns	ns	ns	ns	ns
Portland	2019-FMG1	YSZ	***	ns	ns	**	ns	ns	ns	ns	ns
		DAP	ns	ns	ns	ns	ns	ns	ns	ns	ns
		YSZxDAP	ns	ns	ns	ns	ns	ns	ns	ns	ns

Differences significant at * p<0.10; **p<0.05; *** p<0.01; **** P<0.001

3.4.3. Nitrogen uptake relationship with plant growth rate and grain number

The PGR during the critical period of maize (period around silking, R1 +/- 15 days) ranged from 0.17 and 10 g $plant^{-1}day^{-1}$. Nitrogen uptake, in the grains, biomass, and total, were significantly and positively related to PGR ($p<0.001$) in the period around silking (Fig.6a, b, and c). Generally, late emerging and dominated plants had very low PGR (<2 g $plant^{-1}$ day^{-1}) (Fig. 13, green triangles). The number of grains per plant varied from 38 to 1019 and was significantly related to PGR ($p<0.0001$), showing a curvilinear response (Fig.14a). At similar PGR, Late and Dominated plants set less grains, compared with Early and Dominant ones (i.e. green points generally below the fitted curve and orange generally above). The number of grains per plant was positively related to the N uptake, and most plants with low grain number were Late and Dominated plants (Fig.14b).

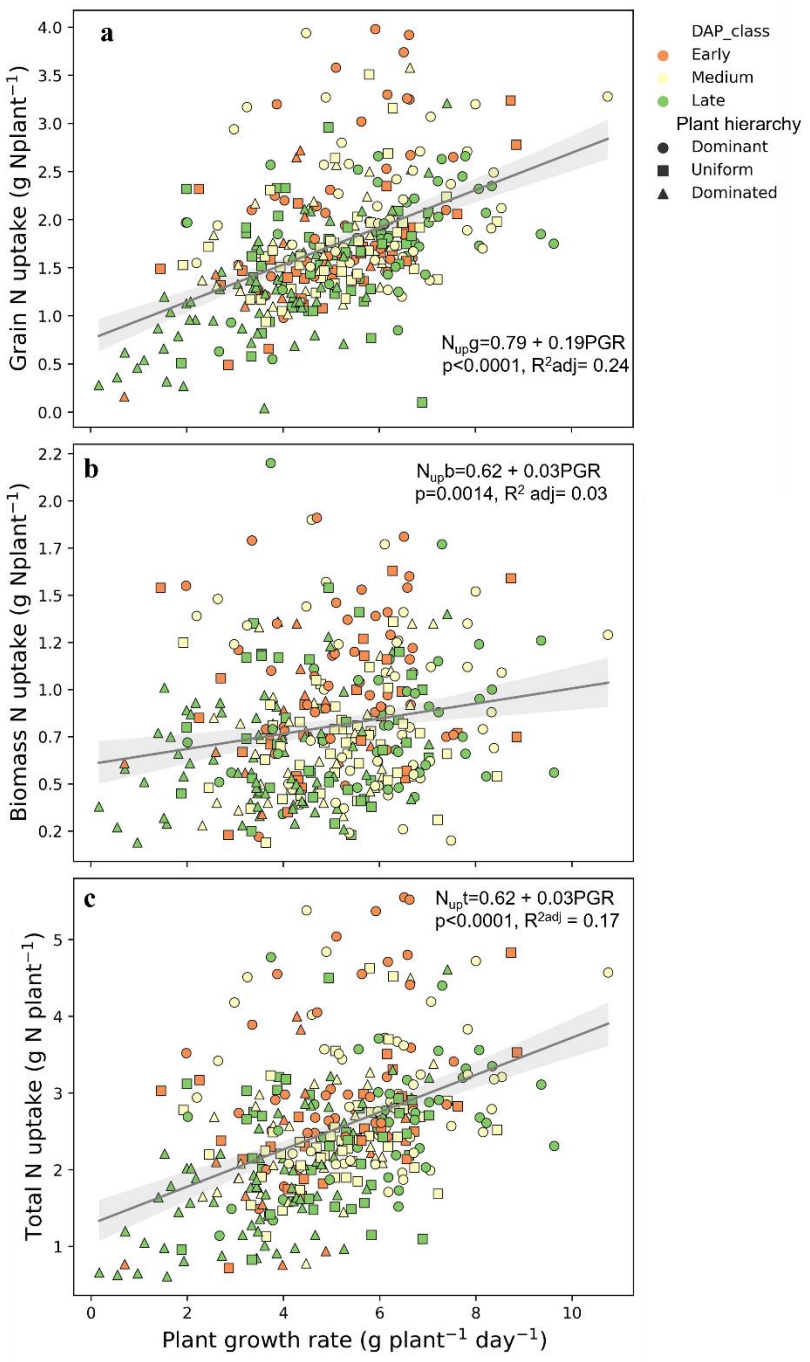

Figure 13. Plant nitrogen uptake in the grains (a), biomass (b), and total (c) (g N plant^{-1}) measured at R6 (following Ritchie et al, 1986), versus plant growth rate (g plant^{-1} day^{-1}) in the period around R1 for 2019-F304, 2019-FMG1, 2020-F308, and 2021-F210 year-fields combinations. Colors denote Early, Medium, and Late emergence class and symbols denote Dominant, Uniform, and Dominated plant hierarchy. Each point represents an individual plant (n= 345).

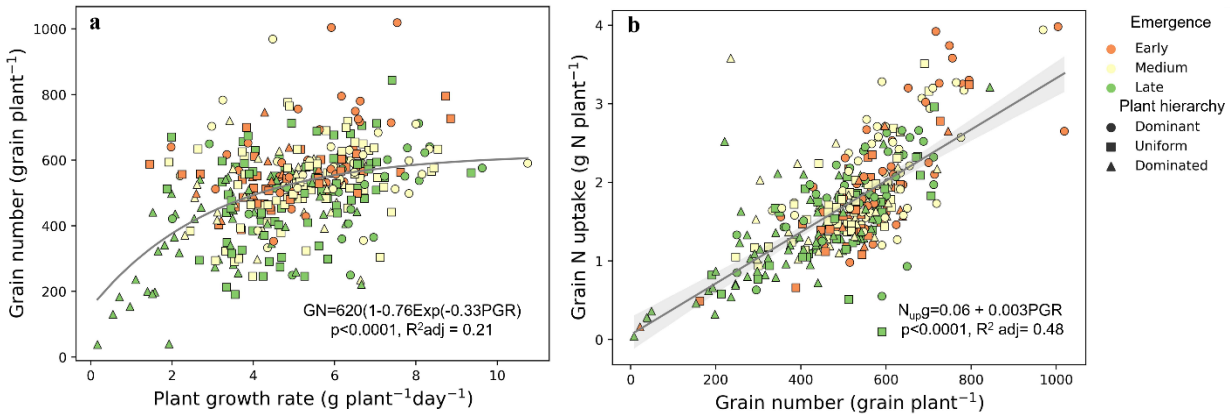

Figure 14. Relationship between a) grain number per plant (GN, grain plant^{-1}) and plant growth rate around R1 (g plant^{-1} day^{-1}), and b) plant nitrogen uptake in grain (g N plant^{-1}) and grain number per plant (grain plant^{-1}) for 2019-F304, 2019-FMG1, 2020-F308, and 2021-F210 year-fields combinations. Colors denote Early, Medium, and Late emergence class and symbols denote Dominant, Uniform, and Dominated plant hierarchy. Each point represents an individual plant (n= 345).

3.4.4. Emergence delay impact on PGR, GN, and N uptake

General linear and bi-linear relationships were fitted for PGR vs GDD_E, GN vs GDD_E, and NHI vs GDD_E, as there were no significant differences between Year-Field in the fitted models (Fig.15 and Fig.16). Plant growth rate was positively affected by emergence (GDD_E) up to a threshold (76 °C day^{-1}) above which, delayed emergence caused a decrease in PGR of 0.05 g per plant per °C day^{-1} of delay (Fig.15a). Similarly, the number of grains per plant showed a significant increase of 2.7 grains per plant in relation to emergence delay up to a threshold (96.7 °C day^{-1}) beyond which, the delay in the emergence caused a decrease of 6 grain per plant °C day^{-1} of delay.

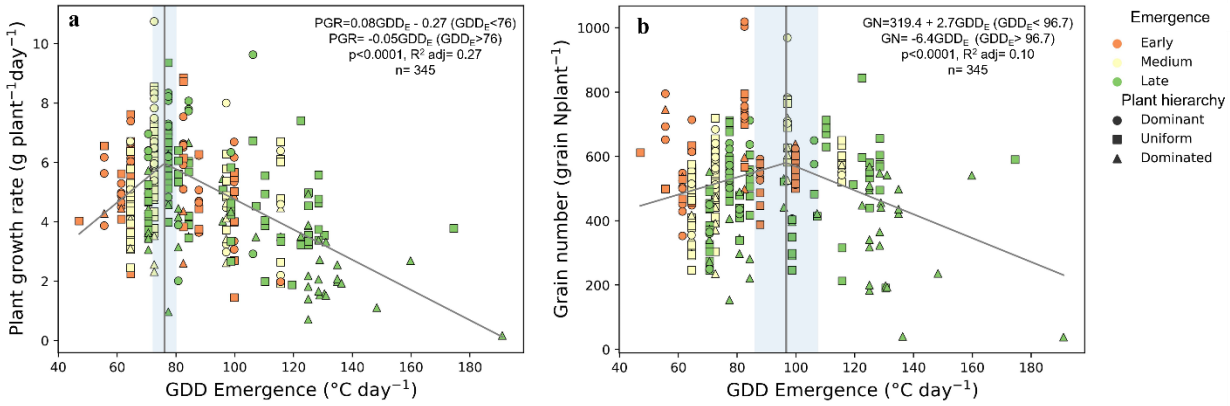

Figure 15. Relationship between plant growth rate around R1 (g plant^{-1} day^{-1}) (a), and grain number per plant (grain plant^{-1}) (b) with emergence in thermal time (°C day^{-1}) for 2019-F304, 2019-FMG1, 2020-F308, and 2021-F210 year-fields combinations. Colors denote Early, Medium, and Late emergence classes and symbols denote Dominant, Uniform, and Dominated plant hierarchy. Each point represents an individual plant (n= 345).

Nitrogen concentration in the grain (%Ng) was not significantly related to emergence (Fig.16a, red symbols), whereas nitrogen concentration in the biomass (Fig.16a, green symbols) was positively affected ($p<0.0001$) by the delay in emergence. Emergence delay caused an increase of 0.01% in the %Nb per °C day^{-1} of delay. Even though %Ng was not affected by emergence, the negative impact of the emergence delay on GN (Fig.16b) and the increase in the %Nb, caused a decrease in the NHI (Fig.16b, blue symbols) when the delay went beyond 73.4 °C day^{-1}.

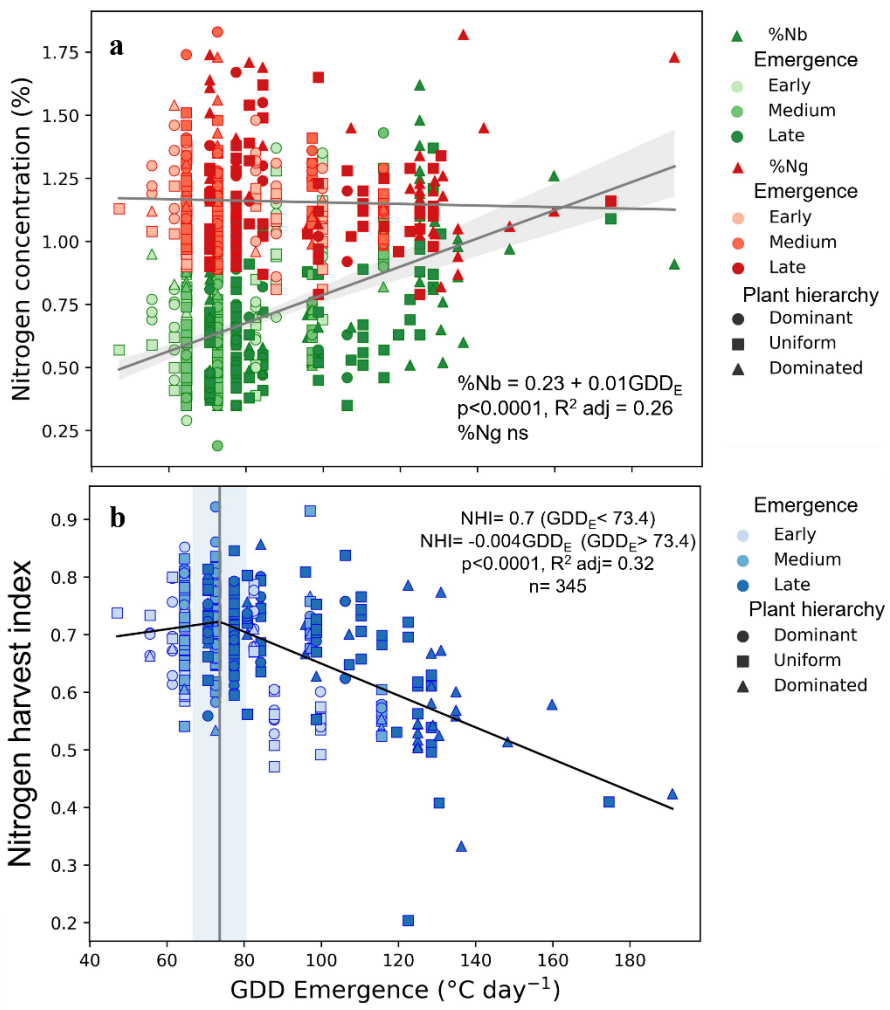

Figure 16. Relationship between a) nitrogen concentration in the grain and biomass (%) and b) nitrogen harvest index (nitrogen uptake in the grain-total nitrogen uptake ratio) versus emergence in thermal time (°C day^{-1}) for 2019-F304 (squares), 2019-FMG1 (triangles), 2020-F308 (diamonds) and 2021-F210 (circles) year-fields combinations. Colors denote Early, Medium, and Late emergence classes and symbols denote Dominant, Uniform, and Dominated plant hierarchy. Each point represents an individual plant (n= 345).

3.5. Discussion

This study provides novel results on the understanding of nitrogen uptake and use efficiency of plants with spatial and temporal variation in emergence in different yield stability zones on commercial farmer fields with a wide range of management practices. Maize emergence was significantly affected by the YSZ. Emergence was mostly slower in the LS (Table 11), and this higher delay in LS zones can be related to the less favorable conditions for

emergence in the low yielding areas (Knappenberger & Köller, 2012), i.e. less plant available water and reduced soil fertility.

Although plant emergence showed variations across YSZ, plant biomass did not show significant differences among YSZ in early stages (V6 and V14), whereas the biomass at R6 was significantly affected by the YSZ and was usually higher in the HS zone (Fig.9a, b, and d). Plant biomass variability was greater at early stages, decreased by R1, and remained consistent from R1 to R6. Plants growing in low yielding zones generally reached lower biomass and showed higher variability (Fig.10) throughout the growing season, suggesting a higher competition for resources between plants in those zones. Rossini et al. (2012), examined the effects of inter-plant competition in maize grown under contrasting nitrogen supply and plant density, and reported differences in accumulated biomass from V8 onwards due to N and from V12 on due to increased plant density. They also reported a decrease in plant biomass CV from V3 to V8, stabilizing around 27%, and mention that fertilization at V6 promoted an increase in biomass and decreased the CV. Similarly, (O'Brien & Hatfield, 2021) reported a decrease in plant-to-plant variability from 16 at V6 to 26% at R6. In contrast with previous research (Maddonni & Otegui, 2004) reported an increase in plant biomass CV from V3 to V9 and the magnitude of the variability persisted to R6. Our results align with the idea that early stressful environmental conditions (i.e. given by different resources supply by YSZ) have greater late impact on plant growth with low resources supply (i.e. LS zones) (Rossini et al., 2011).

Plant nitrogen uptake was related to the PGR around silking, and the relationship of $N_{up}g$ was stronger compared with $N_{up}b$ and $N_{up}t$ (R^2 0.24 vs 0.03 and 0.17) (Fig.13), which may be linked to the fact that grain number set is closely associated with the PGR around R1 (Fig.14a), and the grain number and weight per grain determine the amount of nitrogen that can be taken up

by the grains (Fig.14b). The relationship between grain number and PGR around R1 has been widely reported (Andrade et al., 1999; Maddonni & Otegui, 2004; Echarte et al., 2004; Borrás & Vitantonio-Mazzini, 2018; Parra et al., 2022). In fact, in several crops, grain number per plant is highly dependent on the accumulation of ear biomass, which depends on the PGR around R1 and how much of that biomass is allocated to ear growth (Borrás & Vitantonio-Mazzini, 2018; Fischer, 1985; Rotundo et al., 2012). However, the relationship between PGR around silking and emergence delay has not been reported yet. We found that there is a threshold in emergence beyond which PGR is negatively affected (Fig.15a). Likely, a late emerged and dominated plant will be shorter than its neighbors and will be at a greater disadvantage as the competition for sunlight becomes more intense (Edmeades & Daynard, 1979), particularly during the critical period for grain set (i.e. R1 +/- 15 days) which is the crop's most sensitive period to any stress (Westgate et al., 2004). This may reduce the PGR of the late emerged and dominated plants compared with early emerged and dominant plants affecting their capability to set grains. Grain number decreased by 2.7 grains per growing degree day when emergence went beyond 96°C day^{-1} (Fig.15b). A similar relationship of relative per plant grain weight and soil accumulated growing degree days has been reported (Nemergut et al., 2021). These authors found that relative per plant grain weight was maintained at 103.9% when emergence was within 86.4 °C day^{-1}, and after that the threshold for the relative plant yield was reduced by 0.6%. In this study, most of the plants that showed very low PGR were Late emerged and Dominated plants, and they set less grain compared with medium or early emerged plants (Fig.14a). Maddonni & Otegui (2004), stated that Dominated plants biomass allocation to reproductive structures is already affected at the beginning of active ear growth (ca. V13). Borrás & Vitantonio-Mazzini (2018) mentioned that the proportion of PGR that is allocated to the ear growth during the flowering period is non-

constant. At a low plant growth rate the proportion of assimilates allocated to the ear growth is reduced. In conditions of high plant growth, the consequences of having spatial and temporal variable canopies are relatively insignificant, whereas in reduced growth environments the effect is noticeable.

Plant hierarchy affected plant nitrogen use efficiency (APPENDIX B Fig.27-30), early emerged and dominant plants were more efficient in the use of nitrogen compared with late emerged and dominated plants. These results contrast with those reported by Rossini et al. (2018), as they evaluated the contribution of early-established plant hierarchies to the response of two hybrids to nitrogen fertilization (0 and 200 kg ha^{-1}) and plant density (9 and 12 plant m^{-2}) and found that the dominated and Uniform plants had an increased NUE (grain and biomass) compared with the dominant plants. The reduced response of the dominant plants was attributed to a high leaf-to-stem ratio and leaf N concentration in these plants. Even though %Ng was not affected by the delay in emergence (Fig.16a), the negative impact of the emergence delay on the grain number (Fig.7b) and the increase in the %Nb with emergence delay (Fig.9a), caused a decrease in the NHI (Fig.9b) when emergence went beyond 73.4 °C day^{-1}. We hypothesized that plants that emerge late accumulate less nitrogen than early emerged plants, which is partially true. Even though that %Ng was not affected by the delay in the emergence, late emerged and dominated plants accumulated less nitrogen in the grains due to the reduction in grain number and grain weight per plant (Albarenque et al., 2023, submitted). Late emerged and dominated plants experienced a decrease in total biomass accumulated compared with early and dominant plants, and %Nb increased as a consequence of the reduced accumulation of biomass i.e. no dilution. Apparently, late and dominated plants were able to capture the N from the soil, but they were not able to compete for light and produce enough photo assimilates, their NUE was reduced

compared with early emerged and dominant plants (Table 4). When emergence is delayed, late plants had a reduction in PGR in the period around silking and they set less grains. As such, the N accumulated in the biomass is not remobilized to the grains (i.e. lack of sink not source), increasing the %Nb with the delay.

3.6. Conclusions

Results agreed with our hypothesis, which stated that plants that emerge late accumulate less nitrogen than early emerged plants and the plant nitrogen partition changes with the delay. Nitrogen uptake at the plant level decreased with delayed emergence and was affected by plant hierarchy (dominant>dominated). Although the %Ng remained the same with delayed emergence, there was an increase in %Nb related to lower total biomass which caused a change in N partition related to a lack of sink. The reduction in PGR caused by the delay of emergence was related to a reduction in the number of grains set by the plants. Consequently, nitrogen use efficiency was reduced in the late emerged and dominated plants. Understanding the impact of temporal variation of emergence and plant hierarchies on N uptake and use efficiency can help farmers prescribe N fertilizer on different sub-field yield stability zones.

CHAPTER 4: MAIZE (*Zea Mays* L.) EMERGENCE DERIVED FROM PLANT HEIGHT OBTAINED FROM HIGH-RESOLUTION DRONE IMAGES

4.1. Abstract

Incorporating the spatial and temporal variability of crop emergence into crop models has the potential to enhance field-scale yield prediction. This might provide farmers with a valuable decision-making tool during the growing season and may reduce their economic and environmental risks associated with applying fertilizer inputs at a uniform rate. Our objectives were to i) estimate the spatial and temporal variation in plant emergence using plant height derived from UAV images and Machine learning (ML) techniques, and ii) simulate maize growth and yield incorporating the spatial and temporal variation in crop emergence. We used maize emergence data from six field experiments to train, test, and validate ML to estimate maize emergence. LiDAR images were used to extract plant height at V6, V14, and R1 and estimate spatial variability plant emergence at field-scale. We then simulated maize with uneven emergence (Early, Medium, and Late emergence) and compared the simulation with an even emergence. Observed emergence ranged between 64 and 133 °C day^{-1} and varied among YSZ in four of six fields. The features that most contributed to plant emergence estimation were planting date, plant height at R1 and plant height at V6. The ML was able to accurately predict plant emergence, with RMSE of 9.9, 11.2, and 22.4 °C day^{-1} for the training, testing, and validation dataset. We then developed a map showing the spatial and temporal variation of crop emergence. The Salus model was used to simulate maize under even and uneven emergence conditions. Maize yield was simulated adequately under even and uneven emergence, however, the incorporation of the temporal variability in the simulation improved the late emerged plants simulation, as well as the simulation of the LS and MS zones. Incorporating the spatial and

temporal variation of crop emergence into crop models has the potential to enhance yield prediction at the field scale. This improvement can provide farmers with valuable within-season decision-making tools and reduce economic and environmental risks associated with uniform fertilizer rates across field sites.

4.2. Introduction

Uniformity of maize (Zea mays L.) emergence is essential for minimizing plant-to-plant competition for light, water, and nutrients (Andrade & Abbate, 2005). Emergence variability is associated with variation in soil temperature and moisture (Pommel et al., 2002), and management practices such as planting depth, tillage system, planting speed, and the planter (Knappenberger & Köller, 2012). Plants growing in a stand with temporal variation in the emergence will have a higher variability in plant height, ear size, grain number, and ultimately crop yield. This variability arises from delayed emergence and the impact of interplant competition for resources (D'Andrea et al., 2008; Pagano & Maddonni, 2007; Rossini et al., 2011). Numerous studies have reported the negative effect that uneven emergence of maize causes on crop yield (Carter & Nafziger, 1991; Kolling et al., 2019; Nemergut et al., 2021). The underlying cause of this detrimental effect can be associated with a diminished plant growth rate during the critical period (i.e. 15 days before and after flowering), leading to a reduced number of grains being set by the plants and consequently resulting in a decline in grain yield (Albarenque et al., 2023, Chapter 3).

Although, satellite imagery is an important tool to governmental agencies to monitor agricultural production (Allen, 1990), its adoption at farm-scale applications has been limited due to challenges associated with coarse spatial resolution, variable temporal resolution, cloud cover, and delayed delivery of the information to end users (Mulla, 2013). The advancements in

unmanned aerial vehicle (UAV)-based imaging and image processing technologies have given the possibility of high-resolution crop images collection on a field scale, enabling efficient assessment of crop growth conditions (Zhang & Kovacs, 2012), fulfilling the long-standing demands of farm managers for data acquisition (Hunt & Daughtry, 2017). Additionally, these images can be used to detect diseases, phenotyping, weed mapping, and to prescribe variable input rates (Pajares, 2015). Recent research has demonstrated the effectiveness of utilizing high-resolution UAV equipped with various sensors to assess crop emergence through high-resolution images in several staple crops including corn, wheat, potato, and cotton (Feng et al., 2020; Li et al., 2019; Liu et al., 2017; Shirzadifar et al., 2020; Shuai et al., 2019b; Vong et al., 2022). Vong et al. (2022) estimated plant emergence and produced emergence uniformity field maps using deep learning models and UAV imagery in early growth stages, highlighting the challenge of assessing small plants with a complex background. The availability of high spatial and temporal resolution of plant height data is crucial in obtaining accurate results.

Accurate yield forecasting is important to improve farmers' management and operation decision making (Basso & Liu, 2019). Machine learning (ML) and simulation crop modeling have individually made noteworthy contributions to the accuracy of yield predictions. It has been demonstrated that the combination of the techniques enhances the precision of yield estimation (Shahhosseini et al., 2021). Crop models have demonstrated their capability and versatility to accurately predict crop yield in a wide range of scenarios (Fabbri et al., 2023; Martinez-Feria et al., 2018; Puntel et al., 2016). However, the assumption of uniform spatial and temporal conditions might lead to a biases and inaccurate simulation, in real field conditions of non-uniformity in the crop stand (Batchelor et al., 2002) related to uneven crop emergence. Some efforts have been made to assess the spatial and temporal variation in crop yields using crop

models (Albarenque et al., 2016; Basso et al., 2007, 2011; Sadler et al., 2000), but as pointed out by Batchelor et al. (2002) it is necessary to economically measure inputs to running crop models at several scales.

Capturing and incorporating the spatial and temporal variation of crop emergence into crop models might improve yield prediction at field scale, giving additional within season decision making tools for farmers, reducing their economic risk, as well as the environmental risk associated with uniform fertilizer input rates. In this study we addressed the following research questions: 1) Can we estimate maize emergence using crop height at several stages? 2) Can we simulate the effect of crop emergence spatial and temporal variation on crop yield? Our hypothesis is that incorporating the spatial and temporal variation in the emergence into crop simulation model improves the understanding of yield spatial variability. Through a field-level analysis, we aimed to i) estimate the spatial and temporal variation in plant emergence using plant height derived from UAV images and ML techniques, and ii) simulate maize growth and yield incorporating the spatial and temporal variation in crop emergence.

4.3. Methods

4.3.1. Site description and general characteristics

Field experiments were conducted in six corn commercial fields, located in Springport (MI) (42.3471°N, 84.7097°W), Portland (MI) (42.8971°N, 84.9776°W), and Parana (Argentina) (32.2336°S, 60.5338°W). Fields varied in soils and management practices, such as tillage system, row spacing, hybrid relative maturity, and planting date (Table 14). Fields in Springport were planted with a White planter 9924VE, a John Deere 1770 NT was used in Portland field, and a pneumatic Giorgi Precisa 8000 was used in Parana fields. Yield stability zones (YSZ) delineation was performed as described in the methods section "*Yield stability zones*" of Chapter

2. Table 2 shows in-season and 30 years average cumulative precipitation (May-October and December-April, for Michigan and Parana sites, respectively) and in season average temperature as well as the 30-yr normal (1991-2020) for the same period. Rainfall during the growing season was closer (90 to 110%) to the normal average (1991-2020) for the same period. Temperatures were slightly higher than historical averages in Springport fields, while they were within the range of historical values for Portland and Parana fields (Table 15).

Table 14. Experimental sites and locations with soil and management data.

Site	Year-Field	Tillage System	Cover crop	Planting date	nº plants
Springport	**2019-304**	No-Till	No	8-Jun	1210
	2020-308	No-Till	Yes	11-May	669
	2021-210	No-Till	Yes	15-May	535
Portland	**2019-MG1**	Conventional	No	8-Jun	597
Parana	**2020-4**	No-Till	No	18-Dec	270
	2020-11	No-Till	No	29-Dec	202
				Total	3483

4.3.2. Experimental design and measurements

Emergence was recorded daily by visiting each 5m x 2 rows plot from each field once a day during the period of emergence. Emergence was expressed in thermal time ($GDD_{E,}$ °C day^{-1}), which was calculated as described in *3.2.4. Calculations* section. Each emerged plant was individually labeled using white stakes. At the stages of V6, V14, and R1, the plant height (H_V6, H_V14, and H_R1, respectively) from ground level to the last fully expanded leaf (visible collar) of tagged plants was measured and recorded. At the end of the growing season, each labeled plant was individually harvested (n=3484 plants) to analyze the individual plant grain yield and grain number. Crop yield was estimated using the achieved plant density in every plot.

Table 15. Monthly observed average air temperature (°C) and total precipitation (mm) and 30-year means (1991-2020) during the growing season at Springport, Portland, and Parana sites.

Springport								
	Temperature				Precipitation			
Month	**2019**	**2020**	**2021**	**30-yr**	**2019**	**2020**	**2021**	**30-yr**
May	14.0	14.0	14.0	12.9	91.2	121.7	53.3	97.7
Jun	19.0	21.0	22.0	18.0	124.7	117.9	224.8	84.3
Jul	23.0	24.0	22.0	22.2	65.8	45.7	119.9	92.2
Aug	21.0	22.0	23.0	20.2	36.3	57.9	98.0	89.2
Sep	19.0	16.0	19.0	15.4	101.9	74.9	110.5	83.1
Oct	11.0	9.0	14.0	7.7	115.8	61.5	136.6	78.3
	Portland				**Parana**			
	Temperature		**Precipitation**		**Temperature**		**Precipitation**	
Month	**2019**	**30-yr**	**2019**	**30-yr**	**2020**	**30-yr**	**2020**	**30-yr**
May	13.1	12.4	115.0	95.8	15.2	15.8	66.6	66.0
Jun	18.6	21.0	132.6	89.8	12.4	13.0	19.8	36.0
Jul	22.9	22.4	72.9	82.6	10.9	12.1	8.0	27.0
Aug	20.0	21.7	68.8	97.4	15.5	14.1	4.5	35.0
Sep	18.3	15.1	186.4	88.7	16.0	16.0	32.6	51.0
Oct	9.9	7.0	155.5	87.6	19.6	19.0	84.2	119.0

4.3.3. UAV flight and field data collection

The UAV LiDAR system used was a SICK LD-MRS400001 (Fig.17a) mounted on a DJI Matrice 600 Pro drone with a take-off weight of about 10 kg (Fig.17b). The position of the UAV was provided by GPS (or GLONASS, Global Navigation Satellite System) and a magnetic compass to maintain the flight direction. Images were collected at the same date that plant height was measured at crop stages V6, V14, and R1 in field 2021-210. Flights were conducted 50 m above the ground at a 2.7 m s^{-1} speed. Images were stitched with Pix4D (Pix4D, 2021) creating an orthomosaic image. The UAV LiDAR point cloud images were processed using LAS-Tools (Version: 210, 720, rapidlasso GmbH, Gilching, Germany) in ArcGIS (Environmental Systems Research Institute, 2021) to obtain the digital elevation models (DEM) that were used to extract individual plants height. Additionally, to assess the accuracy of the plant height obtained with LiDAR images, plant height of all the plants in 6 rows 300m long in 2020-308 field (n=8073 plants) (Fig. 18) was measured at R1 stage. This was evaluated using the R^2 of the LiDAR versus observed plant height and the RMSE (Equation 2).

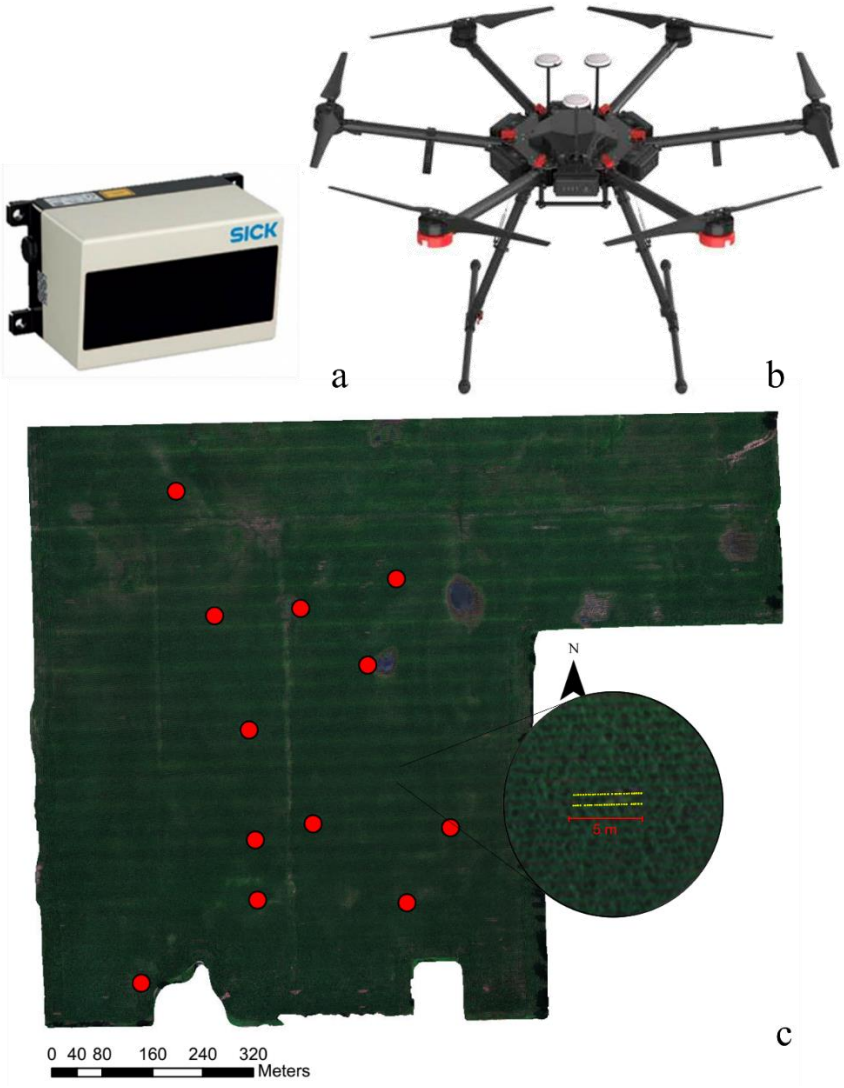

Figure 17. a) Lidar system SICK LD-MRS400001, b) DJI Matrice 600 Pro drone, c) Plot locations in 2021-210 field and plot (2 rows x 5m) details. Each yellow dot represents a plant. The images in a) were taken on July 14th, 2021.

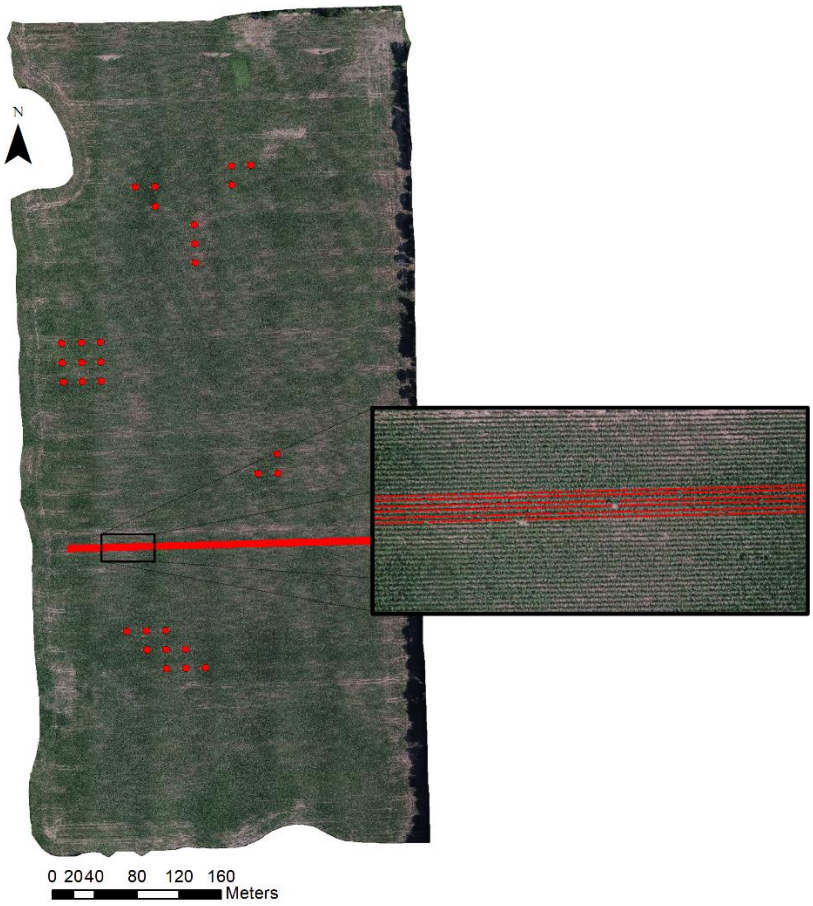

Figure 18. Plot locations in 2020-308 field site with rows measured to assess plant height obtained with LiDAR images. The inset shows the detail of the 6 rows x 300 m where plant heights were measured (n = 8073 plants).

4.3.4. Random forest model

The Random Forest (RF) model was fitted and used to estimate maize emergence in thermal time (°C day^{-1}) at a field level. The RF is a machine learning method that belongs to the supervised learning category, specifically to the ensemble learning method (James et al., 2021). It works by constructing a multitude of decision trees at training time and outputting the class that is the mode of the classes (classification) or mean prediction (regression) of individual trees. Each decision tree is constructed by taking a random subset of the training data and a random subset of the input features (Schonlau & Zou, 2020). The model was developed using the dataset

collected for the six fields (n=3483) described in section 4.2.1 *Site description and general characteristics,* with maize emergence (°C day^{-1}) as response variable and five features: Planting date (PD), Yield Stability Zone (YSZ), Cover crop (CC), Tillage system (TS), and plant height at V6 (H_V6), V14 (H_V14), and R1 (H_R1). The dataset was split 70% training (n= 2439), 15% testing (n=522), and 15% validation (n=522). We used Sklearn package in Python v3 to train, test, and validate the RF model. We then performed a hyperparameter tuning using RandomizedSearchCV class provided by the Sklearn package to find the hyperparameter values that result in the best model performance for emergence estimation. By fine-tuning the hyperparameters, the model's ability to generalize to unseen data could be improved, increasing its predictive accuracy, and reducing the likelihood of overfitting or underfitting (Probst & Bischl, 2019).

The model was evaluated using three accuracy indicators. We regressed the estimated emergence versus the observed and used the coefficient of determination (R^2) to assess the overall agreement between estimated and observed maize emergence. Additionally, we calculated root mean square error (RMSE) (Equation 2) and the mean absolute error (MAE) (Equation 3).

$$RMSE\ (°C\ day^{-1}) = \sqrt{\frac{\sum_{i=1}^{n}(E_i - O_i)^2}{n}} \quad \text{Equation 2}$$

$$MAE\ (°C\ day^{-1}) = \frac{1}{n}\sum_{i=1}^{n}|E_i - O_i| \quad \text{Equation 3}$$

where E_i is the estimated plant emergence (°C day^{-1}), O_i is the observed emergence, n is the total number of observations, and i is the ith observation.

Estimated emergence was classified in Early, Medium, and Late as described in Chapter 3 section 3.2.1. Field experiments and Yield stability zones.

4.3.5. SALUS model description

The Systems Approach to Land Use Sustainability (SALUS) simple crop model was used to simulate maize grain yield in field with uneven crop emergence. The SALUS model is a process-based crop model (Basso et al., 2006) adapted from the CERES (Crop Environment Resource Synthesis) model with soil nutrient and water simulations updates (Basso & Ritchie, 2015). The model is designed to simulate continuous crops, soil, water, and nutrient conditions under different management strategies over multiple years. The model uses daily weather information (solar radiation, maximum and minimum temperature, and rainfall), crop parameters (specie, cultivar/hybrid), soil layer properties (soil water limits, soil texture, bulk density, soil organic carbon, and nitrogen), and management (planting date, planting depth, seeding rate, row spacing, and fertilization). The Salus model has been used and evaluated on several sites (Albarenque et al., 2016; Basso et al., 2006; Basso & Ritchie, 2015; Liu et al., 2021; Liu & Basso, 2017; Shuai et al., 2019).

The SALUS model was calibrated from runs with contrasting emergence dates from experiments 2019-304, 2019-MG1, and 2020-308 (APPENDIX C Fig.32a) to develop three different Subspecies within Maize to account for variation in emergence, namely: Early, Medium, and Late subspecies. Validation was made with data from the year-fields described in Table 14 (APPENDIX C Fig.32b). The simulations were run under non-limited nitrogen and rain-fed conditions. Harvest dates were set to be as measured. The results of uneven emergence simulations were validated against the yield monitor data for the 2021-210 year-field. Model performance was evaluated through RMSE (Equation 2), MAE (Equation 3), and RRMSE (Equation 4).

$$RRMSE\ (\%) = \frac{RMSE}{\frac{1}{n}\sum_{i=1}^{n} O_i} \quad \text{..... Equation 4}$$

where E_i is the estimated plant emergence (°C day^{-1}), O_i is the observed emergence, n is the total number of observations, and i is the ith observation.

4.3.6. Data analysis

For each Yield-Field, data was statistically analyzed using the GLIMMIX procedure in SAS version 9.4 (SAS Inst., Inc.) to determine the yield stability zone effect on emergence and plant height. Individual plants were nested within the plot and included as a random factor to identify them as subsamples. Mean separation between groups was analyzed using Tukey's method, performing pairwise comparisons to identify differences greater than the expected standard error.

4.4. Results

4.4.1. Maize emergence and plant height

Plant emergence ranged between 64 to 133 °C day^{-1} and was significantly affected by the YSZ in four out of six evaluated fields (Table 16). Average emergence range was highest in 2020-308 reaching 100 °C day^{-1}, whereas the lowest range was 24 °C day^{-1} observed in 2019-304 (Appendix C Table 20). In general, the MS and LS zones showed the highest range in GDD_E being between 13 and 144 °C day^{-1}. Plant height ranged from 9 to 19 cm, 48 to 135 cm, and 136 to 232 cm, in V6, V14, and R1, respectively. Even though plant height showed significant differences in one out of the six Year-Field, plants where generally 20-30% shorter and showed an increased variation (i.e. higher CV) in the LS zone, except for 2019-MG1 where the MS zone plants were 30% shorter that plants in the other YSZ.

Table 16. Average plant emergence (°C day-1) and plant height (cm) at V6, V14, and R1 crop growth stages at Springport, MI (42.3471°N, 84.7097°W) and Portland, MI sites (42.8971°N, 84.9776°W) for 2019-F304, 2019-FMG1, 2020-F308, and 2021-F210 season field combinations for High stable (HS), Medium Stable (MS), Low Stable (LS), and Unstable (UN) Yield Stability Zones (YSZ).

Site	Year-Field	YSZ	GDD_E † (°C day^{-1})	Plant height (cm)		
				V6	V14	R1
Springport	2019-304	HS	73 (7) ¶	14 (12)	92 (13)	219 (9)
		MS	73 (7)	13 (13)	80 (22)	196 (15)
		UN	73 (11)	14 (13)	99 (14)	224 (14)
	2020-308	HS	84b (23)	19 (17)	135 (17)	232 (10)
		MS	92a (21)	17 (18)	121 (22)	211 (14)
		LS	94a (17)	15 (26)	96 (32)	185 (15)
		UN	89ab (20)	19 (16)	136 (19)	232 (10)
	2021-210	HS	109b (16)	13a (14)	119 (16)	182 (14)
		MS	110b (17)	13a (15)	117 (17)	179 (15)
		LS	124a (18)	9b (23)	86 (23)	136 (21)
		UN	105b (13)	13a (13)	123 (13)	184 (11)
Portland	2019-MG1	HS	64c (7)	19 (14)	88 (13)	221 (11)
		MS	87a (21)	13 (19)	48 (24)	186 (22)
		LS	67b (6)	17 (18)	62 (25)	195 (12)
		UN	66bc (11)	19 (12)	82 (13)	219 (8)
Parana	2020-11	HS	132ab (11)	15 (12)	124 (7)	183 (7)
		MS	121b (13)	14 (13)	95 (15)	152 (8)
		LS	133ab (17)	13 (15)	93 (16)	145 (12)
	2020-4	HS	107 (13)	11 (16)	87 (14)	187 (11)
		LS	109 (13)	13 (16)	101 (16)	200 (10)

† Means not sharing the same letter within the same column and Year-Field are different ($p<0.05$) from each other.
¶Values in brackets are the variation coefficient.

4.4.2. Machine learning model

The relative importance of each feature in the model's prediction accuracy is represented in Fig.19a. According to this, the feature that contributed the most to the emergence estimation is planting date, followed by plant height at R1 (H_R1) and V6 (H_V6), whereas plant height at V14 (H_V14), yield stability zone (YSZ), cover crop, and tillage system, contributed to emergence estimation in less proportion. However, the feature importance plot does not imply causation it reflects the model's learned associations.

The adjusted ML model was able to accurately estimate plant emergence. The relationship between the predicted values for the training and testing data sets with their corresponding residuals is displayed in Fig.19b. The residuals are well distributed around the

zero line and suggests there is not an evident under or over estimation of the emergence. Even though the model showed a good performance there are some very late emergence values that the model underestimated (residuals < -50 °C day^{-1}) (Fig.19b). The model provided an acceptable estimation of the emergence, with R^2 values of 0.82 and 0.72 for the observed vs estimated training and testing data sets (Fig.19b). Additionally, the RMSE for the training was 9.9 °C day^{-1} and the MAE was 6.7 °C day^{-1} (APPENDIX C Fig. 31a), whereas for the testing the RMSE was 11.2 °C day^{-1}and the MAE was 7.4 °C day^{-1} (APPENDIX C Fig.31b).

The RMSE between estimated and observed plant emergence for the validation dataset (Fig.19c) was 22.4 °C day^{-1} and the MAE was 19.4 °C day^{-1}.

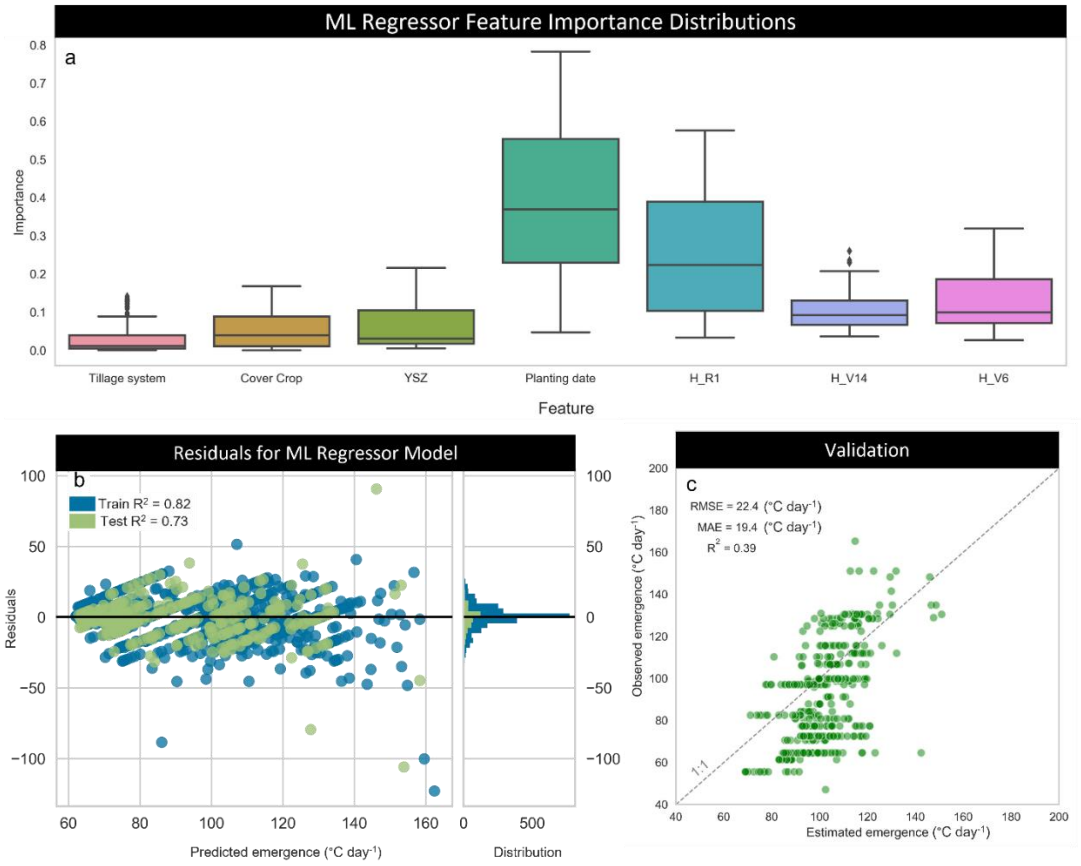

Figure 19. Machine learning feature importance distribution (a), residuals for the ML regressor model (b), and comparison between estimated emergence (°C day^{-1}) and observed emergence (°C day^{-1}) using validation data set (c).

4.4.3. LiDAR plant height

Plant height derived from LiDAR images obtained with UAVs was within the range of observed values and the RMSE was 22.5 cm and MAE 14.5 cm (Fig.20). Even though the overall error was acceptable, when analyzed by stage the RMSE was 4.8, 16.4, and 23.5 cm for H_V6, HV14, and H_R1, respectively (APPENDIX C Fig.32) and the MAE was 4.4, 12, and 20.5 cm which represents a 38, 12, and 10% of error for H_V6, HV14, and H_R1, respectively.

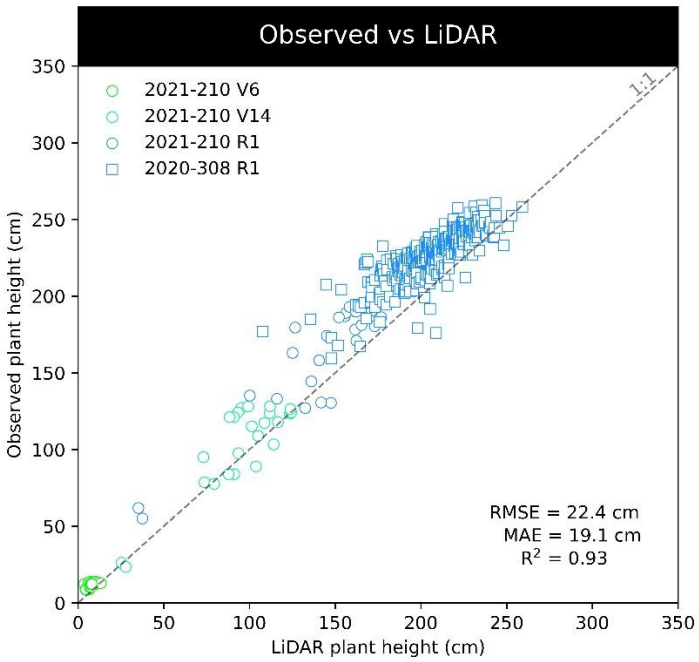

Figure 20. Comparison between observed plant height (cm) and plant height (cm) extracted from LiDAR images at V6, V14, and R1 growth stages at fields 2020-308 and 2021-210 in Springport, MI during the 2020 and 2021 growing seasons.

4.4.4. Emergence estimation with ML

Plant emergence was estimated using the developed ML model, using plant height (at V6, V14, and R1), planting date, tillage system, cover crop, and yield stability zone as features. A map of estimated emergence is shown in Fig.22. As the LiDAR images were obtained in portions of the fields were the plots were located, the map is in patches. The estimated emergence ranged from 77 to 135.5 °C day^{-1} (Fig.22), with an average value of 116.8 °C day^{-1} and standard

deviation of 10.1 °C day^{-1}. The ML model was able to capture the YSZ variation in emergence (Fig.21 and Fig.22), being the average estimated emergence 111.6, 119.3, 123.5, and 114.1 °C day^{-1}, for the HS, MS, LS, and UN zones, respectively. It can be noted that the estimated emergence in the LS zone (Fig.22 and Fig.23 yellow) shows higher values (i.e. more delay) compared with the other zones.

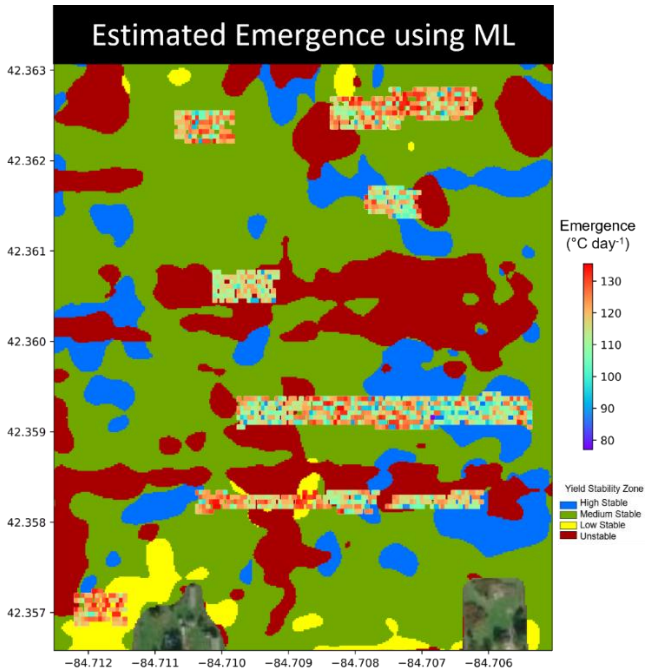

Figure 21. Estimated emergence (°C day^{-1}) using ML model and Yield Stability Zone for field 2021-210 in Springport, MI in 2021.

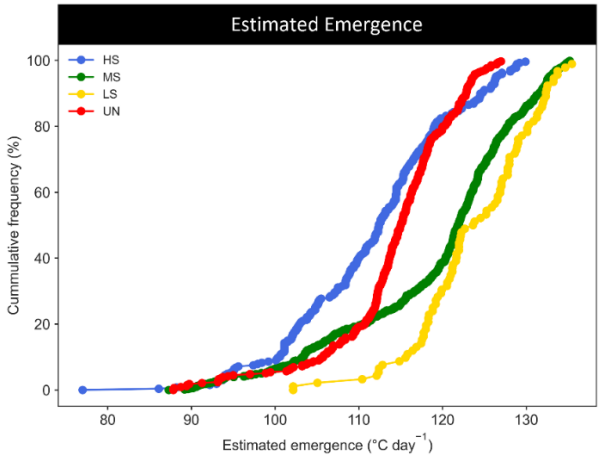

Figure 22. Cumulative frequency of the estimated emergence by Yield Stability Zone in year-field 2021-210. HS: High stable, MS: Medium stable, LS: Low stable, and UN: Unstable. Every point represents a pixel from the generated emergence map.

4.4.5. Simulation of spatial and temporal variable emergence

After the estimation of plant emergence using ML, we simulated maize for even emergence conditions by YSZ and uneven emergence, with three emergence classes: Early, Medium, and Late emergence by YSZ (Fig.23, Table 17). Observed maize yield ranged from 6.5 to 11.9 Mg ha^{-1}, with an average value of 10.1 Mg ha^{-1} and standard deviation of 1.2 Mg ha^{-1}. The average observed yield per emergence class was 10.3, 10.1, and 9.9 Mg ha^{-1}, for the Early, Medium, and Late emergence classes, respectively.

Maize yield using Salus model with even emergence was adequately simulated. The overall RMSE was 1.6 Mg ha^{-1}, whereas RMSE per emergence class was 0.4, 0.8, and 2.7 Mg ha^{-1} for the Early, Medium, and Late emergence class, respectively. The RMSE by YSZ was 1.4, 2.7, 1.7, and 1.2 Mg ha^{-1}, for the HS, MS, LS, and UN zones, respectively (Table 17). The simulation with the temporal variation in maize emergence incorporated into the model (i.e. using three subspecies with different time to emerge within Salus model) gave an adequate yield result. The overall RMSE was 1.5 Mg ha^{-1}, whereas the RMSE per emergence class was 2.2, 0.8, and 1.1 Mg ha^{-1}, for the Early, Medium, and Late emergence class, respectively. The RMSE by YSZ was 1.7, 1.7, 1.4, and 1.1 Mg ha^{-1} for the HS, MS, LS, and UN zones, respectively (Table 17).

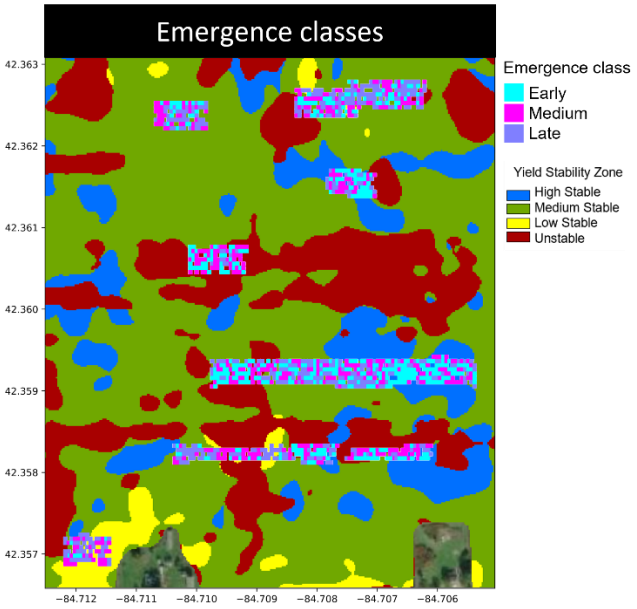

Figure 23. Map of maize emergence classes obtained from the ML estimated emergence for field 2021-210 in Springport, MI (42.3471°N, 84.7097°W).

The incorporation of the temporal variability in the Salus simulation improved the Late emerged class yield estimation by a 25% (Table 17), whereas it decreased the accuracy in the estimation of the early emerged class (uneven emergence 22% RRMSE vs even emergence 3% RRMSE, Table 17). Including the temporal variation in the emergence improved the yield simulation of the LS (uneven emergence 15% error vs even emergence 17% error, Table 17) and the MS (variable emergence 14% error vs uniform emergence 18% error, Table 17) zones.

Table 17. Accuracy metrics to evaluate Salus model performance in simulating the maize under uniform emergence and with spatial and temporal effects of maize emergence on crop yield for early, medium, and late emergence categories and High stable (HS), Medium Stable (MS), Low Stable (LS), and Unstable (UN) Yield Stability Zones.

	Even emergence			**Uneven emergence**		
	RMSE	**MAE**	**%RRMSE**	**RMSE**	**MAE**	**%RRMSE**
Overall	1.6	1.2	13%	1.5	1.3	13%
Early	0.4	0.3	3%	2.2	2.2	22%
Medium	0.8	0.6	6%	0.8	0.6	6%
Late	2.7	2.7	35%	1.1	1.0	10%
HS	1.4	0.9	9%	1.7	1.3	13%
MS	2.1	1.6	18%	1.7	1.4	14%
LS	1.7	1.4	17%	1.4	1.3	15%
UN	1.2	1.0	10%	1.1	1.1	10%

HS: High stable, MS: medium stable, LS: Low stable, and UN: Unstable.

4.5. Discussion

Assuming uniform spatial and temporal maize emergence can result in biased simulated crop yield under uneven crop emergence conditions. Crop models have been used to assess the spatial and temporal variation in crop yields (Basso et al., 2007, 2011; Sadler et al., 2000), but the temporal variation of crop emergence still needs to be incorporated into crop models to improve crop yield prediction accuracy. This study is believed to be the first attempt to integrate spatial and temporal variation in crop emergence, ML, UAV images, and crop modeling.

The LiDAR images showed their usefulness in accurately obtaining plant height in several stages, with lower accuracy in the V6 stage, probably related to the plant size and lower soil coverage increasing the chances to mismatch the coordinate point to extract the data from the actual plant position. LiDAR images have been successfully used to estimate several crop's height (Wang et al., 2023; Zhang et al., 2021). One disadvantage of LiDAR technology that gathers extensive datasets is the high level of analysis and interpretation required and the sensors are highly power-consuming (Debangshi, 2022).

We demonstrated that maize emergence can be adequately estimated using ML and plant height derived from LiDAR images to develop maps with the spatial variability of emergence. Recent studies by Liu et al. (2023) and Vong et al. (2022) have explored maize emergence estimation by combining ML and UAV images with accurate results. The former developed a system to estimate maize emergence uniformity considering seedling count, size, uniformity, and plant distribution with accuracies around 90%. They highlighted the negative effects of shadows and plant density on the estimation accuracy. However, their research was conducted in small plots and lacked a comprehensive investigation of time to emerge and the impact of temporal variability on crop yield. Vong et al. (2022) developed maps of spatial and temporal variability

of maize emergence as well as plant density and plant spatial variability. They estimated plant emergence for several planting depths and showed that with shallower planting depths plants emerge earlier. Even though their studies were made at the field scale, they did not analyze the impact of emergence variability on crop yield. In our study, we estimated emergence spatial and temporal variability and we incorporated this into a crop model to better understand the impact of delayed emergence in crop yield spatial variation.

We conclude from our research that accounting for emergence temporal variation improves Salus maize yield simulation. Although the overall RMSE did not change with the incorporation of variability in emergence, accounting for the delay in emergence improved the estimation of Late emerged plants, which went from 35% RRMSE when simulated with a unique emergence to a 10% RRMSE when emergence delay was considered in the simulation. Previous research has demonstrated the improvement in simulation results when accounting for crop heterogeneity (spatial and temporal) (Pommel et al., 2002), but different planting dates were simulated to generate the temporal variation in emergence. An accurate assessment of crop emergence variability may help farmers make timely field management decisions to increase maize yield and by adjusting spatial fertilizer inputs and potentially reduce environmental impacts of fertilizer applications.

4.6. Conclusions

In this study we have presented a novel approach that integrates UAV imagery, machine learning, and crop model simulations to estimate the spatial and temporal variability of maize emergence and enhance yield simulation. We successfully estimated maize emergence using crop height derived from UAV's images at several stages and incorporated the variation in emergence into the crop model. Incorporating the temporal variation of emergence enhanced

maize yield simulation in the MS and LS yield stability zones. This accurate assessment of crop emergence variability has the potential to provide farmers with valuable information for making timely field management decisions, thereby increasing their profitability while mitigating environmental risks.

CHAPTER 5: CONCLUSIONS

This dissertation has presented the effect of maize plant emergence across commercial fields and within sub-field yield stability zones on crop yield and yield components (Chapter 2), and nitrogen uptake and nitrogen use efficiency (Chapter 3). The data generated on emergence variability was incorporated into crop models through the integration of UAV's images and ML (Chapter 4).

Chapter 1 established the context and significance of this dissertation. It included an overview of maize's importance in the world's agricultural systems and the current state of knowledge about maize emergence spatial and temporal variability.

Chapter 2 presented a comparison of maize plant emergence in several commercial fields and within sub-field YSZ. The analysis evaluated the effect of delayed emergence on crop yield and yield components. Our findings indicate that temporal variability has a greater impact on crop yield and its components compared to spatial variability within rows. The reduction in maize yield resulting from delayed emergence did not show a statistically significant correlation with yield stability zones, but delayed emergence had a more detrimental effect in the low yield stability zones.

Chapter 3 assessed the variability in biomass accumulation, nitrogen concentration, nitrogen uptake, and nitrogen use efficiency in plants with spatial and temporal variability in emergence across YSZ. Maize plants emerging later had a reduction in grain per plant possibly caused by a reduction in PGR around silking (R1) and exhibit lower nitrogen accumulation compared to those plants that emerged earlier, leading to changes in the partitioning of nitrogen within the maize plants. Although the percentage of nitrogen in the grain remained unchanged with delayed emergence, there was an increase in the percentage of nitrogen in the biomass due

to reduced total biomass and altered partitioning possibly due to a lack of sink. As a result, nitrogen use efficiency was diminished in the late-emerging and dominated maize plants.

Chapter 4 assessed the impact of incorporating spatial and temporal variability of maize emergence into crop model simulation on crop yield estimation. We used an innovative methodology combining UAV imagery, machine learning, and crop model simulations to estimate the spatial and temporal variation in maize emergence to improve yield prediction. We successfully estimated maize emergence by analyzing crop height and integrated the variation in emergence into the crop model. We demonstrated that incorporating the temporal variation of emergence has a positive impact on the simulation of maize yield, particularly in the MS and LS yield stability zones.

REFERENCES

Aggarwal, P., Vyas, S., Thornton, P., Campbell, B. M., & Kropff, M. (2019). Importance of considering technology growth in impact assessments of climate change on agriculture. In *Global Food Security* (Vol. 23, pp. 41–48). Elsevier B.V. https://doi.org/10.1016/j.gfs.2019.04.002

Albarenque, S., Basso, B., Caviglia, O. P., & Melchiori, R. J. M. (2016). Spatio-temporal nitrogen fertilizer response in maize: Field study and modeling approach. *Agronomy Journal*, *108*(5). https://doi.org/10.2134/agronj2016.02.0081

Alexandratos, N., & Bruinsma, J. (2012). World Agriculture towards 2030/2050: the 2012 revision. *WORLD AGRICULTURE*. www.fao.org/economic/esa

Allen, D. J. (1990). A Look at the Remote Sensing Applications Program of the National Agricultural Statistics Service. *Journal of Official Statistics*, *6*(4), 393–409.

Andrade, F., Cirilo, A., Uhart, S., Otegui, M. (1996). *Ecofisiología del cultivo de maíz*. Ed La Barrosa, Balcarce, Buenos Aires.

Andrade, F. H., & Abbate, P. E. (2005). Response of maize and soybean to variability in stand uniformity. *Agronomy Journal*, *97*(4), 1263–1269. https://doi.org/10.2134/agronj2005.0006

Andrade, F. H., Vega, C., Uhart, S., Cirilo, A., Cantarero, M., & Valentinuz, O. (1999). Kernel number determination in maize. *Crop Science*, *39*(2), 453–459. https://doi.org/10.2135/cropsci1999.0011183X0039000200026x

Andrade, F., Otegui, M. E., Cirilo, A., & Uhart, S. (2023). *Ecofisiología y manejo del cultivo de maíz* (F. Andrade, M. E. Otegui, A. Cirilo, & S. Uhart, Eds.; 1st ed).

Andrade, J. F., Cassman, K. G., Rattalino Edreira, J. I., Agus, F., Bala, A., Deng, N., & Grassini, P. (2022). Impact of urbanization trends on production of key staple crops. *Ambio*, *51*, 1158–1167. https://doi.org/10.1007/s13280

Basso, B., Bertocco, M., Sartori, L., & Martin, E. C. (2007). Analyzing the effects of climate variability on spatial pattern of yield in a maize-wheat-soybean rotation. *European Journal of Agronomy*, *26*(2), 82–91. https://doi.org/10.1016/j.eja.2006.08.008

Basso, B., & Liu, L. (2019). Seasonal crop yield forecast: Methods, applications, and accuracies. In *Advances in Agronomy* (Vol. 154, pp. 201–255). Academic Press Inc. https://doi.org/10.1016/bs.agron.2018.11.002

Basso, B., & Ritchie, J. T. (2015). *Simulating Crop Growth and Biogeochemical Fluxes in Response to Land Management Using the SALUS Model*.

Basso, B., Ritchie, J. T., Cammarano, D., & Sartori, L. (2011). A strategic and tactical management approach to select optimal N fertilizer rates for wheat in a spatially variable field. *Europ. J. Agronomy*, *35*, 215–222. https://doi.org/10.1016/j.eja.2011.06.004

Basso, B., Ritchie, J. T., Grace, P. R., & Sartori, L. (2006). Simulation of Tillage Systems Impact on Soil Biophysical Properties Using the SALUS Model. In *Ital. J. Agron. / Riv. Agron* (Vol. 4).

Batchelor, W. D., Basso, B., & Paz, J. O. (2002). Examples of strategies to analyze spatial and temporal yield variability using crop models. *European Journal of Agronomy*, *18*, 141–158. www.elsevier.com/locate/eja

Bonelli, L. E., Monzon, J. P., Cerrudo, A., Rizzalli, R. H., & Andrade, F. H. (2016). Maize grain yield components and source-sink relationship as affected by the delay in sowing date. *Field Crops Research*, *198*, 215–225. https://doi.org/10.1016/j.fcr.2016.09.003

Boomsma, C. R., Santini, J. B., Tollenaar, M., & Vyn, T. J. (2009). Maize morphophysiological responses to intense crowding and low nitrogen availability: An analysis and review. *Agronomy Journal*, *101*(6), 1426–1452. https://doi.org/10.2134/agronj2009.0082

Borrás, L., & Vitantonio-Mazzini, L. N. (2018). Maize reproductive development and kernel set under limited plant growth environments. *Journal of Experimental Botany*, *69*(13), 3235–3243. https://doi.org/10.1093/jxb/erx452

Cammarano, D., van Evert, F. K., & Kempenaar, C. (2023). *Progress in Precision Agriculture Precision Agriculture: Modelling* (D. Cammarano, F. van Evert, & C. Kempenaar, Eds.; Vol. 1). Springer.

Carter, P., Nafziger, E., & Lauer, J. (1990). Uneven emergence in corn. *Corn.Agronomy.Wisc.Edu*, *344*.

Carter, P. R., & Nafziger, E. D. (1991). Uneven Emergence in Corn. *North Central Regional Extension Publication*, *344*.

Carter, P. R., Nafziger, E. D., & Hick, D. R. (2019). Effects of Uneven Seedling Emergence in Corn. *Service, Cooperative Extension Lafayette, West*, 1–6.

Casper, B. B., & Jackson, R. B. (1997). Plant competition underground. *Annual Review of Ecology and Systematics*, *337*(6203), 122. https://doi.org/10.1038/337122b0

Cassman, K. G., & Dobermann, A. (2022). Nitrogen and the future of agriculture: 20 years on: This article belongs to Ambio's 50th Anniversary Collection. Theme: Solutions-oriented research. *Ambio*, *51*(1), 17–24. https://doi.org/10.1007/s13280-021-01526-w

Caviglia, O. P., & Melchiori, R. J. M. (2011). Contribution of contrasting plant hierarchies to the response to N fertilizer in maize. *Field Crops Research*, *122*(2), 131–139. https://doi.org/10.1016/j.fcr.2011.03.011

Caviglia, O. P., Sadras, V. O., & Andrade, F. H. (2013). Modelling long-term effects of cropping intensification reveals increased water and radiation productivity in the South-eastern Pampas. *Field Crops Research*, *149*, 300–311. https://doi.org/10.1016/J.FCR.2013.05.003

Ciampitti, I. a., & Vyn, T. J. (2013). Grain nitrogen source changes over time in maize: A review. *Crop Science*, *53*(2), 366–377. https://doi.org/10.2135/cropsci2012.07.0439

Cox, W. J., & Cherney, J. H. (2015). Field-scale studies show site-specific corn population and yield responses to seeding depths. *Agronomy Journal*, *107*(6), 2475–2481. https://doi.org/10.2134/agronj15.0308

D'Andrea, K. E., Otegui, M. E., & Cirilo, A. G. (2008). Kernel number determination differs among maize hybrids in response to nitrogen. *Field Crops Research*, *105*(3), 228–239. https://doi.org/10.1016/j.fcr.2007.10.007

Daynard, T. B., & Muldoon, J. F. (1983). Plant-to-plant variability of maize plants grown at different densities. *Can. J. Plant Sci.*, *63*, 45–59. https://doi.org/10.1163/1937240X-00002218

Debangshi, U. (2022). *LiDAR Sensor: Applications in Agriculture*. https://doi.org/10.5281/zenodo.7051446

Echarte, L., Andrade, F. H., Vega, C. R. C., & Tollenaar, M. (2004). Kernel number determination in argentinean maize hybrids released between 1965 and 1993. *Crop Science*, *44*(5), 1654–1661. https://doi.org/10.2135/cropsci2004.1654

Edmeades, G. O., & DAYNARD, T. B. (1979). The development of plant-to-plant variability in maize at different planting densities. *Canadian Journal of Plant Science*, *59*(3), 561–576.

Egli, D. B., & Rucker, M. (2012). Seed vigor and the uniformity of emergence of corn seedlings. *Crop Science*, *52*(6), 2774–2782. https://doi.org/10.2135/cropsci2012.01.0064

Environmental Systems Research Institute. (2021). *ArcGIS* (10.08.2). ESRI.

Fabbri, C., Basso, B., Napoli, M., Dalla Marta, A., Orlandini, S., & Martinez-Feria, R. A. (2023). Developing a tactical nitrogen fertilizer management strategy for sustainable wheat production. *European Journal of Agronomy*, *144*. https://doi.org/10.1016/j.eja.2023.126746

Feng, A., Zhou, J., Vories, E., & Sudduth, K. A. (2020). Evaluation of cotton emergence using UAV-based imagery and deep learning. *Computers and Electronics in Agriculture*, *177*. https://doi.org/10.1016/j.compag.2020.105711

Fischer, R. A. (1985). Number of kernels in wheat crops and the influence of solar radiation and temperature. *The Journal of Agricultural Science*, *105*(2), 447–461. https://doi.org/10.1017/S0021859600056495

Ford, J. H., & Hicks, D. R. (1992). Corn Growth and Yield in Uneven Emerging Stands. *Journal of Production Agriculture*, *5*(1), 185–188. https://doi.org/10.2134/jpa1992.0185

Gnädinger, F., & Schmidhalter, U. (2017). Digital Counts of Maize Plants by Unmanned Aerial Vehicles (UAVs). *Remote Sensing 2017, Vol. 9, Page 544*, *9*(6), 544. https://doi.org/10.3390/RS9060544

Guo, Y., Xiao, Y., Li, M. W., Hao, F., Zhang, X., Sun, H., de Beurs, K., Fu, Y. H., & He, Y. (2022). Identifying crop phenology using maize height constructed from multi-sources images. In *International Journal of Applied Earth Observation and Geoinformation* (Vol. 115). Elsevier B.V. https://doi.org/10.1016/j.jag.2022.103121

Gupta, S. C. (1985). Predicting Corn Planting Dates for Moldboard and No-till Tillage Systems in the Corn Belt 1. *Agronomy Journal*, *77*(3), 446–455. https://doi.org/10.2134/agronj1985.00021962007700030021x

Hall, A. J., & Richards, R. A. (2013). Prognosis for genetic improvement of yield potential and water-limited yield of major grain crops. *Field Crops Research*, *143*, 18–33. https://doi.org/10.1016/J.FCR.2012.05.014

Hoffmann, M. P., Haakana, M., Asseng, S., Höhn, J. G., Palosuo, T., Ruiz-Ramos, M., Fronzek, S., Ewert, F., Gaiser, T., Kassie, B. T., Paff, K., Rezaei, E. E., Rodríguez, A., Semenov, M., Srivastava, A. K., Stratonovitch, P., Tao, F., Chen, Y., & Rötter, R. P. (2018). How does inter-annual variability of attainable yield affect the magnitude of yield gaps for wheat and

maize? An analysis at ten sites. *Agricultural Systems*, *159*, 199–208. https://doi.org/10.1016/j.agsy.2017.03.012

Hornung, A., Khosla, R., Reich, R., Inman, D., & Westfall, D. G. (2006). Comparison of site-specific management zones: Soil-color-based and yield-based. *Agronomy Journal*, *98*(2), 407–415. https://doi.org/10.2134/agronj2005.0240

Huggins, D. R., & Pan, W. L. (1993). Nitrogen Efficiency Component Analysis: An Evaluation of Cropping System Differences in Productivity. *Agronomy Journal*, *85*(4), 898–905. https://doi.org/10.2134/AGRONJ1993.00021962008500040022X

Hunt, E. R., & Daughtry, C. S. T. (2017). What good are unmanned aircraft systems for agricultural remote sensing and precision agriculture? *Https://Doi.Org/10.1080/01431161.2017.1410300*, *39*(15–16), 5345–5376. https://doi.org/10.1080/01431161.2017.1410300

James, G., Witten, D., Hastie, T., & Tibshirani, R. (2021). *An Introduction to Statistical Learning with Applications in R Second Edition*.

Janssen, B. H. (1996). Nitrogen mineralization in relation to C:N ratio and decomposability of organic materials. *Plant and Soil*, *181*, 39–45.

Kant, S., Bi, Y. M., & Rothstein, S. J. (2011). Understanding plant response to nitrogen limitation for the improvement of crop nitrogen use efficiency. In *Journal of Experimental Botany* (Vol. 62, Issue 4, pp. 1499–1509). https://doi.org/10.1093/jxb/erq297

Kasperbauer, M. J., & Karlen, D. L. (1994). Plant spacing and reflected far-red light effects on phytochrome-regulated photosynthate allocation in corn seedlings. *Crop Science*, *34*(6), 1564–1569. https://doi.org/10.2135/cropsci1994.0011183X003400060027x

Knappenberger, T., & Köller, K. (2012). Spatial assessment of the correlation of seeding depth with emergence and yield of corn. *Precision Agriculture*, *13*(2), 163–180. https://doi.org/10.1007/s11119-011-9235-4

Kolling, D. F., Sangoi, L., Leolato, L. S., Panison, F., Coelho, A. E., & Kuneski, H. F. (2019). Can an increase in nitrogen rate mitigate damages caused by uneven spatial distribution of maize plants at the sowing row? *Acta Scientiarum - Agronomy*, *41*(1). https://doi.org/10.4025/actasciagron.v41i1.39874

Lark, T. J., Spawn, S. A., Bougie, M., & Gibbs, H. K. (2020). Cropland expansion in the United States produces marginal yields at high costs to wildlife. *Nature Communications*, *11*(1). https://doi.org/10.1038/s41467-020-18045-z

Lauer, J. G., & Rankin, M. (2004). Corn response to within row plant spacing variation. *Agronomy Journal*, *96*(5), 1464–1468. https://doi.org/10.2134/agronj2004.1464

Lawles, K., Raun, W., Desta, K., & Freeman, K. (2012). Effect of delayed emergence on corn grain yields. *Journal of Plant Nutrition*, *35*(3), 480–496. https://doi.org/10.1080/01904167.2012.639926

Lemaire, G., & Gastal, F. (2019). Crop responses to nitrogen. In: Crop Science. R. Savin & G. Slafer, Eds. https://doi.org/https://doi.org/10.1007/978-1-4939-2493-6_385-4

Lemaire, G., & Gastal, F. (2019). Crop responses to Nitrogen. In R. Savin & G. A. Slafer (Eds.), *Crop Science* (pp. 0–516). Springer Nature 2019.

Li, B., Xu, X., Han, J., Zhang, L., Bian, C., Jin, L., & Liu, J. (2019). The estimation of crop emergence in potatoes by UAV RGB imagery. *Plant Methods*, *15*(1). https://doi.org/10.1186/s13007-019-0399-7

Liu, J., You, L., Amini, M., Obersteiner, M., Herrero, M., Zehnder, A. J. B., & Yang, H. (2010). A high-resolution assessment on global nitrogen flows in cropland. *Proceedings of the National Academy of Sciences of the United States of America*, *107*(17), 8035–8040. https://doi.org/10.1073/PNAS.0913658107

Liu, L., & Basso, B. (2017). *Spatial evaluation of maize yield in Malawi*. https://doi.org/10.1016/j.agsy.2017.07.014

Liu, L., Danquah, E. O., Weebadde, C., Bessah, E., & Basso, B. (2021). Modeling soil organic carbon and yam yield under different agronomic management across spatial scales in Ghana. *Field Crops Research*, *263*. https://doi.org/10.1016/j.fcr.2020.108018

Liu, M., Su, W. H., & Wang, X. Q. (2023). Quantitative Evaluation of Maize Emergence Using UAV Imagery and Deep Learning. *Remote Sensing*, *15*(8). https://doi.org/10.3390/rs15081979

Liu, T., Li, R., Jin, X., Ding, J., Zhu, X., Sun, C., & Guo, W. (2017). Evaluation of seed emergence uniformity of mechanically sown wheat with UAV RGB imagery. *Remote Sensing*, *9*(12). https://doi.org/10.3390/rs9121241

Liu, W., Tollenaar, M., Stewart, G., & Deen, W. (2004a). Impact of planter type, planting speed, and tillage on stand uniformity and yield of corn. *Agronomy Journal*, *96*(6), 1668–1672. https://doi.org/10.2134/agronj2004.1668

Liu, W., Tollenaar, M., Stewart, G., & Deen, W. (2004b). Response of corn grain yield to spatial and temporal variability in emergence. *Crop Science*, *44*(3), 847–854. https://doi.org/10.2135/cropsci2004.8470

Liu, W., Tollenaar, M., Stewart, G., & Deen, W. (2004c). Within-Row Plant Spacing Variability Does Not affect Corn Yield. *Agronomy Journal*, *96*, 275–280.

Maddonni, G. A., & Otegui, M. E. (2004). Intra-specific competition in maize: Early establishment of hierarchies among plants affects final kernel set. *Field Crops Research*, *85*(1), 1–13. https://doi.org/10.1016/S0378-4290(03)00104-7

Maddonni, G. A., Otegui, M. E., Andrieu, B., Chelle, M., & Casal, J. J. (2002). Maize leaves turn away from neighbors. *Plant Physiology*, *130*(3), 1181–1189. https://doi.org/10.1104/pp.009738

Maestrini, B., & Basso, B. (2018). Predicting spatial patterns of within- fi eld crop yield variability. *Field Crops Research*, *219*(January), 106–112. https://doi.org/10.1016/j.fcr.2018.01.028

Maestrini, B., & Basso, B. (2021). Subfield crop yields and temporal stability in thousands of US Midwest fields. *Precision Agriculture*, *22*(6), 1749–1767. https://doi.org/10.1007/s11119-021-09810-1

Maltese, N. E., Maddonni, G. A., Melchiori, R. J. M., Ciampitti, I. A., & Caviglia, O. P. (2023). Field Crops Research The allometric relationships between biomass and nitrogen of vegetative organs affect crop N status in maize at silking stage. *Field Crops Research*, *294*(January), 108861. https://doi.org/10.1016/j.fcr.2023.108861

Martin, K. L., Hodgen, P. J., Freeman, K. W., Melchiori, R., Arnall, D. B., Teal, R. K., Mullen, R. W., Desta, K., Phillips, S. B., Solie, J. B., Stone, M. L., Caviglia, O., Solari, F., Bianchini, A., Francis, D. D., Schepers, J. S., Hatfield, J. L., & Raun, W. R. (2005). Plant-to-plant variability in corn production. *Agronomy Journal*, *97*(6), 1603–1611. https://doi.org/10.2134/agronj2005.0129

Martinez-Feria, R. A., Castellano, M. J., Dietzel, R. N., Helmers, M. J., Liebman, M., Huber, I., & Archontoulis, S. V. (2018). Linking crop- and soil-based approaches to evaluate system

nitrogen-use efficiency and tradeoffs. *Agriculture, Ecosystems and Environment*, *256*, 131–143. https://doi.org/10.1016/j.agee.2018.01.002

Mayer, L. I., Rossini, M. A., & Maddonni, G. A. (2012). Inter-plant variation of grain yield components and kernel composition of maize crops grown under contrasting nitrogen supply. *Field Crops Research*, *125*, 98–108. https://doi.org/10.1016/j.fcr.2011.09.004

Mead, R., Curnow, R. N., & Hasted, A. M. (2003). Statistical methods in agriculture and experimental biology (C. Chatfield, J. Lindsey, M. Tanner, & J. Zidek, Eds.; Third edition). Chapman & Hall/CRC.

Moll, R. H., Kamprath, E. J., & Jackson, W. A. (1982). Analysis and Interpretation of Factors Which Contribute to Efficiency of Nitrogen Utilization 1 . *Agronomy Journal*, *74*(3), 562–564. https://doi.org/10.2134/AGRONJ1982.00021962007400030037X

Mueller, S. M., Messina, C. D., & Vyn, T. J. (2019). Simultaneous gains in grain yield and nitrogen efficiency over 70 years of maize genetic improvement. *Scientific Reports*, *9*(1). https://doi.org/10.1038/s41598-019-45485-5

Mulla, D. J. (2013). Twenty five years of remote sensing in precision agriculture: Key advances and remaining knowledge gaps. *Biosystems Engineering*, *114*(4), 358–371. https://doi.org/10.1016/J.BIOSYSTEMSENG.2012.08.009

Nafziger, E. D., Carter, P. R., & Graham, E. E. (1991). Response of Corn to Uneven Emergence. *Crop Science*, *31*(3), 811–815. https://doi.org/10.2135/cropsci1991.0011183x003100030053x

Nemergut, K. T., Thomison, P. R., Carter, P. R., & Lindsey, A. J. (2021). Planting depth affects corn emergence, growth and development, and yield. *Agronomy Journal*, *113*(4), 3351–3360. https://doi.org/10.1002/agj2.20701

Nielsen, R. L. (1993). *Planting Speed Effects on Stand Establishment and Grain Yield of Corn*.

Novak, L., & Ransom, J. (2018). Factors Impacting Corn (Zea mays L.) Establishment and the Role of Uniform Establishment on Yield. *Agricultural Sciences*, *09*(10), 1317–1336. https://doi.org/10.4236/as.2018.910092

Novelli, L. E., Caviglia, O. P., Jobbágy, E. G., & Sadras, V. O. (2023). Diversified crop sequences to reduce soil nitrogen mining in agroecosystems. *Agriculture, Ecosystems and Environment*, *341*. https://doi.org/10.1016/J.AGEE.2022.108208

O'Brien, P. L., & Hatfield, J. L. (2021). Plant-to-plant biomass and yield variability in corn–soybean rotations under three tillage regimes. *Agronomy Journal*, *113*(1), 370–380. https://doi.org/10.1002/agj2.20514

Otegui, M. E., Cirilo, A. G., Uhart, S. A., & Andrade, F. H. (2020). Maize. In *Crop Physiology Case Histories for Major Crops* (pp. 2–43). Elsevier. https://doi.org/10.1016/B978-0-12-819194-1.00001-3

Pagano, E., & Maddonni, G. A. (2007). Intra-specific competition in maize: Early established hierarchies differ in plant growth and biomass partitioning to the ear around silking. *Field Crops Research*, *101*(3), 306–320. https://doi.org/10.1016/j.fcr.2006.12.007

Pajares, G. (2015). Overview and current status of remote sensing applications based on unmanned aerial vehicles (UAVs). *Photogrammetric Engineering and Remote Sensing*, *81*(4), 281–329. https://doi.org/10.14358/PERS.81.4.281

Parra, G., Borrás, L., & Gambin, B. L. (2022). Crop attributes explaining current grain yield dominance of maize over sorghum. *Field Crops Research*, *275*(August 2021). https://doi.org/10.1016/j.fcr.2021.108346

Pierce, F. J., & Nowak, P. (1999). *ASPECTS OF PRECISION AGRICULTURE*.

Pilgrim, C. (2021). Piecewise-regression (aka segmented regression) in Python. *Journal of Open Source Software*, *6*(68), 3859. https://doi.org/10.21105/joss.03859

Pommel, B., Mouraux, D., Cappellen, O., & Ledent, J. F. (2002). Influence of delayed emergence and canopy skips on the growth and development of maize plants: A plant scale approach with CERES-Maize. *European Journal of Agronomy*, *16*(4), 263–277. https://doi.org/10.1016/S1161-0301(01)00130-7

Pradhan, P., Fischer, G., Van Velthuizen, H., Reusser, D. E., & Kropp, J. P. (2015). Closing yield gaps: How sustainable can we be? *PLoS ONE*, *10*(6). https://doi.org/10.1371/journal.pone.0129487

Probst, P., & Bischl, B. (2019). Tunability: Importance of Hyperparameters of Machine Learning Algorithms. In *Journal of Machine Learning Research* (Vol. 20). http://jmlr.org/papers/v20/18-444.html.

Puntel, L. A., Sawyer, J. E., Barker, D. W., Dietzel, R., Poffenbarger, H., Castellano, M. J., Moore, K. J., Thorburn, P., & Archontoulis, S. V. (2016). Modeling long-term corn yield

response to nitrogen rate and crop rotation. *Frontiers in Plant Science*, *7*(November 2016), 1630. https://doi.org/10.3389/FPLS.2016.01630/BIBTEX

Raun, W. R., & Johnson, G. V. (1999). Improving Nitrogen Use Efficiency for Cereal Production. *Agronomy Journal*, *91*(3), 357–363.

Ritchie, S.W., Hanway, J.J., Benson, G. O. (1986). How a corn plant develops. *Special Report, Iowa State University of Science and Technology*, *48*, 21.

Robertson, G. P., & Vitousek, P. M. (2009). Nitrogen in agriculture: Balancing the cost of an essential resource. *Annual Review of Environment and Resources*, *34*, 97–125. https://doi.org/10.1146/annurev.environ.032108.105046

Rossini, M. A., Maddonni, G. A., & Otegui, M. E. (2011). Inter-plant competition for resources in maize crops grown under contrasting nitrogen supply and density: Variability in plant and ear growth. *Field Crops Research*, *121*(3), 373–380. https://doi.org/10.1016/j.fcr.2011.01.003

Rossini, M. A., Maddonni, G. A., & Otegui, M. E. (2012). Inter-plant variability in maize crops grown under contrasting N×stand density combinations: Links between development, growth and kernel set. *Field Crops Research*. https://doi.org/10.1016/j.fcr.2012.03.010

Rossini, M. A., Otegui, M. E., Martínez, E. L., & Maddonni, G. A. (2018). Contribution of the early-established plant hierarchies to maize crop responses to N fertilization. *Field Crops Research*. https://doi.org/10.1016/j.fcr.2017.11.015

Rotundo, J. L., Borrás, L., De Bruin, J., & Pedersen, P. (2012). Physiological strategies for seed number determination in soybean: Biomass accumulation, partitioning and seed set efficiency. *Field Crops Research*, *135*, 58–66. https://doi.org/10.1016/j.fcr.2012.06.012

Rutto, E., Daft, C., Kelly, J., Chim, B. K., Mullock, J., Torres, G., & Raun, W. (2014). Effect of Delayed Emergence on Corn (Zea Mays L.) Grain Yield. *Journal of Plant Nutrition*, *37*(2), 198–208. https://doi.org/10.1080/01904167.2013.859691

Sadler, E. J., Bauer, P. J., Busscher, W. J., & Millen, J. A. (2000). Site-Specific Analysis of a Droughted Corn Crop: II. Water Use and Stress. *Agronomy Journal*, *92*, 403–410.

Sangoi, L., Schmitt, A., Vieira, J., José Picoli, G. J., Arruda Souza, C., Trezzi Casa, R., Eduardo Schenatto, D., Giordani, W., Majolo Boniatti, C., Cardoso Machado, G., & Horn, D. (2012). Plant Spatial Variability in the Sowing Row and Mazie Grain Yield. *Revista Brasileira de Milho e Sorgo*, *11*(3), 268–277. http://www.abms.org.br

Schonlau, M., & Zou, R. Y. (2020). The random forest algorithm for statistical learning. *The Stata Journal*, *20*(1), 3–29. https://doi.org/10.1177/1536867X20909688

Semmartin, M., Cosentino, D., Poggio, S. L., Benedit, B., Biganzoli, F., & Peper, A. (2023). Soil carbon accumulation in continuous cropping systems of the rolling Pampa (Argentina): The role of crop sequence, cover cropping and agronomic technology. *Agriculture, Ecosystems & Environment*, *347*, 108368. https://doi.org/10.1016/J.AGEE.2023.108368

Shahhosseini, M., Hu, G., Huber, I., & Archontoulis, S. V. (2021). Coupling machine learning and crop modeling improves crop yield prediction in the US Corn Belt. *Scientific Reports*, *11*(1). https://doi.org/10.1038/s41598-020-80820-1

Shiferaw, B., Prasanna, B. M., Hellin, J., & Bänziger, M. (2011). Crops that feed the world 6. Past successes and future challenges to the role played by maize in global food security. In *Food Security* (Vol. 3, Issue 3, pp. 307–327). https://doi.org/10.1007/s12571-011-0140-5

Shirzadifar, A., Maharlooei, M., Bajwa, S. G., Oduor, P. G., & Nowatzki, J. F. (2020). Mapping crop stand count and planting uniformity using high resolution imagery in a maize crop. *Biosystems Engineering*, *200*, 377–390. https://doi.org/10.1016/J.BIOSYSTEMSENG.2020.10.013

Shuai, G., Martinez-Feria, R. A., Zhang, J., Li, S., Price, R., & Basso, B. (2019). Capturing Maize Stand Heterogeneity Across. *Sensors (Switzerland)*, *19*(20). https://doi.org/doi:10.3390/s19204446

Smil, V. (1999). Nitrogen in crop production: An account of global flows. *Global Biogeochemical Cycles*, *13*(2), 647–662. https://doi.org/10.1029/1999GB900015

Smil, V. (2004). *Enriching the Earth: Fritz Haber, Carl Bosch, and the Transformation of World Food Production*. MIT press. https://books.google.com/books?hl=en&lr=&id=G9FljcEASycC&oi=fnd&pg=PP15&ots=qQ_UOFWTQG&sig=SqJwKuIMeNzfr0ZAj4k2iuuuV2Q#v=onepage&q&f=false

Tollenaar, M., Deen, W., Echarte, L., & Liu, W. (2006). Effect of crowding stress on dry matter accumulation and harvest index in maize. *Agronomy Journal*, *98*(4), 930–937. https://doi.org/10.2134/agronj2005.0336

Tollenaar, M., & Lee, E. A. (2002). Yield potential, yield stability and stress tolerance in maize. *Field Crops Research*, *75*, 161–169.

Tollenaar, M., & Wu, J. (1999). Yield improvement in temperate maize is attributable to greater stress tolerance. *Crop Science*, *39*(6), 1597–1604. https://doi.org/10.2135/cropsci1999.3961597x

UN FAO. (n.d.). *Food and Agriculture Organization of the United Nations*. 2023. Retrieved April 20, 2023, from https://www.fao.org/faostat/es/#data/QCL

USDA ERS - Fertilizer Use and Price. (2023). https://www.ers.usda.gov/data-products/fertilizer-use-and-price.aspx

Van Ittersum, M. K., & Cassman, K. G. (2013). Yield gap analysis-Rationale, methods and applications-Introduction to the Special Issue. *Field Crops Research*, *143*, 1–3. https://doi.org/10.1016/J.FCR.2012.12.012

Velumani, K., Lopez-Lozano, R., Madec, S., Guo, W., Gillet, J., Comar, A., & Baret, F. (2021). *Estimates of Maize Plant Density from UAV RGB Images Using Faster-RCNN Detection Model: Impact of the Spatial Resolution*. https://doi.org/10.34133/2021/9824843

Vitousek, P. M., Naylor, R., Crews, T., David, M. B., Drinkwater, L. E., Holland, E., Johnes, P. J., Katzenberger, J., Martinelli, L. A., Matson, P. A., Nziguheba, G., Ojima, D., Palm, C. A., Robertson, G. P., Sanchez, P. A., Townsend, A. R., & Zhang, F. S. (2009). Nutrient imbalances in agricultural development. In *Science* (Vol. 324, Issue 5934, pp. 1519–1520). https://doi.org/10.1126/science.1170261

Vong, C. N., Conway, L. S., Feng, A., Zhou, J., Kitchen, N. R., & Sudduth, K. A. (2022). Corn emergence uniformity estimation and mapping using UAV imagery and deep learning. *Computers and Electronics in Agriculture*, *198*. https://doi.org/10.1016/j.compag.2022.107008

Wang, H., Zhang, W., Yang, G., Lei, L., Han, S., Xu, W., Chen, R., Zhang, C., & Yang, H. (2023). Maize Ear Height and Ear–Plant Height Ratio Estimation with LiDAR Data and Vertical Leaf Area Profile. *Remote Sensing*, *15*(4). https://doi.org/10.3390/rs15040964

Wang, L. (2021). Data Driven Explanation of Temporal and Spatial Variability of Maize Yield in the United States. *Frontiers in Plant Science*, *12*. https://doi.org/10.3389/fpls.2021.701192

Waqas, M., Hawkesford, M. J., & Geilfus, C.-M. (2023). Feeding the world sustainably: efficient nitrogen use. *Trends in Plant Science*. www.fao.org/3/i6583e/i6583e.pdf

Wu, F., & Guclu, H. (2013). Global Maize Trade and Food Security: Implications from a Social Network Model. *Risk Analysis*, *33*(12), 2168–2178. https://doi.org/10.1111/risa.12064

Zhang, C., & Kovacs, J. M. (2012). The application of small unmanned aerial systems for precision agriculture: A review. *Precision Agriculture*, *13*(6), 693–712. https://doi.org/10.1007/S11119-012-9274-5/FIGURES/3

Zhang, Y., Xia, C., Zhang, X., Cheng, X., Feng, G., Wang, Y., & Gao, Q. (2021). Estimating the maize biomass by crop height and narrowband vegetation indices derived from UAV-based hyperspectral images. *Ecological Indicators*, *129*. https://doi.org/10.1016/j.ecolind.2021.107985

Westgate, M.E., Otegui, M.E., and F.H. Andrade. (2004). Physiology of the corn plant. *In:* C.W. Smith, Beltran, and E.C.A. Runge. Corn: Origin, History, Technology, and Production. John Wiley & Sons, Inc. Hoboken, NJ.

APPENDIX A: CHAPTER 2 SUPPLEMENTAL TABLES AND FIGURES

Table 18. Analysis of variance of emergence (DAP, days after planting), growing space (GS), and yield stability zone (YSZ) on corn plant yield (g plant^{-1}), grain number (grain plant^{-1}), grain weight (g grain^{-1}), and crop yield (Mg ha^{-1}) at 10 field experiments.

Location	**Springport**						**Portland**			**Parana**
Year-Field	**2016-222**	**2017-222**	**2018-105**	**2019-304**	**2020-308**	**2021-210**	**2017-JS1**	**2018-NC12**	**2019-MG1**	**2020-11**
Source	Plant yield (g plant^{-1})									
YSZ	0.0528	0.0046	0.6771	0.6644	0.0003	<.0001	0.1813	0.26	0.2999	0.037
DAP	0.4588	<.0001	0.0001	0.3845	<.0001	<.0001	<.0001	0.066	0.0072	0.0026
DAP*YSZ	0.3663	0.7201	0.1928	0.6161	0.1275	0.0371	0.9189	0.6829	0.6651	0.3033
GS	0.8299	0.0946	0.5646	0.004	<.0001	<.0001	0.0001	0.967	0.0155	0.1271
GS*YSZ	0.0684	0.0313	0.6534	0.9818	0.1895	0.0002	0.3784	0.7024	0.3308	0.6496
	Grain number (grain plant^{-1})									
YSZ	0.0636	0.1741	0.7875	0.2409	0.0442	<.0001	0.1318	0.8005	0.1583	0.0338
DAP	0.4122	<.0001	<.0001	0.9668	<.0001	<.0001	<.0001	0.0605	0.0373	0.0014
DAP*YSZ	0.5309	0.4361	0.0806	0.34	0.4342	0.0007	0.962	0.6581	0.7182	0.1163
GS	0.9999	0.2159	0.9875	0.0632	<.0001	<.0001	0.0004	0.5438	0.7612	0.4498
GS*YSZ	0.0428	0.2737	0.2921	0.7823	0.0008	<.0001	0.4384	0.7351	0.4306	0.6749
	Grain weight (g grain^{-1})									
YSZ	0.9852	0.0291	0.6431	0.6804	<.0001	0.1591	0.8508	0.0832	0.1558	0.7214
DAP	0.5973	0.1138	0.0655	0.2941	0.0415	0.0583	0.1228	0.3982	0.3055	0.8448
DAP*YSZ	0.7009	0.9846	0.4362	0.1129	0.1812	0.0012	0.1137	0.2238	0.5706	0.6787
GS	0.7302	0.2744	0.3943	0.0014	<.0001	0.8159	0.4155	0.3349	0.3353	0.376
GS*YSZ	0.6378	0.0603	0.445	0.6756	0.105	0.0071	0.8557	0.3537	0.4338	0.8999
	Yield (kg ha^{-1})									
YSZ	0.0324	<.0001	0.8799	0.3229	0.0555	0.0005	0.1681	0.3358	0.2242	0.0494
DAP	0.0499	<.0001	0.0003	0.4943	<.0001	<.0001	<.0001	0.1061	0.0023	0.004
DAP*YSZ	0.0652	0.7887	0.4559	0.646	0.7047	0.0118	0.804	0.7131	0.5509	0.2182
GS	0.0368	0.697	0.4996	0.0248	0.0001	0.0011	0.005	0.9325	0.0179	0.2632
GS*YSZ	0.03	0.517	0.3866	0.9402	0.5347	<.0001	0.2539	0.7831	0.2564	0.784

Table 19. Compared models for Springport, Portlan and Parana Sites. Full model, describe resuts using one function per yield stability zone (YSZ) (8 parameters); Simple YSZ model, describes the relationship between variables with one function (5 parameters); Simple model, describes the relationship between variables with one function (2 parameters).

Site	Variable		Model
Springport	Relative Plant yield	Full	RPY= 1.06 -0.07MS -0.14LS -0.23UN -0.03DAP_{HS} -0.02DAP_{MS} -0.02DAP_{LS} -0.02DAP_{UN}
		Simple YSZ	RPY = 0.96 -0.004MS -0.06LS -0.04UN -0.02DAP
		Simple	RPY = 0.97 -0.02DAP
	Relative grain number	Full	RGN= 1.14 -0.10MS -0.16LS -0.23UN -0.04DAP_{HS} -0.03DAP_{MS} -0.02DAP_{LS} -0.02DAP_{UN}
		Simple YSZ	RGN = 1.02 +0.02MS -0.02LS -0.05UN -0.02DAP
		Simple	RGN = 1.01 -0.02DAP
	Relative crop yield	Full	RY= 1.18 -0.12MS -0.43LS - 0.280UN -0.04DAP_{HS} -0.03DAP_{MS} -0.01DAP_{LS} -0.02DAP_{UN}
		Simple YSZ	RY = 1.04 -0.04MS -0.17LS -0.08UN -0.02DAP
		Simple	RY = 0.98 -0.03DAP
Portland	Relative Plant yield	Full	RPY= 1.13 +0.33MS +0.48LS +0.08UN -0.05DAP_{HS} -0.08DAP_{MS} -0.11DAP_{LS} -0.06DAP_{UN}
		Simple YSZ	RPY = 1.47 +0.04MS -0.15LS -0.08UN -0.07DAP
		Simple	RPY = 1.38 -0.06DAP
	Relative grain number	Full	RGN = 1.14 +0.15MS + 0.34LS -0.24UN -0.06DAP_{HS} -0.07DAP_{MS} -0.11DAP_{LS} -0.04DAP_{UN}
		Simple YSZ	RGN = 1.52 -0.02MS -0.21LS -0.09UN -0.06DAP
		Simple	RGN = 1.42 -0.06DAP
	Relative crop yield	Full	RY = 1.25 +0.40MS + 0.50LS +0.17UN -0.05DAP_{HS} -0.08DAP_{MS} -0.11DAP_{LS} -0.07DAP_{UN}
		Simple YSZ	RY = 1.48 +0.05MS -0.14LS -0.06UN -0.07DAP
		Simple	RY = 1.41 -0.06DAP
Parana	Relative Plant yield	Full	RPY = 0.61 +0.58MS + 0.05LS +0.03DAP_{HS} -0.06DAP_{MS} -0.04DAP_{LS}
		Simple YSZ	RPY = 1.02 -0.32MS - 0.20LS -0.04DAP
		Simple	PRY= 1.10 -0.06DAP
	Relative grain number	Full	RGN = 0.80 +0.62MS + 0.001LS +0.01DAP_{HS} -0.07DAP_{MS} -0.05DAP_{LS}
		Simple YSZ	RGN = 1.25 -0.40MS - 0.11LS -0.05DAP
		Simple	RGN = 1.26 -0.07DAP
	Relative crop yield	Full	RY = 1.31 -0.05MS -1.32LS -0.12DAP_{HS} -0.07DAP_{MS} +0.06DAP_{LS}
		Simple YSZ	RY = 0.59 +0.06MS -0.29LS -0.0007DAP
		Simple	RY = 1.15 - 0.06DAP

HS: High and stable, MS: Medium stable, LS: Low stable, and UN: Unstable, DAP_{HS}: emergence in the High stable YSZ, DAP_{MS}: emergence in the Medium stable YSZ, DAP_{LS}: emergence in the Low stable YSZ, DAP_{UN}: emergence in the Unstable YSZ.

Table 20. Mean time (days) to reach 10, 50, and 90% emergence by Year-Field and YSZ in the three evaluated sites.

Site	Year-Field	DAP_{Q10}†	DAP_{Q50}§	DAP_{Q90}‡
Springport	**2016-222**	10.2	11.0	12.1
	2017-222	4.1	5.1	7.2
	2018-105	6.3	7.0	8.2
	2019-304	7.5	7.9	8.9
	2020-308	13.4	14.3	15.7
	2021-210	9.7	11.0	14.2
Portland	**2017-JS1**	9.7	10.4	11.4
	2018-NC12	9.6	10.7	12.6
	2019-MG1	9.1	9.6	11.0
Parana	**2020-11**	6.1	6.7	8.8
YSZ¶		DAP_{Q10}	DAP_{Q50}	DAP_{Q90}
	HS	8.3	9.3	10.8
	MS	9.0	9.5	11.3
	LS	8.5	9.9	11.8
	UN	8.8	9.5	10.7
ANOVA				
Year-Field		0.1165	0.1166	0.1236
YSZ		0.1995	0.5578	0.6069
Year-Field x YSZ		0.3188	0.1019	0.084

†Time to reach 10% of emergence, §time to reach 50% of emergence, ‡time to reach 90% of emergence. ¶Yield stability zone. HS: High stable, MS: Medium stable, LS: Low stable, and UN: Unstable.

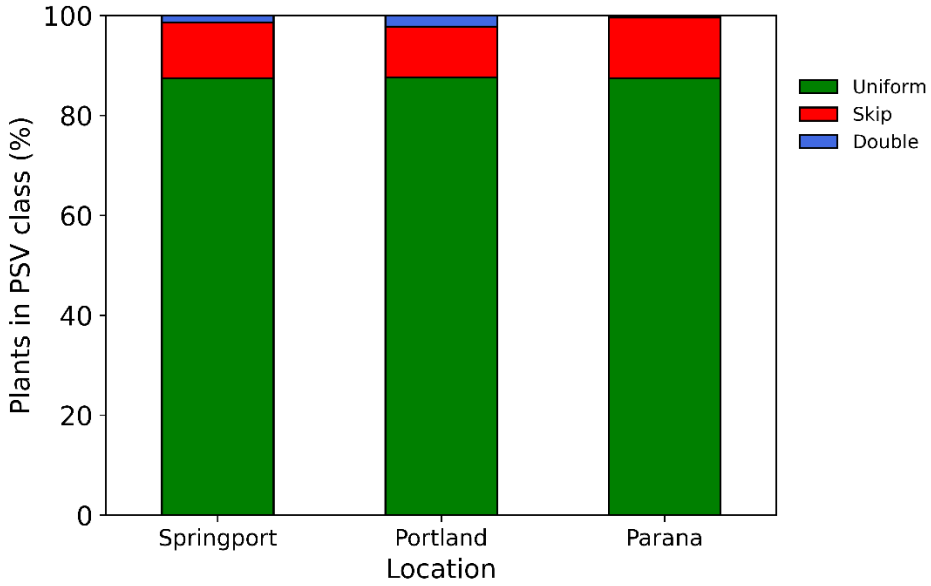

Figure 24. Plant spatial variability within the row as percentage of uniform, skip, and double plants across locations (Springport, Portland, and Parana). Uniform: plants with distances between 5 and 30 cm; Skip: gaps greater than 30 cm, and Double: consecutive plants less than 5 cm from each other.

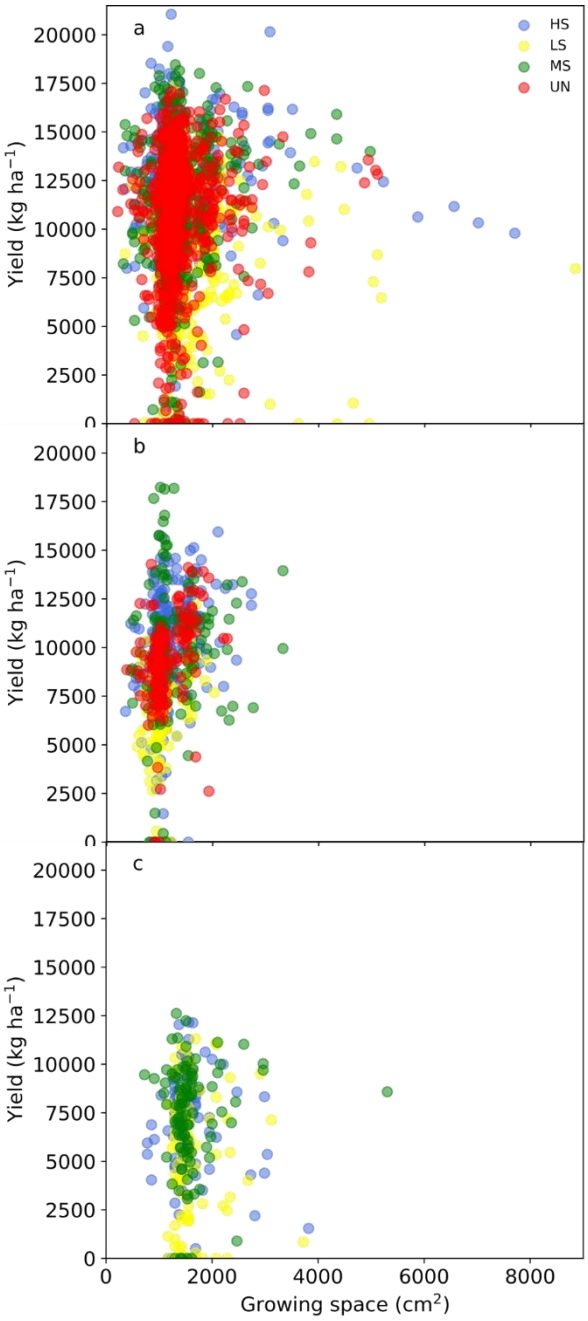

Figure 25. Crop yield (kg ha^{-1}) as affected by growing space (cm^2 plant^{-1}) and yield stability zone by location a) Springport, b) Portland, and c) Parana. HS: High and stable, LS: Low and stable, MS: Medium and Stable, and UN: Unstable.

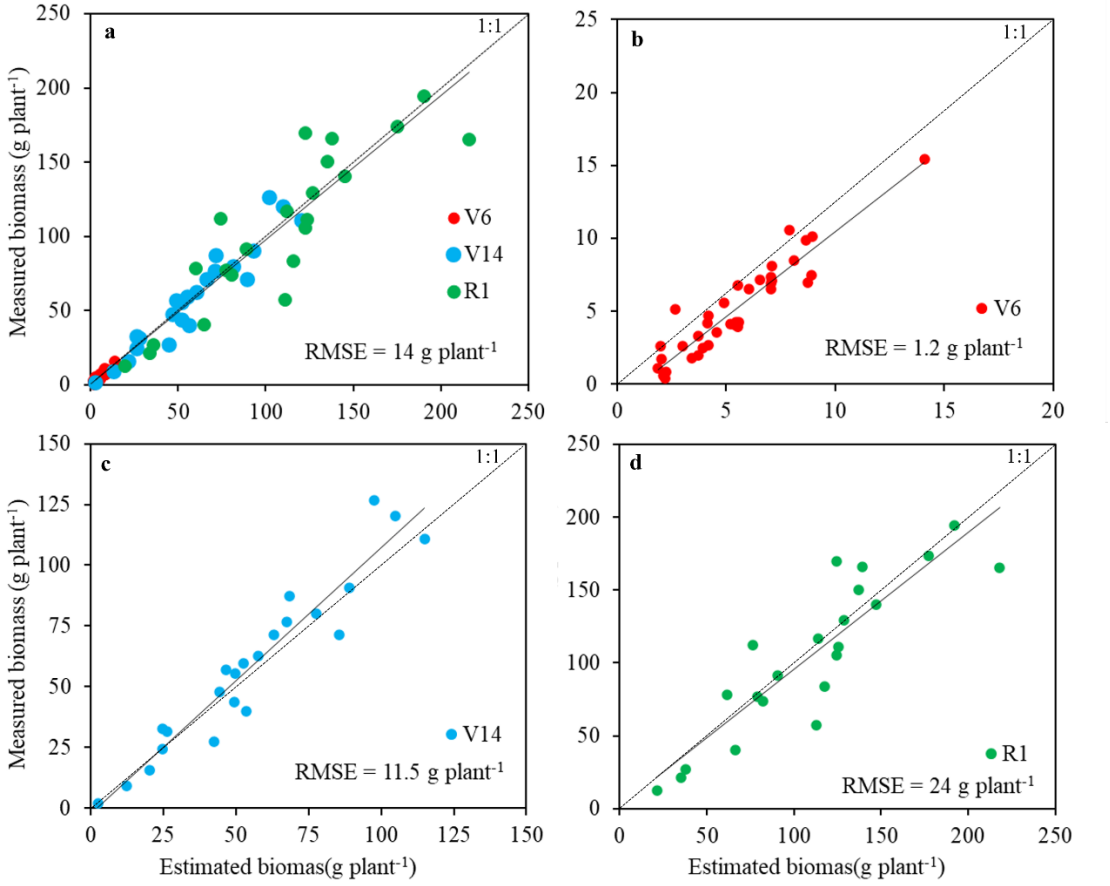

Figure 26. Allometric model validation results a) general model overall, b) general model for V6 stage, c) general model V14 stage, and d) general model R1 stage.

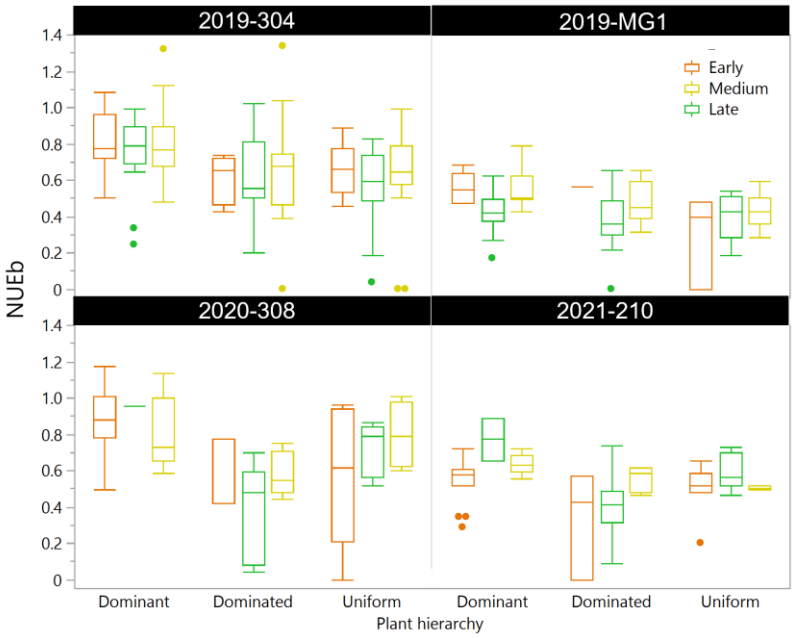

Figure 27. Box plots showing distribution of biomass nitrogen use efficiency (g) in four Year-Fields (2019-304, 2019-MG1, 2021-308, and 2021-210) for three plant emergence classes, Early, Medium, and Late, and three plant hierarchies, Dominant, Dominated, and Uniform.

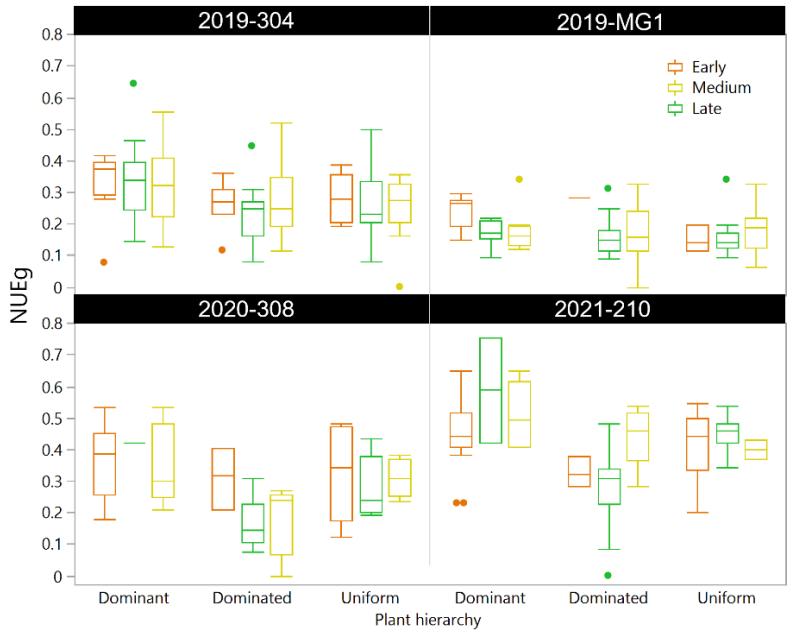

Figure 28. Box plots showing distribution of grain nitrogen use efficiency (g) in four Year-Fields ((2019-304, 2019-MG1, 2021-308, and 2021-210)) for three plant emergence classes, Early, Medium, and Late, and three plant hierarchies, Dominant, Dominated, and Uniform.

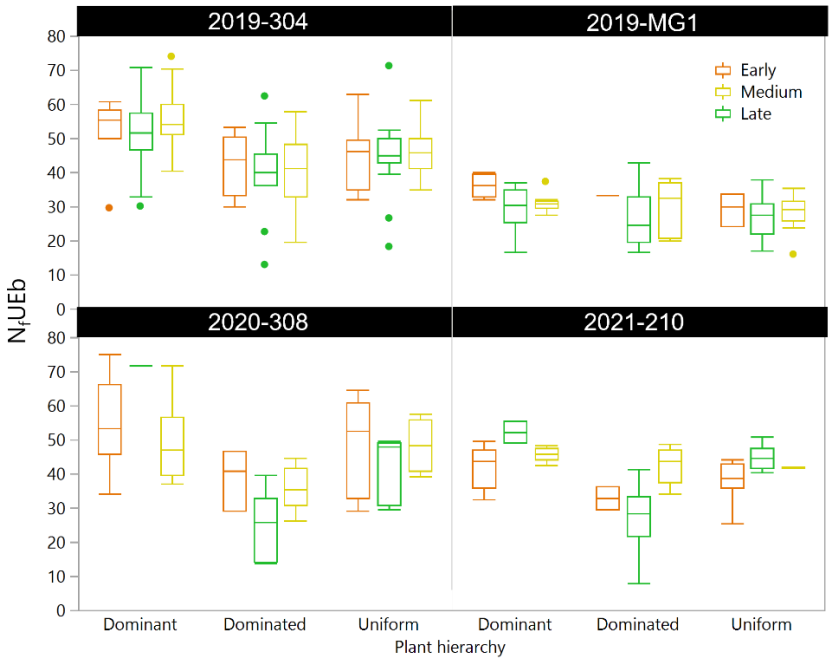

Figure 29. Box plots showing distribution of biomass nitrogen fertilizer use efficiency (g) in four Year-Fields (2019-304, 2019-MG1, 2021-308, and 2021-210) for three plant emergence classes, Early, Medium, and Late, and three plant hierarchies, Dominant, Dominated, and Uniform.

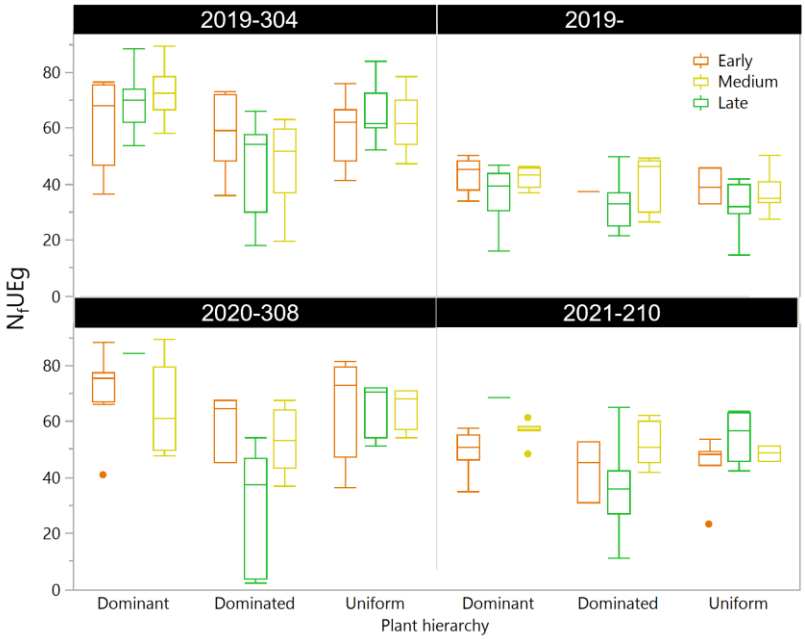

Figure 30. Box plots showing distribution of grain nitrogen fertilizer use efficiency (g) in four Year-Fields (2019-304, 2019-MG1, 2021-308, and 2021-210) for three plant emergence classes, Early, Medium, and Late, and three plant hierarchies, Dominant, Dominated, and Uniform.

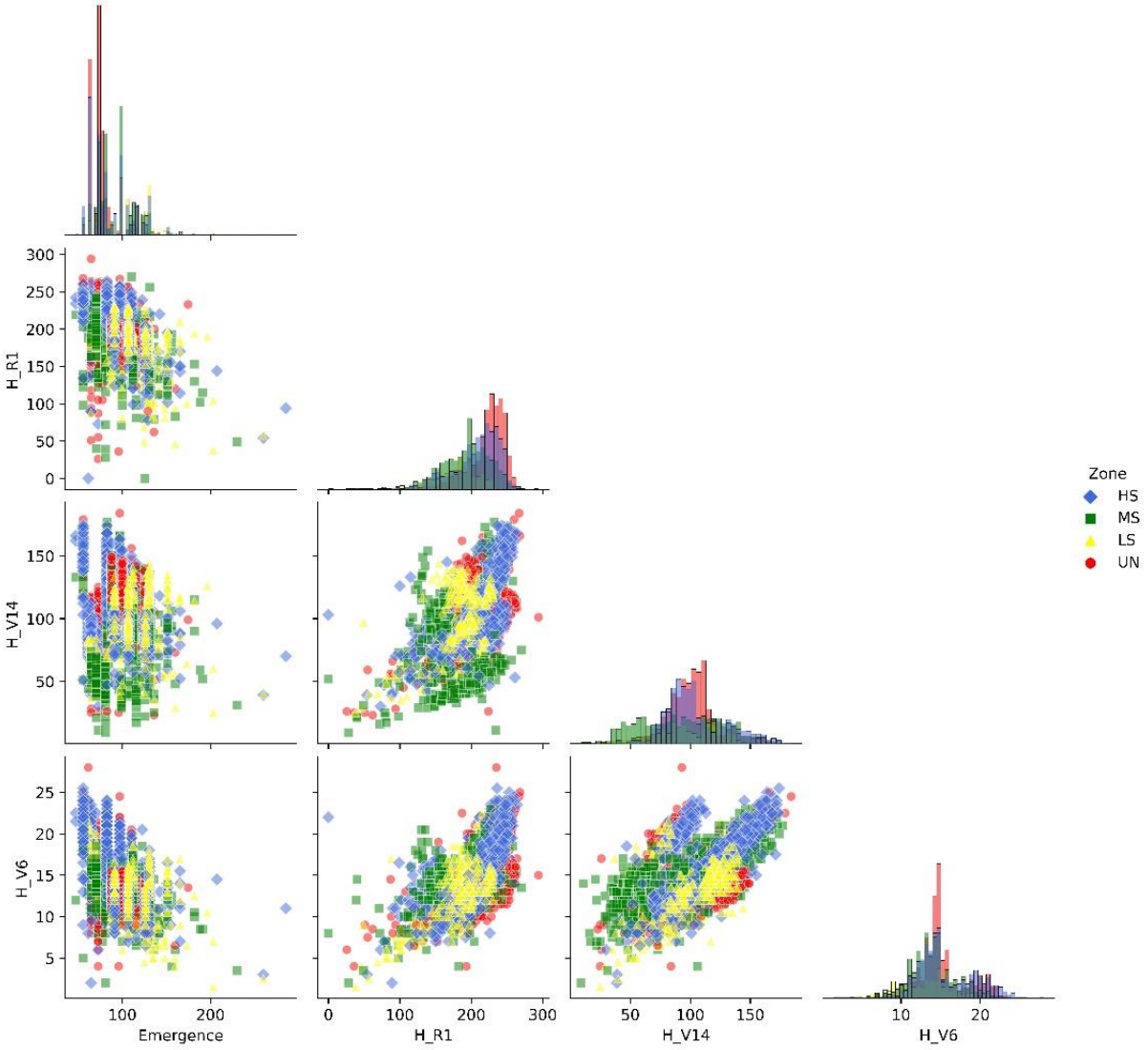

Figure 31. Features pair plot for the maize emergence dataset, which comprises 3483 samples and includes 7 features, 3 being shown. H_V6: plant height (cm) at V6, H_V14: plant height (cm) at V14, and H_R1: plant height (cm) at R1. HS: High stable, MS: Medium stable, LS: Low stable, and UN: Unstable.

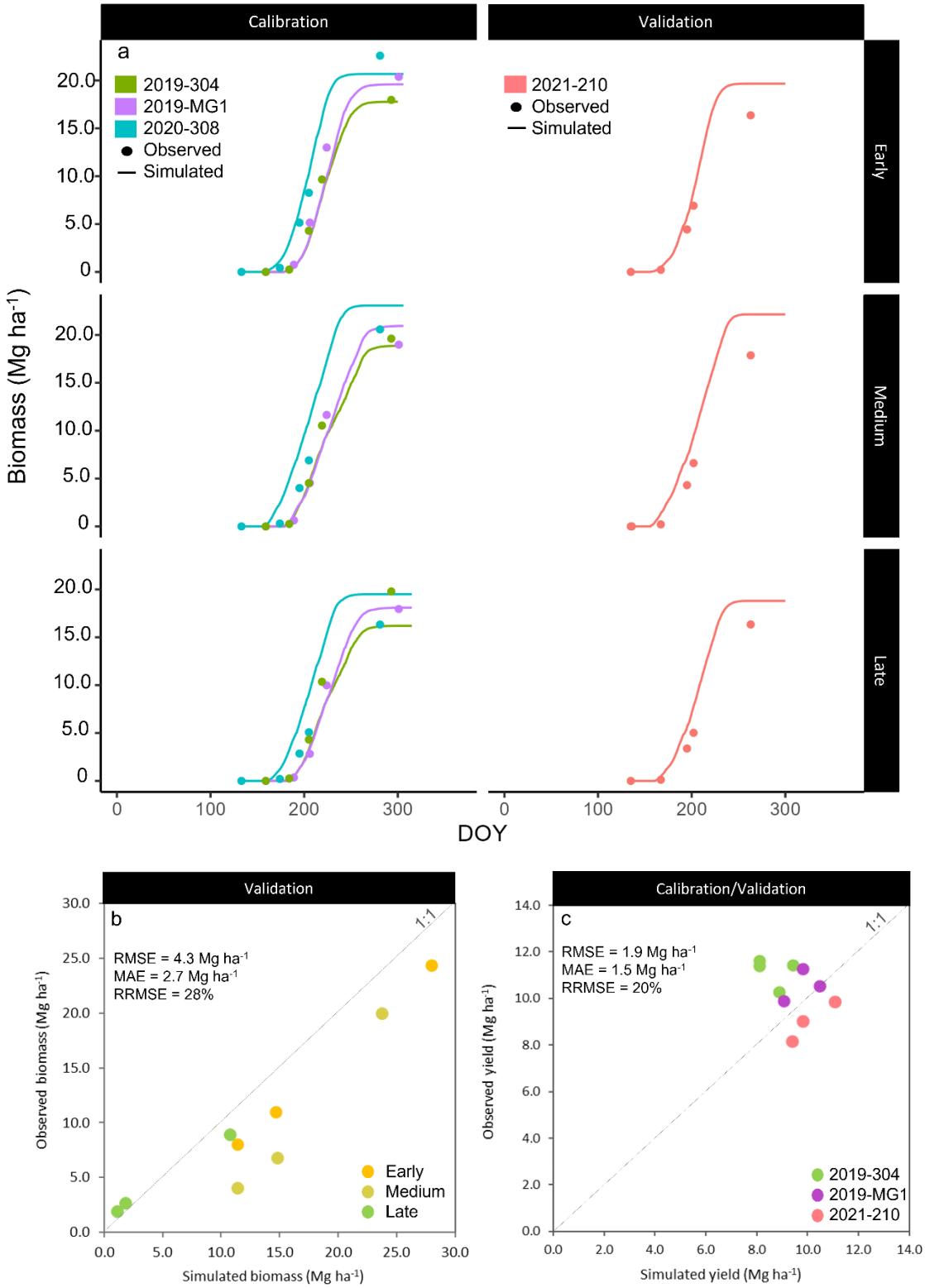

Figure 32. Salus model biomass evolution calibration and validation results (a), comparisons between estimated and observed biomass (b) and yield (c).

Table 21. Emergence descriptive statistics for the evaluated Year-Field by YSZ.

Site	Year-Field	YSZ	Emergence- in thermal time (GDD_E, °C day^{-1})†				
			n	Min	Max	Range	SD
Springport	2019-304	HS	244	64.6	87.7	23.1	5.1
		MS	239	65.5	87.6	22.1	5.4
		UN	727	66.9	94.4	27.4	7.8
	2020-308	HS	220	53.7	125.1	95.1	71.4
		MS	275	63.8	135.8	143.9	72.0
		LS	50	73.5	123.0	80.8	49.5
		UN	124	64.5	129.9	80.8	65.4
	2021-210	HS	150	91.8	172.5	80.7	17.0
		MS	153	87.8	186.5	98.7	19.2
		LS	132	95.8	203.7	107.9	22.5
		UN	100	87.8	144.1	56.3	13.7
Portland	2019-MG1	HS	203	61.4b	76.4b	15.1b	4.3
		MS	193	70.4a	125.7a	55.2a	18.0
		LS	43	62.9ab	75.7b	12.8b	4.2
		UN	158	62.7b	84.3b	21.6b	7.1
Parana	2020-11	HS	96	112.0	176.3	64.3	22.6
		MS	77	112.0	171.4	59.4	15.3
		LS	97	112.0	219.3	107.3	14.8
	2020-4	HS	102	91.2	140.5	49.3	14.0
		LS	100	91.2	149.1	57.9	14.2

†means not sharing the same letter within the same Year-Field and column are significantly different ($p<0.05$).

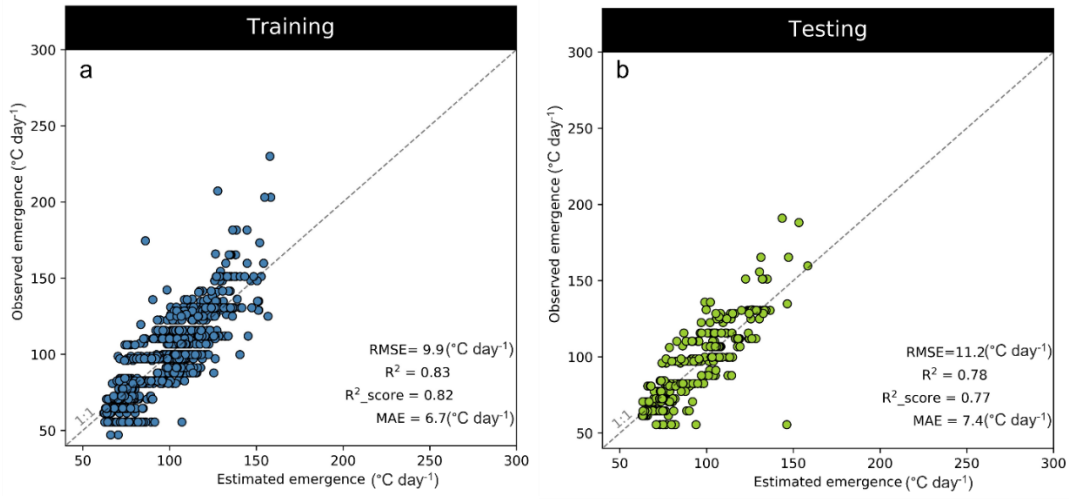

Figure 33. Comparisons between estimated and observed emergence (C day^{-1}) for the training (a) and testing (b) data sets. Data randomly split from six year-field described in *4.2.1. Site description and general characteristics.*

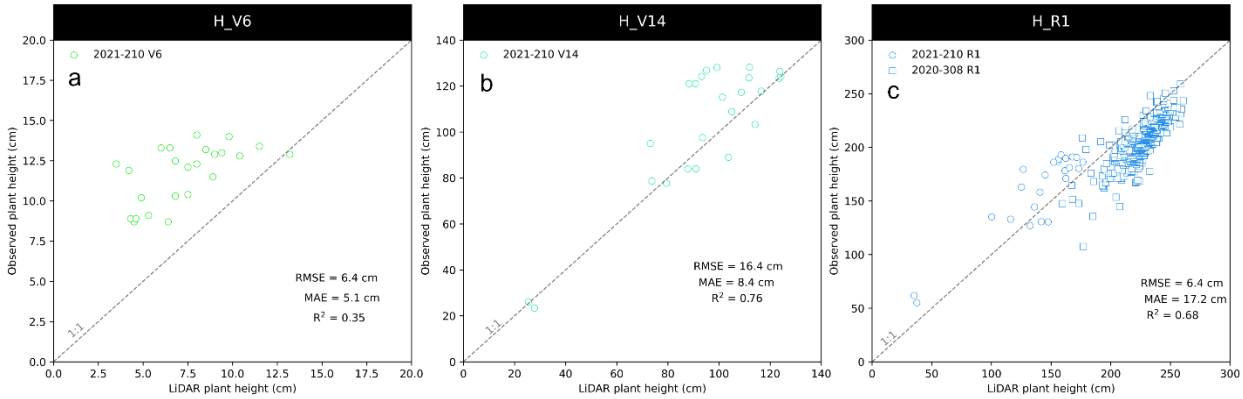

Figure 34. Comparison between observed plant height (cm) and plant height (cm) extracted from LiDAR images obtained at three stages V6 (a), V14 (b), and R1 (c), in two fields 2020-308 and 2021-210.